UC San Diego

UC San Diego Electronic Theses and Dissertations

Title

Bacterial Alteration and Removal of Dissolved Organic Matter in the Surface Ocean /

Permalink

https://escholarship.org/uc/item/4p25h3mg

Author

Sherwood, Byron Pedler

Publication Date

2014

Peer reviewed|Thesis/dissertation

eScholarship.org Powered by the California Digital Library
University of California

UNIVERSITY OF CALIFORNIA, SAN DIEGO

Bacterial Alteration and Removal of Dissolved Organic Matter in the Surface Ocean

A dissertation submitted in partial satisfaction of the requirements for the degree
Doctor of Philosophy

in

Oceanography

by

Byron Pedler Sherwood

Committee in charge:

Professor Farooq Azam, Chair
Professor Eric Allen
Professor Lihini I. Aluwihare
Professor Timithy Baker
Professor Forest Rohwer
Professor T. Frede Thingstad

2014

Copyright

Byron Pedler Sherwood, 2014

All rights reserved.

The Dissertation of Byron Pedler Sherwood is approved, and it is acceptable in quality and form for publication on microfilm and electronically:

_____

_____

_____

_____

_____

_____

Chair

University of California, San Diego

2014

DEDICATION

To my mother, thank you.

EPIGRAPH

"Aho Mitakuye Oyasin."
-*Lakota Sioux*

TABLE OF CONTENTS

Signature Page iii

Dedication iv

Epigraph v

Table of Contents vi

List of Abbreviations viii

List of Figures ix

List of Tables xi

Acknowledgements xiii

Vita xvi

Abstract of the Dissertation xviii

Chapter 1 Introduction: Microbial control of dissolved organic carbon in the ocean 1
- 1.1 Abstract 2
- 1.2 Introduction 2
- 1.3 References 9

Chapter 2 Single bacterial strain capable of significant contribution to carbon cycling in the surface ocean 15
- 2.1 Abstract 16
- 2.2 Significance 17
- 2.3 Introduction 17
- 2.4 Methods 20
- 2.5 Results 24
- 2.6 Discussion 33
- 2.7 Conclusion 39
- 2.8 Acknowledgements 40
- 2.9 References 41
- 2.10 Appendix: Supporting Information 49

Chapter 3 Single strain physiology and community composition of bacteria from coastal and offshore Southern California Bight marine environments 71
3.1 Abstract..... 72
3.2 Introduction 73
3.3 Methods 74
3.4 Results 81
3.5 Discussion..... 100
3.6 Acknowledgements 106
3.7 References 107

Chapter 4 Physiological and genomic insights into the role of bacterial metabolism on the alteration and efficient removal of marine dissolved organic matter 111
4.1 Abstract..... 112
4.2 Introduction 112
4.3 Methods 114
4.4 Results 123
4.5 Discussion..... 136
4.6 Acknowledgments 145
4.7 References 146

LIST OF ABBREVIATIONS

AFM	atomic force microscopy
AFSW	autoclaved filtered seawater
AltSIO	Alteromonas strain SIO
AMC	7-amino-4-methylcoumarin
amol	atto (10^{-18}) mole
ANOVA	analysis of variance
ANI	average nucleotide identity
CCE	California current ecosystem
CHN	carbon, hydrogen, nitrogen
Ci	curie (2.22×10^{12} radioactive decays per minute)
CO_2	carbon dioxide
COG	cluster of orthologous groups
CTD	conductivity, temperature, density
DAPI	4', 6-diamidino-2-phenylindole
DNA	deoxyribonucleic acid
DOC	dissolved organic carbon
DOM	dissolved organic matter
FISH	fluorescence in situ hybridization
FITC	fluorescein isothiocyanate
FSW	filtered seawater
FT-ICR-MS	Fourier transform, ion cyclotron resonance, mass spectrometry
GF/F	glass fiber filter, type F
HCl	hydrochloric acid
KEGG	Kyoto Encyclopedia of Genes and Genomes
LTER	Long-term ecological research
MAR-FISH	microautoradiography fluorescence in situ hybridization
MUF	4-methyl-umbelliferone
NA	noble agar
NPSG	North Pacific subtropical gyre
OD	optical density
OTU	operational taxonomic unit
PCR	polymerase chain reaction
PES	polyethersulfone
POM	particulate organic matter
Pg	peta (10^{15}) gram
SIO	Scripps Institution of Oceanography
SW	seawater
SWC	seawater community
rDNA	ribosomal DNA
RNA	ribonucleic acid
rRNA	ribosomal RNA
TEM	transmission electron microscopy
XRMA	X-ray microanalysis

LIST OF FIGURES

Figure 1. Bacterial growth, cell C, and DOC consumption of three treatments grown in 0.1 μm filtered coastal North Pacific seawater Bacterial growth, cell C, and DOC consumption of three treatments grown in 0.1 μm filtered coastal North Pacific seawater (A–I) 26

Figure 2. Bacterial partitioning of coastal surface ocean DOC during three incubation experiments (A–C) 29

Figure 3. Long-term carbon drawdown of January 2012 incubation 30

Figure 4. Growth dynamics of Alteromonas sp. strain AltSIO cocultured with native microbial assemblages in size-fractionated coastal seawater: (A and D) <0.2 μm FSW, (B and E) < 0.8μm FSW, and (C and F) <50 μm FSW 32

Figure S1. Bacterial size frequency distribution in the California Current Ecosystem 59

Figure 5. Overview of cruise CCE P0810 80

Figure 6. Maximum likelihood tree of phylogentitic distribution of Scripps pier bacterial isolate 16S rRNA 82

Figure 7. Scripps pier isolate growth in 0.1μm-filtered seawater. 88

Figure 8. Cluster analysis of 44 samples across CCE A-Front and adjacent flanking water masses from cruise CCE P0810 93

Figure 9. Summarized results for oxidation of 95 individual substrates by AltSIO relative to phylogentically diverse bacterial strains. 86

Figure 10. Transmission electron microscopy (TEM) images of non-fixed, non-stained, air-dried *Alteromonas* sp. AltSIO cells grown in 0.1 μm filtered, aged seawater 126

Figure 11. AltSIO growth and metabolic response to neutral sugar-amended 0.1 μm-filtered seawater 128

Figure 12. Maximum likelihood phylogenetic tree of the 16S rRNA gene of AltSIO (Alteromonas_sp._ALT199) relative to closely related *Alteromonas macleodii* strains with publicly available genomes (JGI IMG). 131

Figure 13. KEGG pathway of bacterial (*E. coli*) chemotaxis with enzymes present in AltSIO genome highlighted with filled purple boxes 134

Figure 14. Linkage dendrogram of presence/absence FT-ICR-MS peak data of 22 samples calculated from Bray-Curtis distance and Ward's method..... 135

Figure S2. KEGG pathway of glycolysis in AltSIO..... 151

Figure S3. Diagram of KEGG pathways of metabolism..... 153

LIST OF TABLES

Table S1. Quality control analysis of filtration and experimental setup 60

Table S2. Environmental conditions during seawater collection from Scripps Pier 61

Table S3. Bacterial carbon and nitrogen content measured by CHN analysis 62

Table S4. Statistical analysis of three experiments with ambient dissolved organic matter from surface coastal North Pacific seawater after 5 d of incubation 63

Table S5. Heterotrophic bacterial consumption of ambient dissolved organic matter from surface coastal North Pacific seawater after 5 d of incubation 64

Table S6. One-way ANOVA of experimental data from Table S5 65

Table S7. Statistical analysis of long-term (>1 y) carbon drawdown experiment (Figure 3) 66

Table S8. TOC averaged by density horizon in the California Current, North Pacific 70

Table 1. Isolation scheme of 270 marine bacteria isolates. 75

Table 2. Bacterial isolate abundance and DOC utilization 87

Table 3. Bacteria cell biovolume and carbon content across the A-Front study in the CCE (cruise P0810) 90

Table 4. Relative abundance of 16S rDNA sequences for major taxa in the CCE A-Front study. Surface sample 94

Table 5. Relative abundance of 16S rDNA sequences for major taxa in the CCE A-Front study. Mixed layer 95

Table 6. Relative abundance of 16S rDNA sequences for major taxa in the CCE A-Front study. Upper chlorophyll maximum 96

Table 7. Relative abundance of 16S rDNA sequences for major taxa in the CCE A-Front study. Mid chlorophyll maximum 97

Table 8. Relative abundance of 16S rDNA sequences for major taxa in the CCE A-Front study. Lower chlorophyll maximum 98

Table 9. Relative abundance of 16S rDNA sequences for major taxa in the CCE A-Front study. Lower chlorophyll maximum (100 m) 99

Table 10. AltSIO cell-specific hydrolytic enzyme activity 124

Table 11. C:N:P elemental ratios of AltSIO grown in marine DOM. 126

Table 12. Radiolabeled glucose, fructose, galactose, and leucine uptake measured in AltSIO grown in GF/F-filtered, autoclave-sterilized, aged seawater 130

Table S9. General characteristics of AltSIO (ALT99) genome 155

Table S10. Clusters of orthologous groups (COG) of proteins categorized by function for AltSIO genome relative to closely related *Alteromonas macleodii* strains 156

Table S11. Enumeration of COGs with predicted carbohydrate-processing function within genomes of AltSIO and *Alteromonas macleodii* strains AD45, MED64, and DE1 157

Table S12. COGs of predicted transporters present in AltSIO genome but absent from *Alteromonas macleodii* strains AD45, MED64, and DE1 160

Table S13. Biolog GN2 microplate data showing isolate-specific oxidation of 95 screened substrates. 162

ACKNOWLEDGEMENTS

I am sincerely grateful to my advisor, Farooq Azam, for his guidance along this journey. I feel honored and privileged to have had the opportunity to interact with and learn from Farooq. Among many lessons, I have learned to approach the study of the ocean as an ecosystem whose every function is intimately influenced by the ecology and physiology of individual microbes and their interaction with one another. I aspire to bring the same creativity and imagination to my explorations as Farooq has throughout his career.

Thank you to Lihini Aluwihare for being a mentor, advocate, and friend. Lihini's enthusiasm and endless positivity has been a much appreciated source of support and guidance throughout my Ph.D. Thank you to Frede Thingstad for his generosity and hospitality while hosting me in his lab and for his insight and feedback on my work and several research proposals. Thanks to Eric Allen for all the stimulating impromptu Hubbs hallway discussions as well as suggestions and tips for sequencing the genome of AltSIO. Thanks to Forest for all the free advice and insight during our meetings at the University Heights office, Small Bar. Lastly, thank you to Tim Baker for helpful discussions throughout this process. Tim provided an important and fresh perspective as the lone committee member whose research career has been focused outside of the marine realm.

Thank you to all Azam lab members throughout the years who have played a role in welcoming me into the lab and shaping my development as a scientist: Ty, Steve, Francesca, Xavier, Melissa, Krystal, Ryan G., Ryan P., Nirav, and Anne-Claire.

Thanks also to the UCSD STARS undergraduate students, summer REU students, and volunteers who have worked with me in the lab: Kalani Reyes, Benjamin Negrete Jr., Emily Shaffer, and Jasmine Tan. It's been a pleasure working with you, serving as your mentor, and learning from you along the way.

Thank you to all at the J. Craig Venter Institute who have generously supported an ambitions collaborative project to characterize the bacterial and eukaryotic microbial community across the CCE A-Front, much of which did not make it into this dissertation. Andy Allen, Chris Dupont, Hong Zheng, Jing Bai, Ariel Rabines, and Alex Richter are greatly acknowledged for their help processing and analyzing DNA and RNA. Thank you also to Magali Porrachia in the Aluwihare lab for assistance throughout the many years running samples and troubleshooting the TOC analyzer.

A special thank you to Chris Reddy and Benjamin Van Mooy at WHOI. As my WHOI Summer Student Fellow advisor, Chris played a pivotal role in my career development by thrusting me into the realm of analytical and environmental marine chemistry and later encouraged me to apply to the Scripps Ph.D. program. My work with Ben planted the seed of interest and gave me my first hands-on exposure to microbial oceanography, a field unbeknownst to me at the time, would later become the focus of my Ph.D.

Thank you to my family, Mom, Kevin, Farley, and Anastasia for your continued love and support. Thanks to all the great friends I've made at SIO for keeping it real, providing balance, and just being awesome people: Ty, Jillian,

Michelle, Rosa, Sarah, Ryan, Breakfast Club, and the 2007 SIO Cohort. Lastly, thank you to my wonderful wife, Katie, for all your love, support, and encouragement. You probably deserve another Ph.D. just for putting up with me. Duke, our 140 lb. Great Dane puppy, thanks for being dopey, loving, and excited every time I see you, even if it was just five minutes ago.

Chapter 2, in full, is a reprint of the material as it appears in Proceedings of the National Academy of Sciences 2014. Pedler, B. E., Aluwihare, L. I., Azam, F., 2014. The dissertation author was the primary investigator and author of this paper.

Chapter 3, in part, is being prepared for submission for publication of the material. Pedler, B. E., Samo, T. J., Dupont, C. L., Allen, A. E., Landry, M. R., Azam, F. The dissertation author was the primary investigator and author of this material.

Chapter 3, in part, is being prepared for submission for publication of the material. Pedler, B. E., Shaffer, E., Aluwihare, L. I., Azam, F. The dissertation author was the primary investigator and author of this material.

Chapter 4, in part, is being prepared for submission for publication of the material. Pedler, B. E., Leon Zyas, R. I., Aluwihare, L. I., Azam, F. The dissertation author was the primary investigator and author of this material.

VITA

2005	Bachelor of Science in Biology, Department of Biological Sciences, University of New Hampshire
2005 – 2007	Research Assistant II, Department of Marine Chemistry and Geochemistry, Woods Hole Oceanographic Institution
2007 – 2014	Graduate Student Researcher, Scripps Institution of Oceanography, University of California, San Diego
2008-2011	National Science Foundation Graduate Research Fellow, Biological Oceanography
2009	Microbial Oceanography training course*, Center for Microbial Oceanography: Research and Education* (C-MORE), University of Hawaii at Manoa
2012	Teaching Assistant, General Microbiology Laboratory, Department of Biological Sciences, University of California, San Diego
2014	Doctor of Philosophy in Oceanography, Scripps Institution of Oceanography, University of California, San Diego

PUBLICATIONS

Pedler, B. E., Aluwihare, L. I., Azam, F. (2014). Single bacterial strain capable of significant contribution to carbon cycling in the surface ocean. *Proceedings of the National Academy of Sciences*. 111(20), 7202-7207.

Van Mooy, B. A. S., Hmelo, L. R., Fredricks, H. F., Ossolinski, J. E., **Pedler, B. E.**, Bogorff, D. J., Smith, P. J. S. (2014). Quantitative exploration of the contribution of settlement, growth, dispersal and grazing to the accumulation of natural marine biofilms on antifouling and fouling-release coatings. *Biofouling.* 30(2), 223-236.

Guasco, T.L., Cuadra-Rodriguez, L.A, **Pedler, B. E.**, Ault, A.P., Collins, D.B., Zhao, D., Kim, M.J., Ruppel, M.J., Grassian, V.H., Azam, F., Bertram, T.H., Prather, K.A. (2013). Transition metal associations with primary biological particles in sea spray aerosol generated in a wave channel. *Environmental Science & Technology.* 48(2), 1324-1333

Collins, D.B., Ault, A.P., Moffet, R.C., Ruppel, M.J., Cuadra-Rodriguez, L.A, Guasco, T.L., Corrigan, C.E., **Pedler, B. E.**, Azam, F., Aluwihare, L.I., Bertram, T.H., Roberts, G.C., Grassian, V.H., Prather, K.A. (2013). Impact of marine biogeochemistry on the chemical mixing state and cloud forming ability of nascent sea spray aerosol. *Journal of Geophysical Research: Atmospheres*. **118**, 8553-8565.

Prather, K.A., Bertram, T.H., Grassian, V.H., Deane, G.B., Stokes, M.D., DeMott, J., Aluwihare, L.I., Palenik, B.P., Azam, F., Seinfeld, J.H., Moffet, R.C., Molina, M.J., Cappa, C.D., Geiger, F.M., Roberts, G.C., Russell, L.M., Ault, A.P., Baltrusaitis, J., Collins, D.B., Corrigan, C.E., Cuadra-Rodriguez, L.A, Ebben, C.J., Forestieri, S.D., Guasco, T.L., Hersey, S.P., Kim, MJ., Lambert, W., Modini, R.L., Mui, W., **Pedler, B. E.**, Ruppel, M.J., Ryder O.S., Schoepp, N., Sullivan, R.C., Zhao, D. (2013) Bringing the ocean into the laboratory to probe the chemical complexity of sea spray aerosol. *Proceedings of the National Academy of Sciences.* 110(19), 7550-7555.

Samo, T. J., **Pedler, B. E.**, Ball, I., Pasulka, A. L., Taylor, A. G., Aluwihare, L. I., Azam, F., Goericke, R., Landry, M. R. (2012) Microbial distribution and activity across a water mass frontal zone in the California Current Ecosystem. *Journal of Plankton Research.* 34(9), 802-814.

Van Mooy, B. A. S., Fredricks, H., **Pedler, B. E.,** Dyhrman, S.T., Karl, D.M., Koblížek, M., Lomas, M.W., Mincer, T., Moore, L.R., Moutin, T., Rappé, M.S., Webb, E.A. (2009). Phytoplankton in the ocean use non-phosphorus lipids in response to phosphorus scarcity. *Nature.* 458(7234) 69-72.

Pangallo, K., Nelson, R. K., Teuten, E. L., **Pedler, B. E.,** Reddy, C. M. (2008) Expanding the range of halogenated 1-methyl-1,2- bipyrroles. *Chemosphere*. 71(8), 1557-1565.

Teuten, E. L., **Pedler, B. E.,** Hangsterfer, A. N., Reddy, C. M. (2006) Identification of highly brominated analogues of Q1 in marine mammals. *Environmental Pollution.* 144, 336-344.

Teuten, E. L., Saint-Louis, R., **Pedler, B. E.,** Xu, L., Pelletier, E., and Reddy, C. M. (2006) Expanding the range of brominated Q1 analogues. *Marine Pollution Bulletin.* 52(5), 578-582.

ABSTRACT OF THE DISSERTATION

Bacterial Alteration and Removal of Dissolved Organic Matter in the Surface Ocean

by

Byron Pedler Sherwood

Doctor of Philosophy in Oceanography

University of California, San Diego, 2014

Professor Farooq Azam, Chair

The ocean contains one of the largest reservoirs of reduced carbon on Earth in the form of dissolved organic matter (DOM). Heterotrophic bacteria serve as the primary force regulating the degradation of this material, recycling the majority of dissolved organic carbon (DOC) produced in the surface ocean by phytoplankton back to carbon dioxide. While it is known that microbial community structure plays a role in determining the rate and magnitude of DOM turnover, the quantitative contribution of individuals to this process remains unknown. The objective of this dissertation was

to investigate the constraints on DOM turnover by bacterial communities by focusing on how a single bacterial strain makes a living in the sea. I found that a single bacterial strain, *Alteromonas* sp. AltSIO, has the capacity to consume an equivalent magnitude of DOC as diverse bacterial communities, suggesting that bacterial diversity may not be required for the complete removal of labile DOC in the surface ocean. In long-term microcosms, however, bacterial diversity was required for continued degradation of semi-labile DOC. To test the generality of this capacity among individual bacteria, a culture-based study was conducted where >100 phylogenetically diverse bacterial strains were isolated to screen for growth in unamended seawater. No other bacterial strain tested exhibited the capacity to consume a measureable quantity of DOC when grown in isolation, suggesting that this phenomenon may not be common among readily culturable marine bacteria. Physiological investigations of this isolate reveal a broad capacity for processing carbohydrates, yet an apparent preference for disaccharides and inability to metabolize glucose. Genomic analysis confirmed that this strain lacks a glucose-specific permease required for the exogenous uptake of glucose, but is endowed with additional carbohydrate-specific transporters not found in genomes of closely related bacterial strains. Genomic insights also show the potential to reduce nitrate, a high capacity to scavenge iron, and a complete chemotaxis apparatus potentially used for disaccharide acquisition. DOM characterization by ultrahigh resolution mass spectrometry revealed that AltSIO and diverse seawater communities significantly alter the composition of ambient DOM.

CHAPTER 1

Introduction: Microbial control of dissolved organic carbon in the ocean

1.1 ABSTRACT

The oceanic pool of dissolved organic matter (DOM) is one of the largest reservoirs of reduced carbon on Earth (Hedges 1992). By process of primary production, phytoplankton are the main source of DOM while heterotrophic bacteria are the primary sink. Community structure plays an integral role in shaping both the composition and turnover of this material. Microbial ecology seeks to understand the fundamental mechanisms of the ocean as a biogeochemical system by asking who is there, what are they doing, and how are they doing it? Resource niche partition among competing organisms (Hutchinson 1957), a cornerstone of fundamental theory of biodiversity, has played a prominent role in shaping both the direction of research and the framework by which we interpret observations within the field of DOM-bacteria interactions. In this review, I discuss the current state of knowledge and apparent paradoxes on the role that microbial community structure plays in regulating marine DOM turnover.

1.2 INTRODUCTION

The oceanic DOM pool contains as much carbon as there is CO_2 in the Earth's atmosphere (Hedges 1992). Heterotrophic activity of Bacteria and Archaea (collectively referred to as bacteria here) serve as the primary removal mechanism for this material (Azam and Hodson 1977, Ammerman et al. 1984), and results in the consumption of nearly 50% of primary carbon production (Fuhrman and Azam 1982). The efficiency of prokaryotic hydrolysis, uptake, assimilation, and respiration of

dissolved organic carbon (DOC) has ultimate bearing on global carbon cycles, long-term carbon export from the euphotic zone (region of the ocean exposed to sufficient sunlight to support photosynthesis) (Kaiser and Benner 2012), and ocean-atmosphere CO_2 flux (del Giorgio and Cole 1998). The chemical composition of DOM is notoriously complex (Benner 2002), and the control mechanisms of production and consumption (Carlson 2002) and ultimately turnover rate of DOM are highly dynamic (Ogura 1972, Kirchman et al. 1991, Carlson and Ducklow 1996, Cherrier et al. 1996).

1.2.1 Seasonal accumulation of DOC

Seasonal accumulation of DOC in the surface ocean has been observed in correlation with summertime thermal stratification across oceanic regimes with a broad range of productivity from the coastal northeast Pacific (Williams 1995), the coastal North Sea (Sintes et al. 2010), the Baltic Sea (Zweifel et al. 1995), the northwest Mediterranean (Copinmontegut and Avril 1993) to the Sargasso Sea (Carlson et al. 1994). Decoupling of primary production and heterotrophic bacterial consumption results in an estimated 17% of global new production accumulating as DOC in the surface ocean (Hansell and Carlson 1998). The drivers regulating this decoupling vary in time and space with bottom-up inorganic nutrient limitation (Rivkin and Anderson 1997, Mills et al. 2008), and competition for nutrients with autotrophs (Rivkin and Anderson 1997, Thingstad et al. 1997) limiting bacterial growth, and top-down grazing pressure (Thingstad et al. 1997) limiting bacterial abundance, each of which reduce the potential of bacteria to consume otherwise

biologically labile DOM. The relative bioavailabiity of accumulated DOM is highly variable. Repeated studies have shown little to no measurable change in DOC concentration when resident bacterial populations were grown on unamended seawater both in the northwestern Sargasso Sea (Carlson and Ducklow 1996, Carlson 2002, Obernosterer et al. 2003) and in the eastern North Pacific (Cherrier et al. 1996, Cherrier and Bauer 2004) leading these authors, and others previously (Legendre and Lefevre 1995, Sondergaard et al. 2000), to hypothesize that in some instances the accumulated DOM is biologically semi-labile or even recalcitrant to the local heterotrophic community.

1.2.2 Bacterial community structure and the apparent dominance of labile DOC-specific degraders

Microbial community structure has significant influence on the turnover of DOM (Azam et al. 1983, Azam and Worden 2004). Recent metagenomic (Mou et al. 2008) and transcriptomic (McCarren et al. 2010) studies investigating natural marine microbial community utilization of unamended and DOC-enriched mesocosms have shown that a narrow diversity of taxa increase in cell abundance and activity following concomitant drawdown of DOC. Mou et al. (2008) concluded that DOC cycling in the coastal ocean is primarily regulated by generalist species dominated by gammaproteobacteria, and in particular *Alteromonadales*. McCarren et al. (2010) characterized the genomic and transcriptional response of the microbial community in microcosm experiments in which high-molecular-weight DOM was added to surface

waters of the North Pacific subtropical gyre (NPSG). Similar to Mou et al., McCarren and colleagues (2010) found that the community became dominated by three taxanomic clades including *Rhodobacteracea*, *Methylophaga*, and *Alteromonas*. In a follow up deep-sea water mixing experiment in the NPSG designed to loosely simulate deep-water nutrient injection to the surface ocean, Shi and colleagues found that treatment-specific shifts in prokaryotic community composition were comprised entirely of large, high nucleic acid *Alteromonas* populations as determined by flow cytometric and transcriptomic analyses (Shi et al. 2012).

Recent studies tracking the uptake of stable isotope or radiolabeled phytoplankton exudates by specific bacterial phyla and species found similar results in contrasting oceanic regimes. Nelson and Carlson (2012) found that *Alteromonads* dominated uptake of stable isotope-labeled *Synechococcus* exudate-derived DOM in both the euphotic and mesopelagic zone of the northwestern Sargasso Sea. Sarmento and Gasol (2012) used microautoradiography fluorescence in situ hybridization (MAR-FISH) to track bacterial phyla- and species-specific uptake of radiolabeled DOM exudates of six phytoplankton and cyanobacterial species endemic to coastal Mediterranean waters. Sarmento and Gasol (2012) found that *Alteromonas* and *Roseobacter* species accounted for the greatest increase in community biomass across all phytoplankton DOM enrichments after 24 hours. However, both studies noted the conspicuous rarity of these taxa at the initiation of the experiment and in unamended controls.

The rapid response of a few bacterial species following resource pulses has been well documented both in the natural environment and in mesocosm experiments (Acinas et al. 1999, Eilers et al. 2000, Carlson et al. 2004b, Mills et al. 2008, Tada et al. 2012, Teeling et al. 2012) but the interpretation and conclusions drawn from such observations are mixed. Tada et al (2011) observed a disproportionately large contribution of *Alteromonas* to total bacterial production during a natural phytoplankton bloom in the western North Pacific. Tada and collegues (2012) found similar results in a mesocosm experiment wherein *Alteromonas* accounted for 30% of the actively growing bacterial population during the development of diatom bloom.

1.2.3 Is bacterial community metabolic capacity shaped by resource composition?

The narrow phylogenetic diversity of bacterial populations observed to respond to and consume ambient DOC and DOC-enrichment experiments is unexpected given the enormous chemical complexity of the ambient DOC pool (Hedges 1992, Benner and Opsahl 2001). Furthermore, genomic, physiological, and chemical studies have shown distinct differences in metabolic potential and DOC consumption rates between phylogenetically distinct bacterial populations. Shifts in both microbial community composition (Moeseneder et al. 2001) and metabolic potential as a function of increasing water column depth (DeLong et al. 2006), for example, indicate a reflection in changes in available substrate composition and a potential adaptation to utilize more degraded/oxidized DOM with depth (Benner 2002). As an example, Perez and colleagues (2003) measured an increase in D/L-amino acid uptake ratios with

increasing depth. In this study, it was found that mesopelagic microbial communities readily utilized D-amino acids, whereas the L-enantiomers were taken up preferentially and efficiently by surface communities. The shift in uptake ratio of D/L-amino acids indicates adaptations of mesopelagic communities to altered supply ratios and was hypothesized to result from shifts in prokaryotic community composition between the euphotic and mesopelagic zones of the upper ocean (Perez et al. 2003). Carlson et al (2004a) found that seasonally accumulated DOC was functionally recalcitrant to depth-stratified surface heterotrophic community, but was then consumed by phylogenetically distinct mesopelagic populations following annual convective overturning. These observations suggest not only that separate microbial communities harbor distinct metabolic potential that may be adapted to local resource composition, but also that the biotic degradation of semi-labile DOM may likely be an iterative process among communities or individuals with complementary metabolic capacities.

1.2.4 Inferred constraints on DOM turnover. Does DOM labilty scale with microbial diversity?

That phylogenetic diversity is required to achieve significant reductions in semi-labile DOC has been hypothesized from experimental and bioinformatic observations, as it provides a broader repertoire of ectoenzymes (Martinez et al. 1996, Langenheder et al. 2006) and membrane-bound transporters (Poretsky et al. 2010)

within a given community thus potentially facilitating increased hydrolysis and uptake of complex macromolecules of varying biochemical lability (Benner 2002).

At present the mechanisms regulating the strength and nature of coupling between organic matter production and consumption by bacteria remain poorly constrained. Dynamics of DOC consumption have typically been studied in complex environments (either in the field, mesocosm experiments, or seawater cultures), whereas the dynamics of ambient DOC drawdown in the absence of bacterial diversity has been studied to lesser extent (Jannasch 1967, Williams and Carlucci 1976). The magnitude of DOC consumption by single bacterial strains relative to complex microbial communities is largely unknown.

1.2.5 Minimum requirements for significant DOM turnover

This dissertation takes a reductionist approach to an often times overwhelmingly complex system in an attempt to untangle fundamental mechanisms involved in regulating the fate of carbon that has come to pass through the ocean on it's journey through the Earth's ecosystem.

We begin by asking if there is a minimum degree of bacterial diversity required for significant drawdown of ambient DOM, and proceed to test the capacity of individual bacterial strains to degrade an ecologically relevant magnitude of DOC. Then, focusing in on a single individual, we delve deeper into unraveling the specific physiological traits that facilitate rapid and efficient turnover of oceanic DOM.

REFERENCES

Acinas, S., J. Anton, and F. Rodriguez-Valera. 1999. Diversity of free-living and attached bacteria in offshore western Mediterranean waters as depicted by analysis of genes encoding 16S rRNA. Applied and Environmental Microbiology **65**:514-522.

Ammerman, J. W., J. A. Fuhrman, Å. Hagström, and F. Azam. 1984. Bacterioplankton growth in seawater: 1. Growth kinetics and cellular characteristics in seawater cultures. Marine Ecology Progress Series **18**:31-39.

Azam, F., T. Fenchel, J. Field, J. Gray, L. Meyerreil, and F. Thingstad. 1983. The ecological role of water-column microbes in the sea. Marine Ecology-Progress Series **10**:257-263.

Azam, F., and R. E. Hodson. 1977. Size distribution and activity of marine microheterotrophs. Limnology and Oceanography **22**:492-501.

Azam, F., and A. Worden. 2004. Microbes, molecules, and marine ecosystems. Science **303**:1622-1624.

Benner, R. 2002. Chemical composition and reactivity. Pages 59-90 *in* D. A. Hansell and C. A. Carlson, editors. Biogeochemistry of Marine Dissolved Organic Matter. Elsevier Science, USA.

Benner, R., and S. Opsahl. 2001. Molecular indicators of the sources and transformations of dissolved organic matter in the Mississippi river plume. Organic Geochemistry **32**:597-611.

Carlson, C., and H. Ducklow. 1996. Growth of bacterioplankton and consumption of dissolved organic carbon in the Sargasso Sea. Aquatic Microbial Ecology **10**:69-85.

Carlson, C., H. Ducklow, and A. Michaels. 1994. Annual flux of dissolved organic carbon from the euphotic zone in the northwestern sargasso sea. Nature **371**:405-408.

Carlson, C., S. Giovannoni, D. Hansell, S. Goldberg, R. Parsons, and K. Vergin. 2004a. Interactions among dissolved organic carbon, microbial processes, and community structure in the mesopelagic zone of the northwestern Sargasso Sea. Limnology and Oceanography **49**:1073-1083.

Carlson, C. A. 2002. Production and removal processes. Pages 91-151 *in* D. A. Hansell and C. A. Carlson, editors. Biogeochemistry of marine dissolved organic matter. Elsevier Science, USA.

Carlson, C. A., S. J. Giovannoni, D. A. Hansell, S. J. Goldberg, R. Parsons, and K. Vergin. 2004b. Interactions among dissolved organic carbon, microbial processes, and community structure in the mesopelagic zone of the northwestern Sargasso Sea. Limnology and Oceanography **49**:1073-1083.

Cherrier, J., J. Bauer, and E. Druffel. 1996. Utilization and turnover of labile dissolved organic matter by bacterial heterotrophs in eastern north Pacific surface waters. Marine Ecology Progress Series **139**:267-279.

Cherrier, J., and J. E. Bauer. 2004. Bacterial utilization of transient plankton-derived dissolved organic carbon and nitrogen inputs in surface ocean waters. Aquatic Microbial Ecology **35**:229-241.

Copinmontegut, G., and B. Avril. 1993. Vertical-distribution and temporal variation of dissolved organic-carbon in the north-western mediterranean-sea. Deep Sea Research Part I: Oceanographic Research Papers **40**:1963-1972.

del Giorgio, P., and J. Cole. 1998. Bacterial growth efficiency in natural aquatic systems. Annual Review of Ecology and Systematics **29**:503-541.

DeLong, E. F., C. M. Preston, T. Mincer, V. Rich, S. J. Hallam, N. U. Frigaard, A. Martinez, M. B. Sullivan, R. Edwards, B. R. Brito, S. W. Chisholm, and D. M. Karl. 2006. Community genomics among stratified microbial assemblages in the ocean's interior. Science **311**:496-503.

Eilers, H., J. Pernthaler, F. O. Glockner, and R. Amann. 2000. Culturability and in situ abundance of pelagic bacteria from the North Sea. Applied and Environmental Microbiology **66**:3044-3051.

Fuhrman, J., and F. Azam. 1982. Thymidine incorporation as a measure of heterotrophic bacterioplankton production in marine surface waters: Evaluation and field results. Marine Biology **66**:109-120.

Hansell, D., and C. Carlson. 1998. Net community production of dissolved organic carbon. Global Biogeochemical Cycles **12**:443-453.

Hedges, J. 1992. Global biogeochemical cycles: progress and problems. Marine Chemistry **39**:67-93.

Hutchinson, G. E. 1957. Concluding remarks. Pages 414-427 Cold Spring Harbor Symp Quant Biol.

Jannasch, H. W. 1967. Growth of marine bacteria at limiting concentrations of organic carbon in seawater. Limnology and Oceanography:264-271.

Kaiser, K., and R. Benner. 2012. Organic matter transformations in the upper mesopelagic zone of the North Pacific: Chemical composition and linkages to microbial community structure. Journal of Geophysical Research-Oceans **117**.

Kirchman, D., Y. Suzuki, C. Garside, and H. Ducklow. 1991. High turnover rates of dissolved organic carbon during a spring phytoplankton bloom. Nature **352**:612-614.

Langenheder, S., E. Lindstrom, and L. Tranvik. 2006. Structure and function of bacterial communities emerging from different sources under identical conditions. Applied and Environmental Microbiology **72**:212-220.

Legendre, L., and J. Lefevre. 1995. Microbial food webs and the export of biogenic carbon in oceans. Aquatic Microbial Ecology **9**:69-77.

Martinez, J., D. C. Smith, G. F. Steward, and F. Azam. 1996. Variability in ectohydrolytic enzyme activities of pelagic marine bacteria and its significance for substrate processing in the sea. Aquatic Microbial Ecology **10**:223-230.

McCarren, J., J. Becker, D. Repeta, Y. Shi, C. Young, R. Malmstrom, S. Chisholm, and E. DeLong. 2010. Microbial community transcriptomes reveal microbes

and metabolic pathways associated with dissolved organic matter turnover in the sea. Proceedings of the National Academy of Sciences of the United States of America **107**:16420-16427.

Mills, M., C. Moore, R. Langlois, A. Milne, E. Achterberg, K. Nachtigall, K. Lochte, R. Geider, and J. La Roche. 2008. Nitrogen and phosphorus co-limitation of bacterial productivity and growth in the oligotrophic subtropical North Atlantic. Limnology and Oceanography **53**:824-834.

Moeseneder, M. M., C. Winter, and G. J. Herndl. 2001. Horizontal and vertical complexity of attached and free-living bacteria of the eastern Mediterranean Sea, determined by 16S rDNA and 16S rRNA fingerprints. Limnology and Oceanography **46**:95-107.

Mou, X., S. Sun, R. Edwards, R. Hodson, and M. Moran. 2008. Bacterial carbon processing by generalist species in the coastal ocean. Nature **451**:708-711.

Nelson, C., and C. Carlson. 2012. Tracking differential incorporation of dissolved organic carbon types among diverse lineages of Sargasso Sea bacterioplankton. Environmental Microbiology **14**:1500-1516.

Obernosterer, I., N. Kawasaki, and R. Benner. 2003. P-limitation of respiration in the Sargasso Sea and uncoupling of bacteria from P-regeneration in size-fractionation experiments. Aquatic Microbial Ecology **32**:229-237.

Ogura, N. 1972. Rate and extent of decomposition of dissolved organic-matter in surface seawater. Marine Biology **13**:89-93.

Perez, M., C. Pausz, and G. Herndl. 2003. Major shift in bacterioplankton utilization of enantiomeric amino acids between surface waters and the ocean's interior. Limnology and Oceanography **48**:755-763.

Poretsky, R., S. Sun, X. Mou, and M. Moran. 2010. Transporter genes expressed by coastal bacterioplankton in response to dissolved organic carbon. Environmental Microbiology **12**:616-627.

Rivkin, R. B., and M. R. Anderson. 1997. Inorganic nutrient limitation of oceanic bacterioplankton. Limnology and Oceanography **42**:730-740.

Sarmento, H., and J. Gasol. 2012. Use of phytoplankton-derived dissolved organic carbon by different types of bacterioplankton. Environmental Microbiology **14**:2348-2360.

Shi, Y., J. McCarren, and E. DeLong. 2012. Transcriptional responses of surface water marine microbial assemblages to deep-sea water amendment. Environmental Microbiology **14**:191-206.

Sintes, E., K. Stoderegger, V. Parada, and G. J. Herndl. 2010. Seasonal dynamics of dissolved organic matter and microbial activity in the coastal North Sea. Aquatic Microbial Ecology **60**:85-95.

Sondergaard, M., P. J. L. Williams, G. Cauwet, B. Riemann, C. Robinson, S. Terzic, E. M. S. Woodward, and J. Worm. 2000. Net accumulation and flux of dissolved organic carbon and dissolved organic nitrogen in marine plankton communities. Limnology and Oceanography **45**:1097-1111.

Tada, Y., A. Taniguchi, I. Nagao, T. Miki, M. Uematsu, A. Tsuda, and K. Hamasaki. 2011. Differing growth responses of major phylogenetic groups of marine bacteria to natural phytoplankton blooms in the western north pacific ocean. Applied and Environmental Microbiology **77**:4055-4065.

Tada, Y., A. Taniguchi, Y. Sato-Takabe, and K. Hamasaki. 2012. Growth and succession patterns of major phylogenetic groups of marine bacteria during a mesocosm diatom bloom. Journal of Oceanography **68**:509-519.

Teeling, H., B. Fuchs, D. Becher, C. Klockow, A. Gardebrecht, C. Bennke, M. Kassabgy, S. Huang, A. Mann, J. Waldmann, M. Weber, A. Klindworth, A. Otto, J. Lange, J. Bernhardt, C. Reinsch, M. Hecker, J. Peplies, F. Bockelmann, U. Callies, G. Gerdts, A. Wichels, K. Wiltshire, F. Glockner, T. Schweder, and R. Amann. 2012. Substrate-controlled succession of marine bacterioplankton populations induced by a phytoplankton bloom. Science **336**:608-611.

Thingstad, T. F., A. Hagstrom, and F. Rassoulzadegan. 1997. Accumulation of degradable DOC in surface waters: Is it caused by a malfunctioning microbial loop? Limnology and Oceanography **42**:398-404.

Williams, P. J. L. 1995. Evidence for the seasonal accumulation of carbon-rich dissolved organic material, its scale in comparison with changes in particulate material and the consequential effect on net $^{C}/_{N}$ assimilation ratios. Marine Chemistry **51**:17-29.

Williams, P. M., and A. F. Carlucci. 1976. Bacterial utilization of organic matter in the deep sea. Nature **262**:810-811.

Zweifel, U. L., J. Wikner, A. Hagstrom, E. Lundberg, and B. Norrman. 1995. Dynamics of dissolved organic carbon in a coastal ecosystem. Limnology and Oceanography **40**:299-305.

CHAPTER 2

Single bacterial strain capable of significant contribution to carbon cycling in the surface ocean

2.1 ABSTRACT

Marine dissolved organic carbon (DOC) encompasses one of the largest reservoirs of carbon on Earth. Heterotrophic bacteria are the primary biotic force regulating the fate of this material, yet the capacity of individual strains to significantly contribute to carbon cycling is unknown. Here we quantified the ability of a single Alteromonas strain [Alteromonas sp. strain Scripps Institution of Oceanography (AltSIO)] to drawdown ambient DOC in a coastal eco-system. In three experiments, AltSIO alone consumed the entire pool of labile DOC, defined here as the quantity consumed by the submicron size fraction of ambient microbial assemblages within 5 d. These findings demonstrate that complete removal of the labile DOC pool in coastal surface seawater can be achieved by a single taxon. During long-term incubations (>1 y) testing semilabile DOC consumption, AltSIO entered dormancy but remained viable, while the diverse assemblages continued to consume carbon. Given that AltSIO is a large bacterium and thus subject to increased grazing pressure, we sought to determine the ecological relevance of this phenotype. Growth dynamics in natural seawater revealed that AltSIO rapidly outgrew the native bacteria, and despite intense grazing pressure, was never eliminated from the population. A survey in the California Current Ecosystem revealed that large bacteria (≥40 fg $C \cdot cell^{-1}$) were persistent, accounting for up to 12% of total bacterial abundance and 24% of total bacterial biomass. We conclude that large, rapidly growing bacteria have the potential to disproportionately alter the fate of carbon in the mesotrophic ocean and play an important role in ecosystem function.

2.2 SIGNIFICANCE

Primary production generates a reservoir of dissolved organic carbon (DOC) in the ocean as large as the global inventory of atmospheric CO2. Once formed, DOC accumulates on timescales from less than 1 hour to millennia. Bacteria are important contributors to the respiration of DOC to CO2 and the conversion of DOC to refractory biopolymers. Yet, the quantitative contribution of individual species within diverse consortia to DOC cycling remains unknown. We report that a single bacterial strain can consume as much DOC as diverse free-living microbial communities. This taxon is commonly observed in seawater when labile carbon is available, and may serve a key ecosystem function by rapidly recycling and regulating the level of DOC while also supporting ocean food webs.

2.3 INTRODUCTION

Turnover of surface ocean dissolved organic carbon (DOC) by the microbial loop (Azam et al. 1983) represents the largest flux of C through the ocean reservoir (Hansell 2013). The rate and magnitude of this turnover is influenced in part by microbial community structure (Pinhassi et al. 1999, Carlson et al. 2004, Arnosti et al. 2005). For example, seasonally accumulated DOC has been shown to resist consumption by depth-stratified surface microbial communities, but is then readily metabolized by phylogenetically distinct mesopelagic populations following annual convective overturn (Carlson et al. 2004). This supports the hypothesis that distinct microbial communities harbor unique metabolic potential adapted to local resource

composition (Perez et al. 2003). It has been hypothesized from experimental metagenomics (Mou et al. 2008) and transcriptomics (McCarren et al. 2010) that bacterial diversity may enhance the compositional breadth of DOC remineralization as it provides a broader repertoire of enzymes (Martinez et al. 1996, Pinhassi et al. 1999, Arnosti et al. 2005) and transporters (Poretsky et al. 2010) required for bacterial hydrolysis and uptake of complex macromolecules of varying biochemical reactivity (Benner 2002).

The notion that DOC degradation may scale with microbial diversity is in general agreement with fundamental biodiversity theory of resource niche partitioning among competing species (Hutchinson 1957). However, the hypothesis that diversity is required for the degradation of labile DOC has not been explicitly tested. Alternatively, extensive experimental observations suggest that a narrow subset of taxa may disproportionally contribute to the degradation of DOC in the surface ocean. Results from microcosm studies, both nutrient-amended (Eilers et al. 2000b, Mills et al. 2008, Nelson and Carlson 2012) and unamended 'controls' (Eilers et al. 2000a, Schafer et al. 2000, Beardsley et al. 2003, Carlson et al. 2004, Gomez-Consarnau et al. 2012, Nelson et al. 2013), have shown that few taxa, predominantly *Alteromonadales,* rapidly dominate microbial communities. Metagenomic (Mou et al. 2008) and transcriptomic (McCarren et al. 2010, Shi et al. 2012) analyses of DOC-amended microcosms have also shown that *Alteromonadales* accounted for the majority of observed increases in cell abundance and transcriptional activity. Similar results have been observed in experiments tracking species-specific uptake of stable- or

radioisotope-labeled phytoplankton exudates (Nelson and Carlson 2012, Sarmento and Gasol 2012). While the manipulation of predator abundance in microcosm studies has been shown to select for some phylotypes (Eilers et al. 2000a, Beardsley et al. 2003), in situ field observations have corroborated a high proportional abundance of *Alteromonas* spp. in the natural environment (Acinas et al. 1999, Teeling et al. 2012). Furthermore, Tada et al. (Tada et al. 2011) reported that *Alteromonas* spp. accounted for up to 30% of the actively growing bacterial population during a phytoplankton bloom in the western North Pacific.

These findings suggest that single physiotypes, such as *Alteromonas,* may serve as a central conduit for a significant flux of DOC and nutrient mineralization in the upper ocean. In this study, we sought to address the most fundamental component required to elicit such observations by quantifying the maximum potential contribution of a single bacterial isolate to DOC degradation, particularly in the absence of other cells that may inhibit or facilitate the growth performance of the individual strain. We tested this by quantifying *Alteromonas*-specific DOC consumption in pure culture and in co-culture relative to conventionally assessed DOC drawdown of free-living bacterial seawater communities (Carlson and Ducklow 1996, Cherrier et al. 1996). Thus, our null hypothesis stated that the physiological capacity encoded within a single bacterial genome is not metabolically sufficient to consume ambient DOC to a measurable degree. We interpret our results from three separate DOC drawdown experiments with the single isolate alongside additional competition and grazing studies in size-fractionated natural seawater, and in the context of field measurements

of bacterial size frequency distribution and TOC concentrations in the California Current Ecosystem (CCE).

2.4 METHODS

2.4.1 Sampling, experimental setup, and Alteromonas sp. AltSIO isolation

AltSIO (GenBank accession no. KC758958 as "ALT199") was isolated by plating whole seawater collected from the Ellen Browning Scripps Memorial Pier (hereafter "Scripps Pier"), Scripps Institution of Oceanography, La Jolla, California USA, (32° 52.02' N, 117° 15.43' W) onto Noble agar (15 g L^{-1} GF/F filtered seawater). AltSIO shares ~99% 16S rDNA sequence homology with *Alteromonas macleodii*, a globally cosmopolitan gammaproteobacteria described as an opportunistic copiotroph (Lopez-Perez et al. 2012) with wide strain-specific niche specialization (Ivars-Martinez et al. 2008).

2.4.2 DOC drawdown experiments

Drawdown experiments were conducted with 0.1 μm filtered Scripps Pier seawater collected at ~1 m depth. Filtration used polyethersulfone (PES) membranes (PALL, Supor-100, Ann Arbor, MI) previously flushed with 2L Milli-Q water then 0.5 L seawater to remove leachable carbon (*SI Methods*). TOC concentration was measured in three treatments: 1) seawater culture (SWC) (10% GF/F filtered seawater (FSW); 90% 0.1 μm FSW); 2) AltSIO in pure culture; and 3) SWC inoculated with AltSIO. Filter-sterilized seawater served as a control to test abiotic effects on TOC

concentration. All experiments were conducted in the dark at ambient temperature (14 - 16 ± 1^{o} C).

Microbial abundance. Bacteria and protists were enumerated by epifluorescence microscopy using the nucleic acid stain 4', 6-diamidino-2-phenylindole (DAPI) (Porter and Feig 1980). An *Alteromonas* sp. AltSIO strain-specific rDNA fluorescence in situ hybridization (FISH) probe was designed, tested, and optimized as described (Fuchs et al. 2007). Absolute concentration of AltSIO in co-cultures was determined by multiplying the relative proportion of probe-positive cells within FISH processed samples by total bacterial abundance determined from non-FISH processed filters as described (Fuchs et al. 2007).

2.4.3 Direct measure of cell carbon and nitrogen by CHN analysis

Jan. 2012 samples (~2L) were gravity filtered onto pre-combusted 25 mm GF/F filters, acidified in a desiccator to remove inorganic carbonates, then dried at 50^{o} C. CHN was measured by high temperature combustion using an Organic Elemental Analyzer (*SI Methods*). Bacterial biomass C in SWC and AltSIO treatments was determined from direct measurement of treatment-specific cell C (Table S2) multiplied by respective cell abundance. Bacterial biomass C of the combined SWC+AltSIO treatment was calculated from the proportional abundance and cell-specific C content of AltSIO and SWC at each time point as determined by FISH. Because all samples were inoculated into 0.1-μm FSW, non-bacterial particulate organic C was negligible.

2.4.4 TOC and DOC

Incubation carboys were sampled in a laminar flow hood using aseptic technique. TOC concentrations were measured by high temperature combustion using a Shimadzu 500 V-CSN/TNM-1 TOC analyzer as described (Samo et al. 2012), and calculated from the average of 5 sample injections (100 μL) per 2-3 replicate vials. Samples from each experiment were analyzed in a single run to limit instrument variability, and interspersed with low DOC deep seawater reference material (Hansell 2005) (*SI Methods*). Following standard convention (Carlson and Ducklow 1996, Carlson et al. 2004, Nelson et al. 2013), DOC concentration from incubation experiments was calculated by subtracting bacterial biomass C (Table S4) from TOC measurements of unfiltered samples to avoid contamination from sample handling. Assuming a single C conversion factor for all bacteria (e.g. 20 fg C $cell^{-1}$) proved erroneous owing to the significantly greater C content of AltSIO. Thus, direct measurement of cell C proved critical to accurately measure treatment-specific DOC consumption. TOC included bacterial C and therefore measured decreases were directly attributed to bacterial respiration of C. Likewise, DOC consumption reported here is the cumulative of C respired and C incorporated into biomass, and thus reflects total bacterial C demand (del Giorgio and Cole 1998).

2.4.5 Frequency distribution of bacterial cell volume in the California Current Ecosystem

Frequency distribution of bacterial cell volume in the Southern California Bight. Samples (n = 29) were collected from 6 depths (0 - 100 m) from 5 CTD rosette hydrocasts across a 29-km transect in the California Current (Samo et al. 2012). Length and width of 17,388 bacterial cells was measured by DAPI fluorescence and used to calculate biovolume (Bratbak 1985), and cell-specific carbon content (Simon and Azam 1989) as described (Samo et al. 2012). Autofluorescent cyanobacteria were manually eliminated from all measurements. Biovolume of AltSIO cells (n = 79) was measured by atomic force microscopy (AFM) as described for dry AFM samples (Malfatti et al. 2010).

2.4.6 Alteromonas sp. AltSIO survival in size-fractionated seawater

Whole seawater was collected from the Scripps Pier, passed through 50 μm Nytex nylon mesh, 0.7 μm GF/F filters, and 0.2 μm nuclepore polycarbonate filters, respectively. AltSIO was added to each size fraction at ~10^4 cells mL^{-1} and incubated at 15^o C on a 12 h light:dark cycle at a light level of 100 μE m^{-2} s^{-1}, and sampled daily for microbial abundance.

2.4.7 Statistical analysis

Statistical analyses were preformed using GraphPad Prism® for Mac OS X version 6.0C (GraphPad Software, Inc., La Jolla, CA). Significant differences between treatments were tested for in May and Nov. 2011 data by conducting analysis of variance (one-way ANOVA) and Tukey's post-hoc multiple comparison tests at the

95% confidence interval ($\alpha = 0.05$) on delta TOC between d 0-5. Insufficient biological replication precluded statistical analysis on short-term (5 d) Jan 2012 data. Long-term (379 d) DOC drawdown data from Jan 2012 was analyzed by repeated measures two-way ANOVA and Sidak's multiple comparison test ($\alpha = 0.05$) comparing the change in TOC concentration between AltSIO and AltSIO+SWC treatments individually against the SWC treatment over time.

2.5 RESULTS

2.5.1 Experimental quality control

Whole seawater, and filtrate used as ambient DOM growth media showed a reduction in TOC concentration after each filtration step (0.7 μm nominal GF/F, 0.1 μm PES) ensuring contamination-free methodology (Table S1). Concurrent replicated (3x) bacteria-free control incubations showed no growth of bacteria and no change in TOC concentration after 5 d, confirming sterility of controls and the absence of abiotic reductions in DOC (Table S1). In situ seawater conditions including TOC and nutrient concentrations at the time of seawater collection are reported in Table S2.

2.5.2 Cell retention on GF/Fs and CHN-derived cell carbon and nitrogen

Cell C was directly measured in Jan. 2012. Cell retention was calculated as the difference in cell abundance between whole and GF/F filtered water and measured 69%, 99%, and 66% for the free-living bacteria seawater community (SWC), AltSIO, and SWC+AltSIO treatments, respectively, after 3 d. After 5 d, cell retention increased

to 79%, 99.5%, and 76% for SWC, AltSIO, and SWC+AltSIO, respectively (Table S3). The SWC averaged 19 fg C $cell^{-1}$, whereas AltSIO averaged 75 fg C $cell^{-1}$ on d 3, and decreased slightly to 17.5 and 63.0 fg C $cell^{-1}$, respectively on d 5 (Table S3). AltSIO contained 4.4-fold greater cell-specific N than the average seawater community bacterial cell. C and N values for the SWC are within the range of those reported for coastal bacteria (Lee and Fuhrman 1987, Fukuda et al. 1998).

2.5.3 Bacterial abundance

Bacterial abundance increased in all treatments in each DOC drawdown experiment (Fig. 1*A, B, C;* Table S4). In all experiments, the free-living seawater community (SWC) reached the highest cell abundance, followed by SWC inoculated with AltSIO (SWC+AltSIO). The AltSIO-only treatment consistently showed the lowest maximum cell abundance of ~10^8 cells L^{-1}, ~10x less than the SWC (Fig. 1*A, B, C;* Table S4). All treatments yielded greater cell abundance in Jan. relative to May and Nov. It is possible, but unknown, whether greater incubation volume (20 L vs. 200 mL; see *SI Text*) contributed to this observation. There was no significant difference at any time point between abundance of AltSIO grown in isolation and that grown in co-culture (Table S4, ANOVA, Tukeys's $P > 0.05$). AltSIO was inoculated into each co-culture at ~1% of the total starting bacterial abundance and reached a final proportional abundance of 17, 26, and 30% of the total bacterial assemblage (total DAPI-stained cells) in May 2011, Nov. 2011, and Jan. 2012, respectively as determined by fluorescence in situ hybridization (FISH).

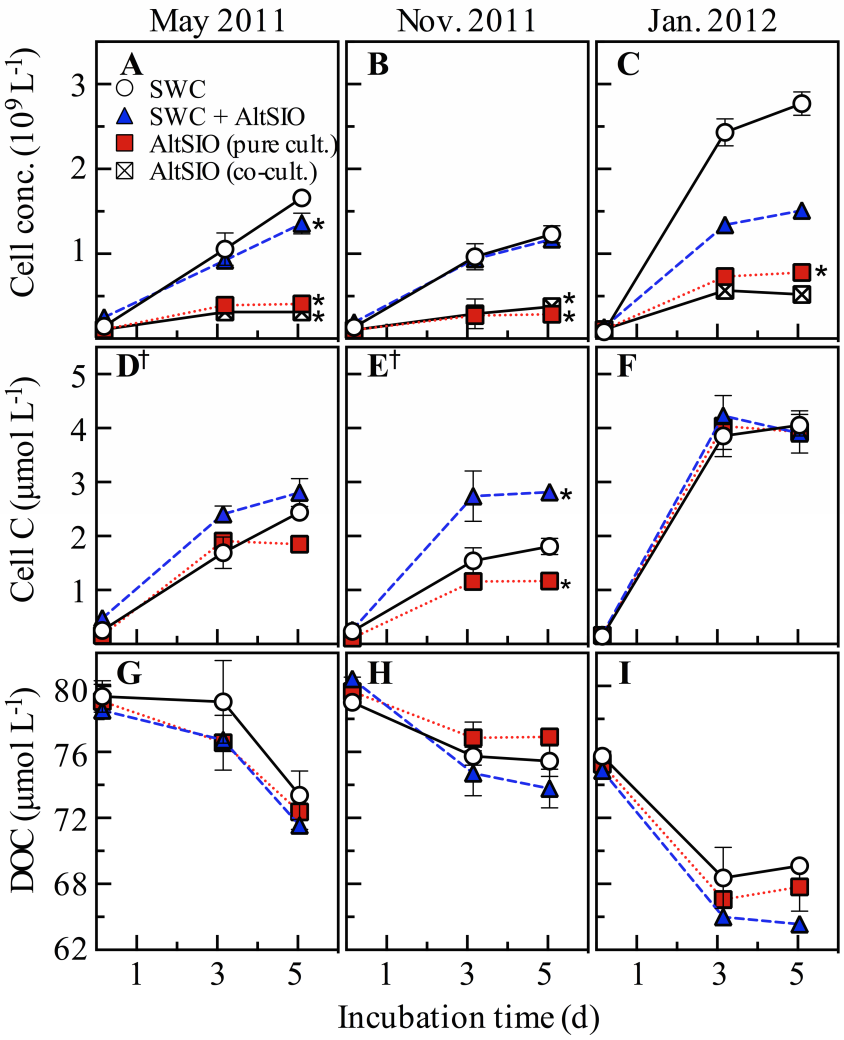

Figure 1. Bacterial growth, cell C, and DOC consumption of three treatments grown in 0.1 µm filtered coastal North Pacific seawater (A–I). Treatment abbreviations are as follows: AltSIO (cocult.) represents FISH-derived abun-dance of AltSIO in coculture, AltSIO (pure cult.) represents Alteromonas sp. strain AltSIO pure culture, SWC represents seawater community comprised of 10% GF/F-filtered seawater, and SWC + AltSIO represents coculture of treatments above. All data are mean ± SD of two to three biological repli-cates. SWC + AltSIO January 2012 was plotted from a single incubation. In D and E, † represents cell C calculated from direct CHN measurements of each treatment from the January 2012 experiment (Table S4). DOC calculated by subtraction of cell C from TOC. *Significantly different from SWC by ANOVA, Tukey's $P < 0.05$.

2.5.4 Bacterial biomass

Mean treatment differences in C biomass within each experiment were low relative to treatment-specific differences across experiments (Table S4). The average of all treatments within each experimental date showed the highest C biomass in January 2012 relative to May 2011 and November 2011 (3.87, 2.32, and 1.88 μmol C·L−1, respectively; Fig. 1 and Table S4). The SWC + AltSIO treatment yielded significantly greater bacterial C biomass relative to other treatments in November (Fig. 1 and Table S4) (ANOVA, Tukey's $P < 0.05$). No significant difference was measured in total bacterial C biomass between the SWC and AltSIO-only treatments in May 2011 (Fig. 1 D–F and Table S4).

2.5.5 DOC utilization

One of 3 SWC treatment replicates became contaminated in May 2011 as measured by elevated TOC concentration and was eliminated from all calculations. All other treatments and replicates resulted in a reduction of TOC concentration after 5 d (Fig. 1, Table S4). Among all experiments, no significant difference (ANOVA, $P > 0.05$) was measured between treatment-specific means of absolute change in TOC, or biomass-corrected DOC concentration after 5 d (Table S4). While the SWC+AltSIO treatment consistently resulted in the greatest proportion and rate of DOC drawdown across all experiments (Fig. 1 and Fig. 2), significant differences were only detected in Nov. 2011 (Table S5). No significant differences were measured in the proportion or rate of DOC drawdown between AltSIO and SWC treatments (Table S5).

2.5.6 Long-term laboratory incubation and TOC drawdown rates of coastal seawater

Incubation and measurement of TOC from the Jan. 2012 experiment was continued for >1 year. No decrease in TOC concentration was detected in the AltSIO-only treatment beyond 3 d (Fig. 3). In contrast, the TOC concentration of the SWC treatment decreased from 70.2 μM to 57.8 μM between 3-379 d and the SWC+AltSIO treatment decreased from 68.1 to 59.6 μM C (Fig. 3). The two seawater culture incubations, with and without AltSIO, were combined and averaged by time point to determine a mean long-term (>30 d) drawdown rate of 6.5 μmol L^{-1} yr^{-1}. Cell abundance (cells mL^{-1} ± s.e.) after 379 d of incubation in the SWC, AltSIO-only, and SWC+AltSIO treatments measured 4.2 x 10^5 ± 1.1 x 10^5, 3.9 x 10^5 ± 1.5 x 10^5, and 8.6 x 10^5 ± 5.3 x 10^4, respectively. All treatments and replicates contained viable cells that produced colony-forming units on both 2216 ZoBell agar and Noble agar plates without nutrient amendment.

2.5.7 Alteromonas sp. AltSIO survival in size-fractionated seawater

AltSIO was grown in size-fractionated natural seawater collected from the Scripps Pier to determine growth and survival when faced with bottom-up and top-down control. The < 0.2 μm size fraction was intended to serve as a bacterial-free control to gauge the growth of AltSIO unchallenged by competition or grazing mortality, but was found to contain 1.5 x 10^5 cells mL^{-1} after filtration of natural seawater. Thus, this treatment instead served to test the ability of AltSIO to compete with the smallest filterable size class of bacteria (Haller et al. 2000). AltSIO

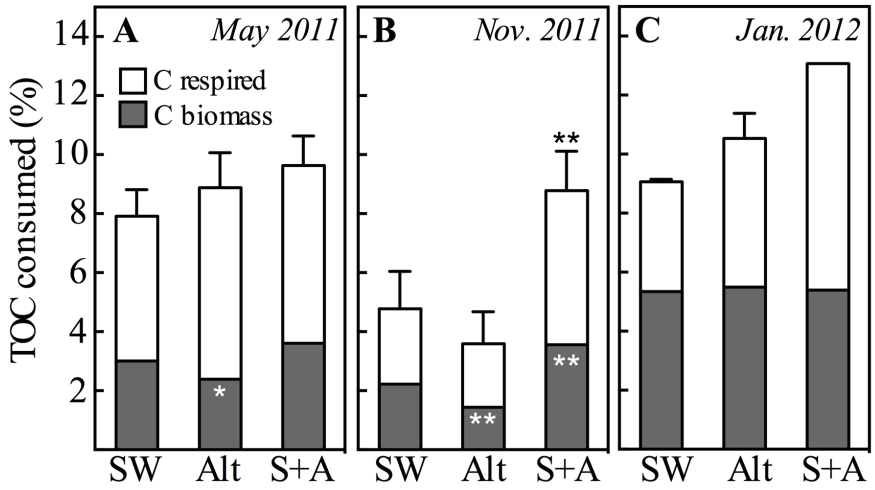

Figure 2. Bacterial partitioning of coastal surface ocean DOC during three incubation experiments (A–C). Stacked bar graph of bacterial biomass (lower bar), C respired (upper bar), and total C consumed (sum of both bars) dis-played as a percentage of initial TOC concentration. Alt, Alteromonas sp. AltSIO pure culture; SW, seawater community; S + A, coculture of SWC and AltSIO. All values are mean ± SD of two to three biological replicates. January 2012 S + Ais a single incubation. Significant differences relative to SWC (ANOVA, Tukey's) were detected in bacterial biomass in May and November, but no differ-ences were detected in the proportion of C respired between treatments in any experiment. The S + A treatment in November 2011 was the only to show a significant difference in total C consumed. *$P < 0.05$; **$P < 0.01$.

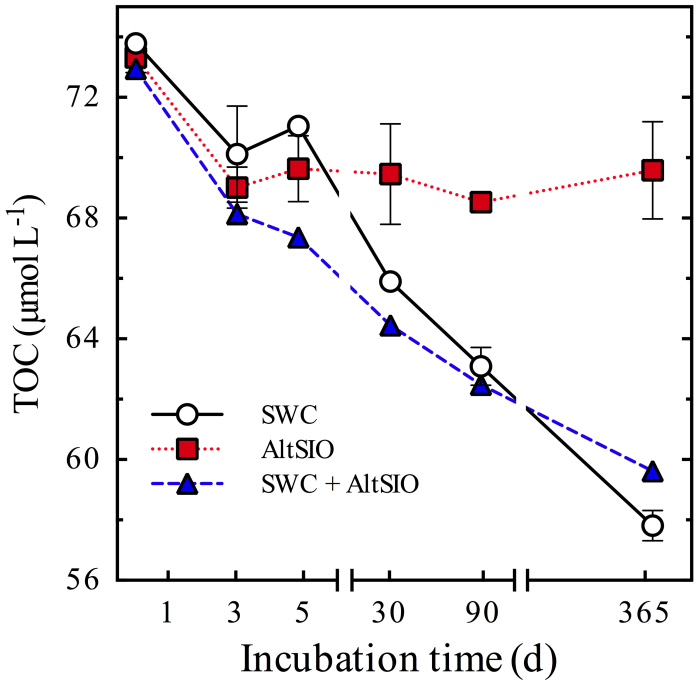

Figure 3. Long-term carbon drawdown of January 2012 incubation. Data are mean ± SD of two biological replicates. SWC + AltSIO is a single incubation. TOC concentrations of AltSIO are significantly different from SWC and SWC + AltSIO on and after time points 31 and 89, respectively [repeated-measures two-way ANOVA, Sidak's multiple comparison post hoc test $P < 0.05$ (Table S7)]. Except on day 5, no significant difference was detected between SWC and SWC + AltSIO treatments.

abundance increased from 10^4 to 10^5 cells mL^{-1} within 24 h in both treatments without grazers (< 0.2 and < 0.7 μm size fractions) (Fig. 4*A*, *B, D, E*). After 24 h, the proportion of AltSIO to total bacterial cell abundance increased from 8 to 68% in the < 0.2 μm size fraction, and from 0.4 to 3.0 % in the < 0.7 μm size fraction (Fig. 4*A, B,* respectively). Within the same time period, AltSIO abundance decreased nearly 10-fold in the treatment with grazers, while protist abundance increased (Fig. 4*C*). AltSIO abundance then increased 25-fold following a decrease in protist abundance (Fig. 4*C*). By the end of the experiment AltSIO comprised 19%, 1%, and 0.05% of the total bacterial abundance in the < 0.2, < 0.7, and < 50 μm treatments, respectively (Fig. 4).

2.5.8 Biovolume of AltSIO and cell size distribution frequency in the California Current Ecosystem

AltSIO measured 0.72 μm^3 and 72 fg C $cell^{-1}$. The average of 17,388 individual cells from 29 samples from the California Current Ecosystem measured 0.13 μm^3 and 21 fg C $cell^{-1}$, respectively, and ranged in volume from 0.02 - 1.79 μm^3, and C content from 6.6 - 107.6 fg C $cell^{-1}$. Averaged within samples, mean values between samples ranged 0.08 - 0.18 μm^3 and 16.2 - 26.0 fg C $cell^{-1}$. The distribution frequency of cell biovolume of each sample was binned into 0.2 μm^3 increments (Fig. S1*A*). Across all samples, the smallest size class (0 - 0.2 μm^3) accounted for 69 - 95% of total bacterial abundance (Fig. S1*A*). Large cells, defined here as ≥ 0.3355 μm^3 or ≥ 40 fg C $cell^{-1}$, comprised up to 12% of the total bacterial abundance and up to 24% of the total bacterial carbon biomass (Fig. S1*B*). In all 29 samples from the CCE, large

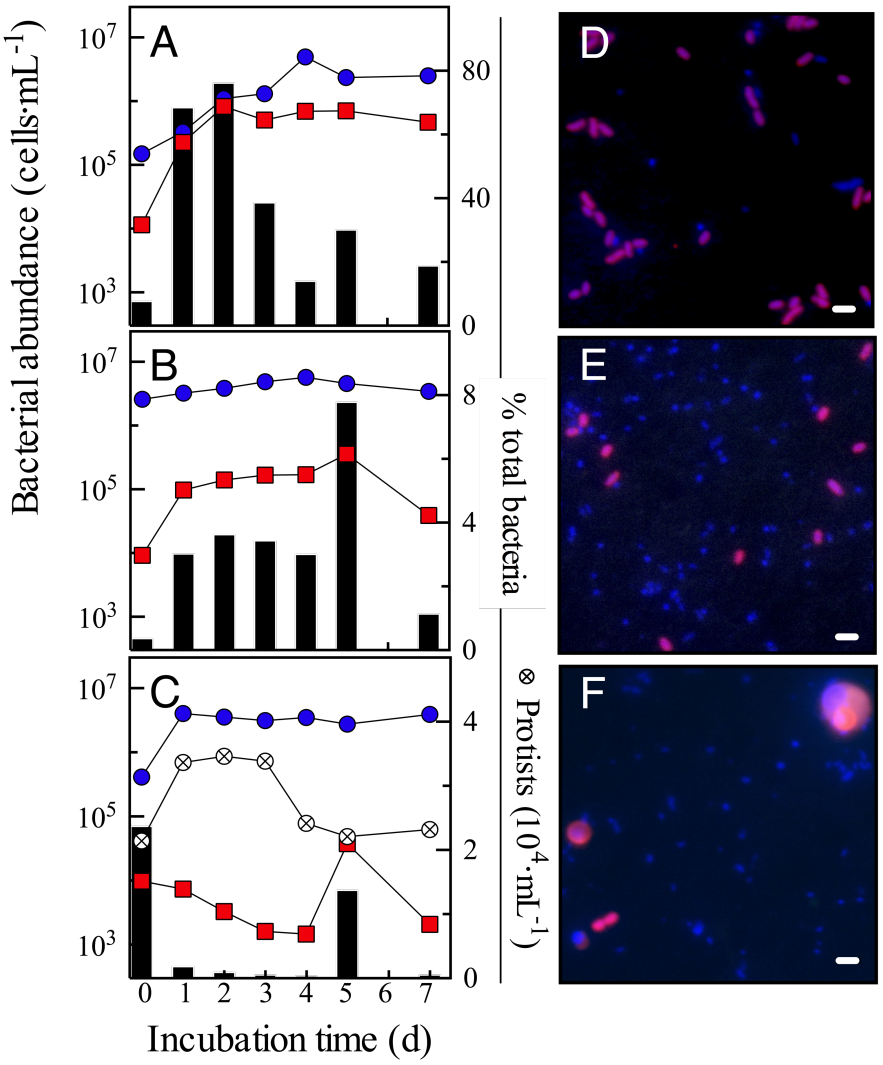

Figure 4. Growth dynamics of Alteromonas sp. strain AltSIO cocultured with native microbial assemblages in size-fractionated coastal seawater: (A and D) <0.2 μm FSW, (B and E) <0.8 μm FSW, and (C and F) <50 μm FSW. (A– C) Abundances of AltSIO (red squares) and total bacteria (blue circles) are shown on the left y axis. Black bars are the proportion of AltSIO to total bacterial abundance (right y axis). Crosshatched circles (in C) show protist abundance (right y axis). D–F are representative images from day 3. Each image is a composite of three epifluorescence micrographs (1,000× magnification) with exposure/emission for Cyanine 3 (Cy3; FISH probe), DAPI (DNA), and FITC (autofluorescent photopigments). AltSIO-specific FISH probe-labeled cells appear red/cyan. A protist is imaged in the upper right corner of F. (Scale bar: 2 μm.)

cells comprised ≥ 1% of the total bacterial community abundance (Fig. S1*B*). We note the strong agreement between microscopy-derived estimates of bacterial carbon and those derived from direct CHN measurements for both AltSIO and the mixed bacterial assemblages.

2.6 DISCUSSION

2.6.1 A single species is capable of complete drawdown of the labile DOC pool

We hypothesized that owing to the sheer chemical complexity of DOM, heterotrophic bacterial consumption of DOC may be dependent upon the iterative processing by multiple species bearing complimentary metabolic capacities. Specifically, we tested the hypothesis that a single bacterial strain, alone, cannot consume a measureable degree of ambient DOC during non-bloom (phytoplankton), non-amended conditions. Here, we explicitly define 'labile' and 'semi-labile' DOC fractions in our microcosms as those that are degraded by the free-living bacterial community (SWC treatment) in the short term (0-5 d), and long-term (> 30 d), respectively. This operational nomenclature is in accordance with the universal definitions proposed by Hansell (2013) based upon apparent decay rates of major bulk DOC fractions.

Our findings demonstrate, unequivocally, that a single bacterial strain does in fact have the capacity to consume the labile DOC pool without the assistance of other members of the microbial community. This finding is derived from the repeated observations that a single strain consumed an equivalent magnitude of ambient DOC

as three separate free-living microbial assemblages sampled over three seasons (Fig. 1). We note that these data cannot determine whether a single taxon necessarily remineralized the same chemical components of the DOM pool as complex microbial communities. In each experiment, the microbial and chemical community species composition was justifiably presumed different, yet the response of each treatment was consistent and robust. These data provide conclusive evidence that key individual taxa have the potential to exhaust the extant labile DOC pool in coastal surface seawater. This demonstrates that the fundamental biogeochemical process of labile DOC turnover does not require a complex community. This finding contributes to the ongoing discussion of functional redundancy within microbial ecosystems (Pedros-Alio 2006, Allison and Martiny 2008, Comte and del Giorgio 2011), and has important implications for our understanding of the relationship between bacterial community composition and the ocean's role in global carbon cycling.

2.6.2 Semilabile DOC decay may require bacterial community diversity

During long-term incubation (>1 yr) of coastal seawater, AltSIO unexpectedly ceased to consume DOC beyond 3 days (Fig. 3). This lack of measurable C consumption, despite maintenance of a relatively high abundance of viable cells, suggests that AltSIO entered a state of prolonged physiological dormancy (del Giorgio and Gasol 2008). Our data do not support the hypothesis that growth became limited by N or P availability as dissolved nutrients were in excess of its cellular requirement (*SI Text, Table S2 and S3*). This leaves open the possibility of an undetermined

micronutrient requirement, or bioavailable-carbon limitation. In support of the latter, some gammaproteobacteria with similar physiological traits have been found to exhibit varying concentration threshold dependencies for metabolic activation following reintroduction to substrates after prolonged C-starvation (Eilers et al.). With respect to DOC quality, Cherrier and Bauer (Cherrier and Bauer) concluded from short-term incubations that the growth of bacterial populations in the eastern North Pacific became limited by the availability of readily catabolized sources of energy. Whether AltSIO growth became limited by bulk carbon concentration or quality is not known. In either case, that AltSIO remained culturable points to its ability to emerge from dormancy following increased nutrient supply, and supports the notion that similar "feast and famine" strategists (Koch 1971, Eilers et al. 2000a) may persist in the environment by virtue of such physiological capacity (Morita 1982, Lennon and Jones 2011). Lastly, the functional inability of AltSIO to consume DOC after 3 days, while parallel incubations of mixed microbial assemblages continued to consume DOC for > 1 year (Fig. 3) suggests that substantial semi-labile DOC decay may require broader community diversity. While AltSIO appears incapable of consuming operationally defined semi-labile DOC on its own, it is unknown whether other isolates, e.g. from the mesopelagic, possess such capacity.

2.6.3 DOC concentration thresholds and apparent decay in the CCE

A minimum average concentration of ~ 54 μmol C kg^{-1} was associated with upwelling waters in the near shore region of the CCE (< 210 km from shore) (Table

S8). We interpret this data as representing the region-specific maximum DOC drawdown potential of resident microbial communities in the surface ocean (0-200 m), i.e. 54 μM C operationally demarks the transition between the semi-labile and semi-refractory DOC fraction as defined by Hansell (2013). Within this context, given that the seawater culture microcosms consumed carbon to 58 μM after 1 year (Fig. 3), we conclude that the field equivalent of operationally defined semi-labile DOC pool was nearly exhausted. Others have shown that depth stratified bacterial communities have specific limitations for DOC drawdown capability (Carlson et al. 2004). If the same constraints hold true here, it would suggest that the microcosms populated by consortia originally collected from coastal surface waters may not have the capacity to consume DOC below ~54 μM. This prediction assumes that the physiological limitation of the community is sculpted by the chemical composition and concentration of the local nutrient supply.

2.6.4 Large bacteria are important players in the ocean carbon cycle

Alteromonas sp. strain AltSIO is a model organism that represents an ecologically adaptive strategy for survival in the ocean: It is a large, fast growing bacterium capable of rapidly responding to increased substrate supply, reduced competition, or reduced grazing pressure. In general, large cells are characterized by high nucleic acid content (Gasol et al. 1999), high frequency of division (Hagström et al. 1979), and exhibit high apparent growth and carbon production rates (Gasol et al. 1995, Bernard et al. 2000).

The nearly 4-fold greater C content of AltSIO (Table S3) led to a C demand equal to the free-living bacterial community (Table S5). Competition for resources did not have a measurable impact on the growth of AltSIO, as it rapidly outgrew the free-living bacterial seawater community and the smallest sized bacteria in both carbon drawdown and grazing/competition microcosm experiments (Fig. 4*A*, *D*), despite the theoretical competitive advantage of smaller bacteria to acquire dissolved nutrients (Jumars et al. 1993). When added to size-fractionated natural seawater communities (Fig. 4), AltSIO retained its large size, yet was never eliminated from the population and exhibited an increase in abundance following a decrease in protist abundance (Figure 4*C*). This suggests that preferential feeding of protists upon a single morphotype may be prey density threshold dependent, as has been observed in some freshwater heterotrophic nanoflagellages when feeding exclusively upon large bacteria (Pfandl and Boenigk 2006). However, even preferred prey populations have been shown to survive and persist during sustained grazing, albeit at low levels, during tight coupling between predator and prey populations (Bohannan and Lenski 1999). Thus, despite elevated grazing pressures, large bacteria such as AltSIO with similar survival strategies theoretically remain among those best poised to consume ephemeral substrate pulses following temporary release from top-down control. During periods of high predation they serve a critical ecosystem function as a substantial nutrient link via protozoa to higher trophic levels (Sherr and Sherr 2002).

In the CCE, we found that large cells ($\geq$ 40 fg C cell^{-1}) comprised 1-12% of the total bacterial abundance, but accounted for as much as 24% of the total bacterial

carbon (Fig. S1). Furthermore, large cells never decreased below 1% of total bacterial abundance (Fig. S1*B*). Field and mesocosm data presented here, suggest that large pelagic bacteria may at times achieve a refuge in rarity, thereby persisting in the environment by function of decreased predator encounter rate as has been predicted for the rare biosphere (Pedros-Alio 2006). The range in the proportional frequency of large bacteria in the CCE also highlights the fact that bacterivorous grazer populations are themselves highly variable and tightly regulated by top-down control (Fenchel 1987, Taylor et al. 2012). Given the inherent fluctuations in microbial predator-prey populations, the competitive advantage for the consumption of labile substrates remains with those whose physiology enables the most rapid response following decoupling from top-down control. The genomic basis enabling such physioptypes to rapidly mobilize from numerical obscurity to dominance has been described (Lauro et al. 2009, Yooseph et al. 2010). Furthermore, several recent studies have shown that typically rare members of the microbial assemblage are often highly active, suggesting a decoupling between abundance and specific activity in the environment and highlighting the importance of "rare" species in geochemical cycling and ecosystem function (Campbell et al. 2011, Hugoni et al. 2013, Hunt et al. 2013).

2.7 CONCLUSION

The labile DOC pool encompasses the single greatest flux of C, up to ~25 Pg C $year^{-1}$, through the DOM reservoir in the global ocean (Hansell). The majority of this reduced carbon is processed through the microbial loop in the upper ocean. While the

role of microbial community structure in carbon cycling has been of interest for decades, the quantitative contribution of individual bacterial strains remains almost entirely unknown. We have provided quantitative evidence that a single bacterial strain, or 'physiotype', can consume as much DOC as the diverse sub-micron size-fraction of the ambient microbial assemblage within 5 d. Longer incubations showed that microbial diversity, while not required for labile DOM consumption, may instead be central to the recycling of semi-labile DOM. These data imply that biotic degradation of more recalcitrant fractions of the DOM pool may scale with bacterial diversity and associated metabolic potential, but remains open for further investigation. Microcosm experiments and field data of bacterial size frequency in the CCE both showed that while large bacteria are preferentially grazed, they persist and contribute a significant proportion of total bacterial carbon in the environment. Together, these findings suggest that rarely dominant bacteria, otherwise intensely grazed or in a temporary survival state may be responsible for a disproportionately large fraction of DOM recycling. Their outsized potential to influence the fate of carbon in the surface ocean suggests that rapidly growing large bacteria play an important role in ecosystem function and should be considered in global models of ocean carbon cycling (Allison and Martiny 2008).

2.8 ACKNOWLEDGMENTS

We thank M. Porrachia, B. Stephens, G.I. Ball, C. Carlson, and F. Malfatti for analytical support and technical advice, and T. Samo for providing raw bacterial size

data from the CCE. We are grateful to K. Barott, T. Samo, and three anonymous reviewers for substantially improving this manuscript. This work was supported by the National Science Foundation (NSF) Graduate Research Fellowship Program to B.E.P., grants NSF OCE0962721 and the Gordon and Betty Moore Foundation Marine Microbial Initiative to F.A., and NSF CAREER OCE-05-28475 to L.I.A. Field sampling was supported by NSF OCE 04–17616 and 10-26607 for the CCE-LTER Program, and made possible by the captain and crew of the R/V *Melville.*

Chapter 2, in full, is a reprint of the material as it appears in Proceedings of the National Academy of Sciences 2014. Pedler, B. E., Aluwihare, L. I., Azam, F., 2014. The dissertation author was the primary investigator and author of this paper.

2.9 REFRENCES

Acinas, S., J. Anton, and F. Rodriguez-Valera. 1999. Diversity of free-living and attached bacteria in offshore western Mediterranean waters as depicted by analysis of genes encoding 16S rRNA. Applied and Environmental Microbiology **65**:514-522.

Allison, S., and J. Martiny. 2008. Resistance, resilience, and redundancy in microbial communities. Proceedings of the National Academy of Sciences of the United States of America **105**:11512-11519.

Arnosti, C., S. Durkin, and W. H. Jeffrey. 2005. Patterns of extracellular enzyme activities among pelagic marine microbial communities: implications for cycling of dissolved organic carbon. Aquatic Microbial Ecology **38**:135-145.

Azam, F., T. Fenchel, J. Field, J. Gray, L. Meyerreil, and F. Thingstad. 1983. The ecological role of water-column microbes in the sea. Marine Ecology-Progress Series **10**:257-263.

Beardsley, C., J. Pernthaler, W. Wosniok, and R. Amann. 2003. Are readily culturable bacteria in coastal North Sea waters suppressed by selective grazing mortality? Applied and Environmental Microbiology **69**:2624-2630.

Benner, R. 2002. Chemical composition and reactivity. Pages 59-90 *in* D. A. Hansell and C. A. Carlson, editors. Biogeochemistry of Marine Dissolved Organic Matter. Elsevier Science, USA.

Bernard, L., C. Courties, P. Servais, M. Troussellier, M. Petit, and P. Lebaron. 2000. Relationships among bacterial cell size, productivity, and genetic diversity in aquatic environments using cell sorting and flow cytometry. Microbial Ecology **40**:148-158.

Bohannan, B. J. M., and R. E. Lenski. 1999. Effect of prey heterogeneity on the response of a model food chain to resource enrichment. American Naturalist **153**:73-82.

Bratbak, G. 1985. Bacterial biovolume and biomass estimations. Applied and Environmental Microbiology **49**:1488-1493.

Campbell, B., L. Yu, J. Heidelberg, and D. Kirchman. 2011. Activity of abundant and rare bacteria in a coastal ocean. Proceedings of the National Academy of Sciences of the United States of America **108**:12776-12781.

Carlson, C., and H. Ducklow. 1996. Growth of bacterioplankton and consumption of dissolved organic carbon in the Sargasso Sea. Aquatic Microbial Ecology **10**:69-85.

Carlson, C., S. Giovannoni, D. Hansell, S. Goldberg, R. Parsons, and K. Vergin. 2004. Interactions among dissolved organic carbon, microbial processes, and community structure in the mesopelagic zone of the northwestern Sargasso Sea. Limnology and Oceanography **49**:1073-1083.

Cherrier, J., J. Bauer, and E. Druffel. 1996. Utilization and turnover of labile dissolved organic matter by bacterial heterotrophs in eastern north Pacific surface waters. Marine Ecology Progress Series **139**:267-279.

Cherrier, J., and J. E. Bauer. 2004. Bacterial utilization of transient plankton-derived dissolved organic carbon and nitrogen inputs in surface ocean waters. Aquatic Microbial Ecology **35**:229-241.

Comte, J., and P. del Giorgio. 2011. Composition Influences the Pathway but not the Outcome of the Metabolic Response of Bacterioplankton to Resource Shifts. Plos One **6**.

del Giorgio, P., and J. Cole. 1998. Bacterial growth efficiency in natural aquatic systems. Annual Review of Ecology and Systematics **29**:503-541.

del Giorgio, P. A., and J. M. Gasol. 2008. Physiological Structure and Single-Cell Activity in Marine Bacterioplankton. Pages 243-298 Microbial Ecology of the Oceans. John Wiley & Sons, Inc.

Eilers, H., J. Pernthaler, and R. Amann. 2000a. Succession of pelagic marine bacteria during enrichment: a close look at cultivation-induced shifts. Applied and Environmental Microbiology **66**:4634-4640.

Eilers, H., J. Pernthaler, F. O. Glockner, and R. Amann. 2000b. Culturability and in situ abundance of pelagic bacteria from the North Sea. Applied and Environmental Microbiology **66**:3044-3051.

Fenchel, T. 1987. Ecology of protozoa: the biology of free-living phagotrophic protists. Springer-Verlag, Berlin.

Fuchs, B. M., J. Pernthaler, and R. Amann. 2007. Single cell identification by fluorescence in situ hybridization. Pages 886-896 *in* C. A. Reddy, T. J. Beveridge, J. A. Breznak, G. Marzluf, T. M. Schmidt, and L. R. Snyder, editors. Methods for General and Molecular Microbiology. ASM Press, Washington D.C.

Fukuda, R., H. Ogawa, T. Nagata, and I. Koike. 1998. Direct determination of carbon and nitrogen contents of natural bacterial assemblages in marine environments. Applied and Environmental Microbiology **64**:3352-3358.

Gasol, J., P. del Giorgio, R. Massana, and C. Duarte. 1995. Active versus inactive bacteria: Size-dependence in a coastal marine plankton community. Marine Ecology Progress Series **128**:91-97.

Gasol, J., U. Zweifel, F. Peters, J. Fuhrman, and Å. Hagström. 1999. Significance of size and nucleic acid content heterogeneity as measured by flow cytometry in natural planktonic bacteria. Applied and Environmental Microbiology **65**:4475-4483.

Gomez-Consarnau, L., M. Lindh, J. Gasol, and J. Pinhassi. 2012. Structuring of bacterioplankton communities by specific dissolved organic carbon compounds. Environmental Microbiology **14**:2361-2378.

Hagström, Å., U. Larsson, P. Horstedt, and S. Normark. 1979. Frequency of dividing cells, a new approach to the determination of bacterial growth rates in aquatic environments. Applied and Environmental Microbiology **37**:805-812.

Haller, C. M., S. Rolleke, D. Vybiral, A. Witte, and B. Velimirov. 2000. Investigation of 0.2 μm filterable bacteria from the Western Mediterranean Sea using a molecular approach: dominance of potential starvation forms. Fems Microbiology Ecology **31**:153-161.

Hansell, D. A. 2005. Dissolved organic carbon reference material program. Eos, Transactions American Geophysical Union **86**:318-318.

Hansell, D. A. 2013. Recalcitrant dissolved organic carbon fractions. Annual review of marine science **5**:421-445.

Hugoni, M., N. Taib, D. Debroas, I. Domaizon, I. J. Dufournel, G. Bronner, I. Salter, H. Agogue, I. Mary, and P. E. Galand. 2013. Structure of the rare archaeal biosphere and seasonal dynamics of active ecotypes in surface coastal waters. Proceedings of the National Academy of Sciences of the United States of America **110**:6004-6009.

Hunt, D., Y. Lin, M. Church, D. Karl, S. Tringe, L. Izzo, and Z. Johnson. 2013. Relationship between abundance and specific activity of bacterioplankton in open ocean surface waters. Applied and Environmental Microbiology **79**:177-184.

Hutchinson, G. E. 1957. Concluding remarks. Pages 414-427 Cold Spring Harbor Symp Quant Biol.

Ivars-Martinez, E., A. Martin-Cuadrado, G. D'Auria, A. Mira, S. Ferriera, J. Johnson, R. Friedman, and F. Rodriguez-Valera. 2008. Comparative genomics of two ecotypes of the marine planktonic copiotroph *Alteromonas macleodii* suggests alternative lifestyles associated with different kinds of particulate organic matter. Isme Journal **2**:1194-1212.

Jumars, P. A., J. W. Deming, P. S. Hill, L. Karp-Boss, P. L. Yager, and W. B. Dade. 1993. Physical constraints on marine osmotrophy in an optimal foraging context. Marine Microbial Food Webs **7**:121-159.

Koch, A. L. 1971. The adaptive responses of *Escherichia coli* to a feast and famine existence. Advances in microbial physiology **6**:147-217.

Lauro, F., D. McDougald, T. Thomas, T. Williams, S. Egan, S. Rice, M. DeMaere, L. Ting, H. Ertan, J. Johnson, S. Ferriera, A. Lapidus, I. Anderson, N. Kyrpides, A. Munk, C. Detter, C. Han, M. Brown, F. Robb, S. Kjelleberg, and R. Cavicchioli. 2009. The genomic basis of trophic strategy in marine bacteria. Proceedings of the National Academy of Sciences of the United States of America **106**:15527-15533.

Lee, S., and J. Fuhrman. 1987. Relationships between biovolume and biomass of naturally derived marine bacterioplankton. Applied and Environmental Microbiology **53**:1298-1303.

Lennon, J. T., and S. E. Jones. 2011. Microbial seed banks: the ecological and evolutionary implications of dormancy. Nature Reviews Microbiology **9**:119-130.

Lopez-Perez, M., A. Gonzaga, A. Martin-Cuadrado, O. Onyshchenko, A. Ghavidel, R. Ghai, and F. Rodriguez-Valera. 2012. Genomes of surface isolates of *Alteromonas macleodii*: the life of a widespread marine opportunistic copiotroph. Scientific Reports **2**:1-11.

Malfatti, F., T. Samo, and F. Azam. 2010. High-resolution imaging of pelagic bacteria by atomic force microscopy and implications for carbon cycling. Isme Journal **4**:427-439.

Martinez, J., D. C. Smith, G. F. Steward, and F. Azam. 1996. Variability in ectohydrolytic enzyme activities of pelagic marine bacteria and its significance for substrate processing in the sea. Aquatic Microbial Ecology **10**:223-230.

McCarren, J., J. Becker, D. Repeta, Y. Shi, C. Young, R. Malmstrom, S. Chisholm, and E. DeLong. 2010. Microbial community transcriptomes reveal microbes and metabolic pathways associated with dissolved organic matter turnover in the sea. Proceedings of the National Academy of Sciences of the United States of America **107**:16420-16427.

Mills, M., C. Moore, R. Langlois, A. Milne, E. Achterberg, K. Nachtigall, K. Lochte, R. Geider, and J. La Roche. 2008. Nitrogen and phosphorus co-limitation of bacterial productivity and growth in the oligotrophic subtropical North Atlantic. Limnology and Oceanography **53**:824-834.

Morita, R. Y. 1982. Starvation-survival of heterotrophs in the marine environment. Advances in Microbial Ecology **6**:171-198.

Mou, X., S. Sun, R. Edwards, R. Hodson, and M. Moran. 2008. Bacterial carbon processing by generalist species in the coastal ocean. Nature **451**:708-711.

Nelson, C., and C. Carlson. 2012. Tracking differential incorporation of dissolved organic carbon types among diverse lineages of Sargasso Sea bacterioplankton. Environmental Microbiology **14**:1500-1516.

Nelson, C., S. Goldberg, L. Kelly, A. Haas, J. Smith, F. Rohwer, and C. Carlson. 2013. Coral and macroalgal exudates vary in neutral sugar composition and differentially enrich reef bacterioplankton lineages. Isme Journal **7**:962-979.

Pedros-Alio, C. 2006. Marine microbial diversity: can it be determined? Trends in Microbiology **14**:257-263.

Perez, M., C. Pausz, and G. Herndl. 2003. Major shift in bacterioplankton utilization of enantiomeric amino acids between surface waters and the ocean's interior. Limnology and Oceanography **48**:755-763.

Pfandl, K., and J. Boenigk. 2006. Stuck in the mud: suspended sediments as a key issue for survival of chrysomonad flagellates. Aquatic Microbial Ecology **45**:89-99.

Pinhassi, J., F. Azam, J. Hemphala, R. A. Long, J. Martinez, U. L. Zweifel, and A. Hagstrom. 1999. Coupling between bacterioplankton species composition, population dynamics, and organic matter degradation. Aquatic Microbial Ecology **17**:13-26.

Poretsky, R., S. Sun, X. Mou, and M. Moran. 2010. Transporter genes expressed by coastal bacterioplankton in response to dissolved organic carbon. Environmental Microbiology **12**:616-627.

Porter, K., and Y. Feig. 1980. The use of DAPI for identifying and counting aquatic microflora. Limnology and Oceanography **25**:943-948.

Samo, T., B. Pedler, G. Ball, A. Pasulka, A. Taylor, L. Aluwihare, F. Azam, R. Goericke, and M. Landry. 2012. Microbial distribution and activity across a water mass frontal zone in the California Current Ecosystem. Journal of Plankton Research **34**:802-814.

Sarmento, H., and J. Gasol. 2012. Use of phytoplankton-derived dissolved organic carbon by different types of bacterioplankton. Environmental Microbiology **14**:2348-2360.

Schafer, H., P. Servais, and G. Muyzer. 2000. Successional changes in the genetic diversity of a marine bacterial assemblage during confinement. Archives of Microbiology **173**:138-145.

Sherr, E., and B. Sherr. 2002. Significance of predation by protists in aquatic microbial food webs. Antonie Van Leeuwenhoek International Journal of General and Molecular Microbiology **81**:293-308.

Shi, Y., J. McCarren, and E. DeLong. 2012. Transcriptional responses of surface water marine microbial assemblages to deep-sea water amendment. Environmental Microbiology **14**:191-206.

Simon, M., and F. Azam. 1989. Protein content and protein synthesis rates of planktonic marine bacteria. Marine Ecology Progress Series **51**:201-213.

Tada, Y., A. Taniguchi, I. Nagao, T. Miki, M. Uematsu, A. Tsuda, and K. Hamasaki. 2011. Differing growth responses of major phylogenetic groups of marine bacteria to natural phytoplankton blooms in the western north pacific ocean. Applied and Environmental Microbiology **77**:4055-4065.

Taylor, A. G., R. Goericke, M. R. Landry, K. E. Selph, D. A. Wick, and M. J. Roadman. 2012. Sharp gradients in phytoplankton community structure across a frontal zone in the California Current Ecosystem. Journal of Plankton Research **34**:778-789.

Teeling, H., B. Fuchs, D. Becher, C. Klockow, A. Gardebrecht, C. Bennke, M. Kassabgy, S. Huang, A. Mann, J. Waldmann, M. Weber, A. Klindworth, A. Otto, J. Lange, J. Bernhardt, C. Reinsch, M. Hecker, J. Peplies, F. Bockelmann, U. Callies, G. Gerdts, A. Wichels, K. Wiltshire, F. Glockner, T. Schweder, and R. Amann. 2012. Substrate-controlled succession of marine bacterioplankton populations induced by a phytoplankton bloom. Science **336**:608-611.

Yooseph, S., K. Nealson, D. Rusch, J. McCrow, C. Dupont, M. Kim, J. Johnson, R. Montgomery, S. Ferriera, K. Beeson, S. Williamson, A. Tovchigrechko, A. Allen, L. Zeigler, G. Sutton, E. Eisenstadt, Y. Rogers, R. Friedman, M. Frazier,

and J. Venter. 2010. Genomic and functional adaptation in surface ocean planktonic prokaryotes. Nature **468**:60-66.

2.10 APPENDIX: SUPPORTING INFORMATION (SI)

2.10.1 SI METHODS

2.10.1.1 Sampling, experimental setup, and Alteromonas AltSIO isolation

Seawater was collected from the Ellen Browning Scripps Memorial Pier, Scripps Institution of Oceanography, La Jolla, California USA, (32° 52.02' N, 117° 15.43' W), at ~1 m depth in May 2011, November 2011, and January 2012 using 20 L polycarbonate carboys rinsed with 1.2 N trace metal grade hydrochloric acid (HCl) followed by three rinses of Millipore Q water (MilliQ) and flushed with two volumes of seawater prior to sample collection. In May and November seawater was pre-filtered through glass fiber filters (GF/F, 0.7 μm nominal pore size) using an all glass filter apparatus and flask. GF/F filtrate was then filtered through 0.1 μm 142 mm polyethersulfone (PES) membranes (PALL, Supor-100, Ann Arbor, MI) using a peristaltic pump fitted with acid-washed, platinum-cured silicone tubing. Prior to 0.1 μm filtrate collection, PES filters were flushed with 2 L of MilliQ water, followed by 0.5 L of GF/F filtered seawater to remove potential water-soluble leachable organic matter (Carlson and Ducklow 1996). The January 2012 seawater was filtered directly through the 0.1 μm PES filters without GF/F prefiltration. All glassware used for filtration, incubation, sampling, and chemical analysis was acid washed (as above) and combusted (450^{o}C, 8 hr.) before use. GF/F filters were combusted prior to sample filtration.

Alteromonas sp. strain AltSIO was isolated in 2010 by plating seawater collected from the Scripps pier onto Noble agar (15 g Noble agar L^{-1} in GF/F filtered

seawater) with no carbon or inorganic nutrient amendment, and subsequently purified by sequential plating and isolation on ZoBell 2216 agar. This isolate (GenBank accession no. KC758958 identified as "ALT199") shares ~99% 16S rDNA sequence homology with *Alteromonas macleodii*, a globally cosmopolitan gammaproteobacteria described as an opportunistic copiotroph (Lopez-Perez et al. 2012) and characterized by wide strain-specific niche specialization (Ivars-Martinez et al. 2008).

Three experimental treatments were set up to quantify the magnitude and rate of ambient DOC consumption by AltSIO relative to the native free-living bacterial community: 1) seawater culture (SWC) (10% GF/F filtered seawater; 90% 0.1 μm FSW); 2) *Alteromonas* strain AltSIO in pure culture; and 3) SWC inoculated with AltSIO. Filter-sterilized (0.1 μm) seawater with no bacterial addition served as the control for potential abiotic effects on measured DOC concentration. Sterility of the 0.1 μm-filtrate was confirmed by epifluorescence microscopy. May and November experimental treatments were incubated in separate 200 mL glass flasks in triplicate. The January 2012 experiment was conducted using 20 L polycarbonate carboys in duplicate for SWC and AltSIO-only treatments. A single 20 L carboy was used for the SWC + AltSIO treatment. All experiments were conducted in the dark at ambient seawater temperature at the time of collection (14 - 16 ± 1^{o} C).

Prior to DOC drawdown experimental setup, a pure culture -80^{o} C glycerol stock of *Alteromonas* sp. strain AltSIO was streaked onto a noble agar plate and incubated in the dark at 16^{o} C for 3 days. A single colony was used to inoculate 50 mL of 0.7μm-filtered, autoclave-sterilized seawater, grown at 16^{o} C for 2 days. While in mid-

exponential growth, the culture was transferred to freshly filtered 0.1μm-filtered (non-autoclaved) seawater collected from the Ellen Browning Scripps Memorial Pier. After 2 days of growth, the "pre-conditioned" culture was used to inoculate experimental treatments in a new batch of freshly filtered seawater used as the starting microcosm water.

2.10.1.2 Total organic carbon analysis

Seawater was sampled from each flask or carboy in a laminar flow hood with 20 mL sterile borosilicate glass serological pipets using aseptic technique. Seawater was dispensed into 40 mL precombusted borosilicate vials (I-CHEM, Chase Scientific), pre-rinsed with 10 mL of sample, acidified to pH 2 with 12 M trace metal-grade HCl to remove inorganic carbon, capped with acid-washed Teflon-lined septa, and stored at 15^{o} C in the dark until analysis. TOC concentrations were quantified with a Shimadzu 500 V-CSN/TNM-1 TOC analysis system using a seven-point carbon standard curve and calculated from the average of 5 sample injections (100 μL) per vial of between 2-3 replicate sample vials. Samples from each experiment were analyzed in a single run to limit instrument variability. Low carbon deep seawater provided by the Hansell CRM Program (Hansell 2005) was measured every ninth sample analysis to ensure instrument precision, and consistently measured between 41-43 μmol C L^{-1}.

2.10.1.3 Direct measure of bacterial cell carbon and nitrogen by CHN analysis

On days 3 and 5 of the January 2012 experiment, samples were collected in duplicate for bacterial carbon and nitrogen analysis by gravity filtration of ~2 L of seawater onto pre-combusted 25 mm GF/F filters placed inside acid washed polysulfone in-line filter holders (Whatman). Filters were transferred to pre-combusted 40 mL borosilicate vials, placed in a desiccator in the presence of concentrated hydrochloric acid (HCl, 12M) vapors to remove inorganic carbonates, then dried at 50^{o} C. Carbon, hydrogen, and nitrogen were analyzed by high temperature combusting using an Organic Elemental Analyzer (Control Equipment Corp., model CEC 440HA) by the Marine Science Institute Analytical Laboratory at the University of California, Santa Barbara. Triplicate filters with no sample were handled, stored, and processed in tandem and used as procedural blanks. The total number of cells captured on each filter was calculated by difference between the bacterial concentration of the unfiltered sample and GF/F filtrate, then multiplied by the volume filtered. Average cell-specific carbon and nitrogen content was calculated by dividing blank-subtracted total carbon and nitrogen of each filter by the total number of bacterial cells on each filter.

2.10.1.4 Bacterial abundance

Between 2 - 25 mL (depending on time point) sample was collected, fixed with 0.2 µm filtered formaldehyde (2% final concentration) at 4^{o} C for 15 min, filtered (at ≤ 20 kPa) onto 0.2 µm black polycarbonate filters (Millipore), air dried at room temperature, stained with the nucleic acid stain 4', 6-diamidino-2-phenylindole (DAPI,

2 μg mL^{-1}) (Porter and Feig 1980), mounted with freshly prepared antifade mounting solution made of 0.1% *p*-phenylenediamine in phosphate buffered saline:glycerol at 1:1 concentration (Suttle and Fuhrman 2010), and enumerated by epifluorescence microscopy (excitation: 488 nm; emission: long pass filter). At least 200 cells from at least 10 fields were counted on an Olympus BX51 microscope at 1000x magnification.

2.10.1.5 Fluorescence in situ hybridization

An *Alteromonas* sp. AltSIO strain-specific rDNA-targeted FISH probe was designed, tested, and optimized as described by Fuchs et al. (Fuchs et al. 2007). In short, the probe was designed using the full-length 16S sequence with the sequence 5'GCGCCGAAGCCTAAGCCC, located at *E. coli* nucleotide position 199 and synthesized with the flurochrome CY3 conjugated to the 5' end (Integrated DNA Technologies, San Diego, CA). A range of hybridization buffer denaturant concentrations spanning 0-50% formamide was tested at 5% step increments to determine optimum hybridization conditions to differentiate two *Alteromonas* strains of 99% 16S similarity and possessing one base pair mismatch in the center of the 18-mer oligonucleotide target region. Final optimized conditions used for the detection and enumeration of AltSIO included hybridization with 45% formamide at 46^{o}C for 2 h, followed by a wash in 40 mM NaCl at 48^{o}C for 15 m. Samples were counterstained with DAPI prior to observation.

To enumerate AltSIO growth and abundance in mixed cocultures with the native free-living seawater community, 10-mL aliquots were fixed with 2% (vol/vol)

formaldehyde (final con-centration) at 4 °C for 1–24 h, then filtered onto 25-mm white 0.2-μm polycarbonate filters (Millipore), air dried at room temperature, then stored at −20 °C until analysis by FISH. Samples were imaged at 1,000× magnification using a Nikon TE2000-U inverted epifluorescence microscope using a CoolSnapHQ CCD camera and analyzed using Nikon NIS-Elements 3.2 software. Relative proportion of probe-positive cells to total DAPI-labeled cells was calculated, then multiplied by the total bacterial abundance measured on separate, non-FISH–processed filters to calculate absolute concentration of AltSIO cells in mixed microbial populations.

2.10.1.6 Alteromonas AltSIO survival in size-fractionated seawater

A microscosm experiment was conducted to test the survival of AltSIO when challenged with grazing pressure and competition for nutrients. Whole seawater was collected from the Scripps Pier as described above and passed through 50 μm Nytex nylon mesh, 0.8 μm nuclepore polycarbonate filters, and 0.2 μm nuclepore polycarbonate filters, respectively to achieve three size fractions. AltSIO was first grown as a pure culture in autoclave-sterilized 0.7 μm GF/F-FSW then added to 2 L of each treatment at a final cell concentration of ~10^4 cells mL^{-1}. Microcosm treatments were incubated at 15^o C on a 12 h light:dark cycle at a light level of 100 μE m^{-2} s^{-1}. Each treatment was sampled for total bacterial abundance (2 mL) and AltSIO abundance via FISH (10 mL) as described above every 24 h for five days, with a final sampling on day 7. Protist abundance was enumerated by DAPI fluorescence from the 10 mL samples of the < 50 μm size fraction treatment.

2.10.1.7 Frequency distribution of bacterial cell volume in the California Current Ecosystem

A total of 29 samples were collected from 6 depths (0 - 100 m) from 5 conductivity, temperature, density (CTD) rosette hydrocasts across a 29-km North-South transect during a cruise in the California Current in October 2008 (Samo et al. 2012). The length and width of 17,388 bacterial cells were measured using DAPI fluorescence and used to calculate biovolume (Bratbak 1985) and cell-specific carbon content (Simon and Azam 1989) as detailed in Samo et al. (Samo et al. 2012). Autofluorescent cyanobacteria were manually eliminated from all measurements. Biovolume was calculated from 79 cells of the bacterial isolate *Alteromonas* sp. AltSIO by preparing samples in an identical manner as samples from the CCE, but length and width were measured by atomic force microscopy (AFM) as described by Malfatti et al. (Malfatti et al. 2010) for dry AFM samples.

2.10.2 SI RESULTS

We note the strong agreement between microscopy-based [both 4′,6-diamidino-2-phenylindole (DAPI) epifluorescence, and atomic force] estimates of average bacterial carbon and those derived from direct CHN measurements: Alteromonas sp. strain Scripps Institution of Oceanography (AltSIO) measured 72 vs. 75 fg C·cell^{-1}, and natural bacterial assemblages measured 21 vs. 19 fg C·cell^{-1} by microscopy and CHN, respectively.

2.10.3 SI DISCUSSION

Our data do not support the hypothesis that dormancy or growth limitation of AltSIO resulted from N or P limitation. First, cellular biomass (Fig. 1) and cell-specific C:N ratios (Table S3) were comparable between treatments precluding excess N requirement or N limitation by AltSIO. Second, total dissolved N and P concentrations at the beginning of the experiment (Table S2) had a stoichiometry that provided P in excess of that reported in bacterial biomass during P-limitation or exponential growth (Vrede et al. 2002). This leaves open the possibility of an undetermined micronutrient requirement, or bioavailable carbon limitation.

2.10.4 SI REFERENCES

Bratbak, G. 1985. Bacterial biovolume and biomass estimations. Applied and Environmental Microbiology **49**:1488-1493.

Carlson, C., and H. Ducklow. 1996. Growth of bacterioplankton and consumption of dissolved organic carbon in the Sargasso Sea. Aquatic Microbial Ecology **10**:69-85.

Fuchs, B. M., J. Pernthaler, and R. Amann. 2007. Single cell identification by fluorescence in situ hybridization. Pages 886-896 *in* C. A. Reddy, T. J. Beveridge, J. A. Breznak, G. Marzluf, T. M. Schmidt, and L. R. Snyder, editors. Methods for General and Molecular Microbiology. ASM Press, Washington D.C.

Hansell, D. A. 2005. Dissolved organic carbon reference material program. Eos, Transactions American Geophysical Union **86**:318-318.

Ivars-Martinez, E., A. Martin-Cuadrado, G. D'Auria, A. Mira, S. Ferriera, J. Johnson, R. Friedman, and F. Rodriguez-Valera. 2008. Comparative genomics of two ecotypes of the marine planktonic copiotroph *Alteromonas macleodii* suggests alternative lifestyles associated with different kinds of particulate organic matter. Isme Journal **2**:1194-1212.

Lopez-Perez, M., A. Gonzaga, A. Martin-Cuadrado, O. Onyshchenko, A. Ghavidel, R. Ghai, and F. Rodriguez-Valera. 2012. Genomes of surface isolates of *Alteromonas macleodii*: the life of a widespread marine opportunistic copiotroph. Scientific Reports **2**:1-11.

Malfatti, F., T. Samo, and F. Azam. 2010. High-resolution imaging of pelagic bacteria by atomic force microscopy and implications for carbon cycling. Isme Journal **4**:427-439.

Porter, K., and Y. Feig. 1980. The use of DAPI for identifying and counting aquatic microflora. Limnology and Oceanography **25**:943-948.

Samo, T., B. Pedler, G. Ball, A. Pasulka, A. Taylor, L. Aluwihare, F. Azam, R. Goericke, and M. Landry. 2012. Microbial distribution and activity across a

water mass frontal zone in the California Current Ecosystem. Journal of Plankton Research **34**:802-814.

Simon, M., and F. Azam. 1989. Protein content and protein synthesis rates of planktonic marine bacteria. Marine Ecology Progress Series **51**:201-213.

Suttle, C. A., and J. A. Fuhrman. 2010. Enumeration of virus particles in aquatic or sediment samples by epifluorescence microscopy. Pages 145-153 *in* S. W. Wilhelm, M. G. Weinbauer, and C. A. Suttle, editors. Manual of Aquatic Viral Ecology. ASLO.

Vrede, K., M. Heldal, S. Norland, and G. Bratbak. 2002. Elemental composition (C, N, P) and cell volume of exponentially growing and nutrient-limited bacterioplankton. Applied and Environmental Microbiology **68**:2965-2971.

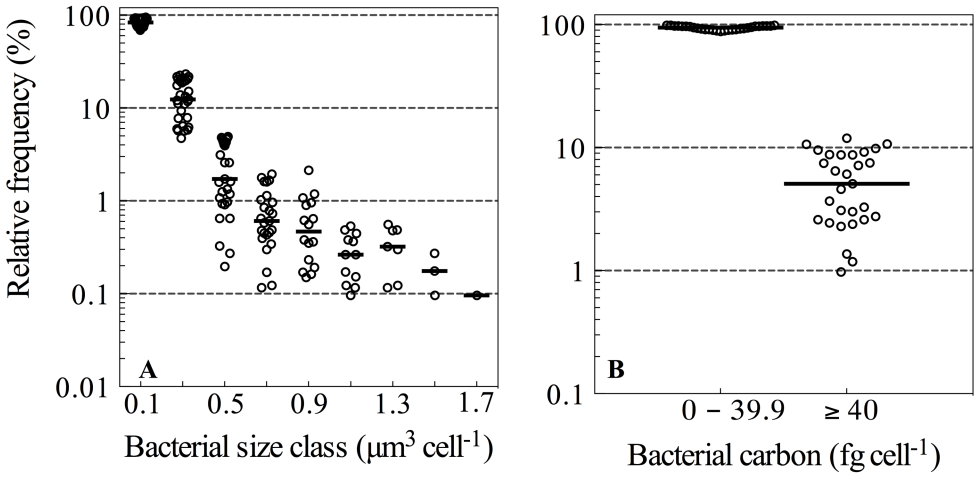

Figure S1. Bacterial size frequency distribution in the California Current Ecosystem. (A) Cell volume (n = 17,388) from 29 samples was binned in 0.2-μm^3 increments denoted on the x axis by the bin center. Each sample was treated as a distinct population, with the relative frequency of each size class calculated separately for each population. All samples are displayed in aggregate as a scatter dot plot. (B) Bacterial volume converted to cell-specific carbon and binned into two classes: average (0–39.9 fg C·$cell^{-1}$) and large (≥40 fg C·$cell^{-1}$). The median of each bin is displayed as a horizontal bar. Note the difference in the y-axis scale between A and B.

Table S1. Quality control analysis of filtration and experimental setup. Total organic carbon (TOC) concentrations at each stage of filtration and in filter-sterilized bacteria-free controls used to test abiotic effects of incubation on TOC concentration.

	TOC (µM ± s.d.)				
Experiment	Whole SW (*in situ*)	GF/F filtrate (< 0.7 µm)	PES filtrate (< 0.1 µm)	Bac-free control d 0	Bac-free control d 5
May 2011	90.0 ± 0.9	78.4 ± 0.3	77.8 ± 1.0	77.80 ± 1.0	78.26 ± 1.16
Nov 2011	81.6 ± 2.4	76.4 ± 0.8	75.6 ± 0.63	76.69 ± 1.53	77.24 ± 0.27
Jan 2012	70.3 ± 1.0*	ns	ns	nc	nc

TOC concentrations at each stage of filtration and in filter-sterilized bacteria-free controls used to test abiotic effects of incubation on TOC concentration. TOC data are mean ± SD of three vials. Bac, bacteria; GF/F, combusted glass fiber filter, type F; NC, not conducted; NS, not sampled. *SD of two vials.

Table S2. Environmental conditions during seawater collection from Scripps Pier

Experiment date	Temp (^{o} C)	Slinity (PSU)	TOC (µM)	Chl-*a* (µg L^{-1})	Silicate (µM)	Nitrate (µM)	Nitrite (µM)	Ammonium (µM)	Phosphate (µM)
May 2011	16.7	33.5	90.0 ± 0.9	1.2	1.65	0.28	0.10	0.74	0.19
Nov 2011	15.9	33.3	81.6 ± 2.4	0.53	4.42	1.56	0.15	0.82	0.31
Jan 2012	14.3	33.3	70.3 ± 1.0*	0.45	3.27	0.30	0.05	0.34	0.23

Nutrient data was provided by the Pier Based Regional Harmful Algal Bloom Program of the Southern California Coastal Ocean Observing System (La Jolla, CA). TOC data are mean ± SD of three vials. PSU, practical salinity units. *SD of two vials.

Table S3. Bacterial carbon and nitrogen content measured by CHN analysis

Time (d)	Treatment	C cell^{-1} (fg)	N cell^{-1} (fg)	C/N (molar)	Cell retention on GF/F (%)
3	SWC	18.9 ± 1.4	4.1 ± 0.6	5.5 ± 0.4	68.7 ± 16.9
	AltSIO	74.6 ± 4.3	17.7 ± 1.2	4.9 ± 0.1	99.1 ± 0.1
	SWC + AltSIO	38.6*	9.1*	5.0*	66.3*
5	SWC	17.5 ± 0.5	4.0 ± 0.1	5.1 ± 0.0	79.3 ± 0.4
	AltSIO	67.4 ± 11.4	17.1 ± 3.9	4.6 ± 0.3	99.5 ± 0.0
	SWC + AltSIO	37.7 ± 2.8†	9.5 ± 0.3†	4.6 ± 0.4†	75.9 ± 5.2†

Bacteria grown in unamended 0.1 μm filtered coastal North Pacific seawater. Values are mean ± SD of two biological replicates. AltSIO, Alteromonas sp. strain AltSIO pure culture; SWC, free-living seawater community; SWC + AltSIO, SWC inoculated with AltSIO.

*Single determination.

†Error calculated from duplicate analytical replicates of a single biological replicate.

Table S4. Statistical analysis of three experiments with ambient dissolved organic matter from surface coastal North Pacific seawater after 5 d of incubation.

					One-way ANOVA				Unpaired *t* test
Measurement	Experiment	Treatment	Mean	SD	*P* value	*F*(DFn,DFd)	R^2	Tukey's, $\alpha = 0.05$	*P* value, two-tailed
Bacterial abundance, cells·L^{-1}	May 2011	SW	1.61E+09	8.49E+07	<0.0001	$F(4,10) = 155.5$	0.9842	A	
		Alt	3.13E+08	1.98E+07	<0.0001	$F(4,10) = 155.5$	0.9842	B	
		SW + Alt	1.26E+09	1.24E+08	<0.0001	$F(4,10) = 155.5$	0.9842	C	
		Alt (cocult.)	2.13E+08	2.63E+07	<0.0001	$F(4,10) = 155.5$	0.9842	B	
		SW (coinc)	1.04E+09	1.13E+08	<0.0001	$F(4,10) = 155.5$	0.9842	C	
	Nov 2011	SW	1.18E+09	1.02E+08	<0.0001	$F(4,10) = 165.1$	0.9851	A	
		Alt	1.90E+08	6.66E+06	<0.0001	$F(4,10) = 165.1$	0.9851	B	
		SW + Alt	1.07E+09	6.66E+07	<0.0001	$F(4,10) = 165.1$	0.9851	A	
		Alt (cocult.)	2.77E+08	8.39E+06	<0.0001	$F(4,10) = 165.1$	0.9851	B	
		SW (coinc)	7.97E+08	6.10E+07	<0.0001	$F(4,10) = 165.1$	0.9851	C	
	Jan 2012	SW	2.72E+09	1.41E+08					0.0030
		Alt	6.83E+08	7.14E+07					0.0030
		SW + Alt	1.41E+09						
		Alt (cocult.)	4.23E+08						
		SW (coinc)	9.88E+08						
Bacterial biomass, μmol C·L^{-1}	May 2011	SW	2.34	0.13	<0.0001	$F(4,10) = 35.60$	0.9344	A B	
		Alt	1.85	0.12	<0.0001	$F(4,10) = 35.60$	0.9344	A D	
		SW + Alt	2.78	0.27	<0.0001	$F(4,10) = 35.60$	0.9344	B	
		Alt (cocult.)	1.26	0.16	<0.0001	$F(4,10) = 35.60$	0.9344	C	
		SW (cocult.)	1.52	0.16	<0.0001	$F(4,10) = 35.60$	0.9344	C D	
	Nov 2011	SW	1.72	0.15	<0.0001	$F(4,10) = 135.7$	0.9819	A	
		Alt	1.13	0.04	<0.0001	$F(4,10) = 135.7$	0.9819	B	
		SW + Alt	2.80	0.13	<0.0001	$F(4,10) = 135.7$	0.9819	C	
		Alt (cocult.)	1.64	0.05	<0.0001	$F(4,10) = 135.7$	0.9819	A	
		SW (cocult.)	1.16	0.09	<0.0001	$F(4,10) = 135.7$	0.9819	B	
	Jan 2012	SW	3.95	0.21					NS, 0.7552
		Alt	3.84	0.40					NS, 0.7552
		SW + Alt	3.82						
		Alt (cocult.)	2.38						
		SW (cocult.)	1.44						
ΔTOC, μmol C·L^{-1}·5 d^{-1}	May 2011	SW	3.80	0.64	NS, 0.3259	$F(2,6) = 1.359$	0.3118		
		Alt	5.00	0.94	NS, 0.3259	$F(2,6) = 1.359$	0.3118		
		SW + Alt	4.63	0.78	NS, 0.3259	$F(2,6) = 1.359$	0.3118		
	Nov 2011	SW	1.97	0.99	0.0434	$F(2,6) = 5.539$	0.6487	A	
		Alt	1.68	0.87	0.0434	$F(2,6) = 5.539$	0.6487	A	
		SW + Alt	4.10	1.05	0.0434	$F(2,6) = 5.539$	0.6487	A	
	Jan 2012	SW	2.75	0.06					NS, 0.1599
		Alt	3.69	0.60					NS, 0.1599
		SW + Alt	5.60						
ΔDOC, μmol C·L^{-1}·5 d^{-1}	May 2011	SW	6.14	0.52	NS, 0.3405	$F(2,6) = 1.296$	0.3017		
		Alt	6.85	1.05	NS, 0.3405	$F(2,6) = 1.296$	0.3017		
		SW + Alt	7.40	0.67	NS, 0.3405	$F(2,6) = 1.296$	0.3017		
	Nov 2011	SW	3.68	1.08	NS, 0.0062	$F(2,6) = 13.33$	0.8163		
		Alt	2.81	0.83	NS, 0.0062	$F(2,6) = 13.33$	0.8163		
		SW + Alt	6.90	1.13	NS, 0.0062	$F(2,6) = 13.33$	0.8163		
	Jan 2012	SW	6.70	0.15					NS, 0.2943
		Alt	7.72	1.02					NS, 0.2943
		SW + Alt	9.52						

Bacterial abundance and biomass values are stocks on day 5. For bacterial biomass, the SD between treatment means of each experiment was 0.35, 0.42, and 0.08 μmol C·L^{-1} in May, November, and January, respectively, whereas the SD within each treatment across experiments measured 1.15, 1.40, and 0.98 μmol C·L^{-1} for SWC, AltSIO, and SWC + AltSIO, respectively. Within each experiment, statistically significant differences among treatments (Tukey's $P < 0.05$) are noted by different letters. Treatments with the same letter are not significantly different. ANOVA and Tukey's results are derived from within experiment (date) treatment comparisons only. NS, not significant. SW, seawater culture; SW (coinc), dynamics of seawater bacteria within coculture; SW + Alt, combined coculture of both treatments.

Table S5. Heterotrophic bacterial consumption of ambient dissolved organic matter from surface coastal North Pacific seawater after 5 d of incubation

		Proportional change, %			Rate, μmol C·L^{-1}·d^{-1}			
Date	Treatment	C incorporated*	C respired†	Total C consumed‡	C production§	C respiration¶	C consumption§	BGE‖
May 2011	SWC	**3.0 ± 0.13 A**	4.9 ± 0.9	7.7 ± 0.8	**0.48 ± 0.03 A B**	0.78 ± 0.13	1.26 ± 0.11	**0.39 ± 0.05 A**
	AltSIO	**2.4 ± 0.13 B**	6.5 ± 1.2	8.7 ± 1.3	**0.37 ± 0.02 A**	1.02 ± 0.19	1.40 ± 0.22	**0.27 ± 0.03 B**
	SWC + AltSIO	**3.6 ± 0.36 A**	6.0 ± 1.0	9.6 ± 0.8	**0.57 ± 0.06 B**	0.95 ± 0.16	1.51 ± 0.14	**0.38 ± 0.05 A**
Nov 2011	SWC	**2.2 ± 0.19 A**	2.6 ± 1.3	**4.6 ± 1.4 A**	**0.35 ± 0.03 A**	0.40 ± 0.20	**0.75 ± 0.22 A**	0.49 ± 0.11
	AltSIO	**1.5 ± 0.07 B**	2.2 ± 1.1	**3.5 ± 1.0 A**	**0.23 ± 0.01 B**	0.34 ± 0.18	**0.57 ± 0.17 A**	0.43 ± 0.13
	SWC + AltSIO	**3.6 ± 0.17 C**	5.2 ± 1.3	**8.8 ± 1.4 B**	**0.57 ± 0.03 C**	0.84 ± 0.22	**1.41 ± 0.23 B**	0.41 ± 0.06
Jan 2012	SWC	5.4 ± 0.30	3.7 ± 0.1	9.0 ± 0.2	0.78 ± 0.04	0.54 ± 0.01	1.31 ± 0.03	0.59 ± 0.01
	AltSIO	5.5 ± 0.62	5.0 ± 0.9	10.2 ± 1.4	0.79 ± 0.08	0.73 ± 0.12	1.52 ± 0.21	0.52 ± 0.01
	SWC + AltSIO	5.4	7.7	13.1	0.77	1.10	1.87	0.41

Proportional C flux (% change) calculated relative to treatment-specific initial C concentration. All values are mean ± SD. May and November values are derived from three biological replicates. January values are derived from two biological replicates. Values without associated error are from a single incubation. Significant differences (one-way ANOVA $P < 0.05$) within experiments are highlighted in bold. Significant differences between treatments (Tukey's $P < 0.05$) indicated by different letters (A–C). Means with the same letters indicate no significant differences between means. Insufficient replication precluded statistical evaluation of January 2012 data. AltSIO, Alteromonas sp. strain AltSIO pure culture; BGE, bacterial growth efficiency; SWC, seawater community; SWC + AltSIO, SWC inoculated with AltSIO.

* Carbon incorporated = bacterial biomass C calculated as cell abundance x treatment-specific carbon content (Table S1).

† Carbon respired = ΔTOC

‡ Total carbon consumed = ΔTOC + Δ bacterial C

§ Carbon production and consumption derived from Δ bacterial C vs. time and Δ DOC vs. time, respectively. DOC = TOC-bacterial C

¶ C respiration rate = ΔTOC/time

‖ BGE, Bacterial growth efficiency = C production/C consumption

Table S6. One-way ANOVA analysis of experimental data from Table S5

		Bacterial carbon flux						
		Proportional change, %			Rate, μmol C·L^{-1}·d^{-1}			
Date	ANOVA results	C incorporated*	C respired†	Total C consumed‡	C production§	C respiration¶	C consumption§	BGE‖
May 2011	$F(2,6)$	**23.52**	1.43	1.77	**18.52**	1.31	1.26	**7.89**
	P	**0.0014**	0.3101	0.2488	**0.0049**	0.3378	0.3505	**0.0209**
	R^2	**0.8869**	0.3231	0.3710	**0.8811**	0.3036	0.2949	**0.7246**
Nov 2011	$F(2,6)$	**154.60**	5.43	**13.66**	**140.80**	5.53	**13.60**	0.45
	P	**<0.0001**	0.0451	**0.0058**	**<0.0001**	0.0435	**0.0059**	0.6595
	R^2	**0.9810**	0.6442	**0.8199**	**0.9791**	0.6484	**0.8192**	0.1296

Significant results ($P < 0.05$) are highlighted in bold.

Table S7. Statistical analysis of long-term (>1 y) carbon drawdown experiment (Fig. 3). Two-way RM ANOVA and Sidak's multiple comparison post hoc test. Analyses conducted separately for SWC vs. AltSIO (A), SWC vs. SWC + AltSIO (B), and AltSIO vs. SWC + AltSIO (C). CI, confidence interval; df, degrees of freedom; MS, mean square; NS, not significant; N1, group 1 sample size; N2, group 2 sample size; RM, repeated measure; SS, sum of squares; t, student's t ratio.

Table S7. Statistical analysis of long-term (>1 y) carbon drawdown experiment (Fig. 3). Continued

A	Table analyzed	STATS_TOC_Jan_2012							
	Two-way RM ANOVA	Matching: stacked							
	Alpha	0.05							
	Source of variation	% of total variation	*P* value	*P* value summary	Significant?				
	Interaction	29.97	<0.0001	****	Yes				
	Time	55.61	<0.0001	****	Yes				
	Column factor	11.98	0.051	NS	No				
	Subjects (matching)	1.321	0.0205	*	Yes				
	ANOVA table	SS	df	MS	*F*(dfn,dfd)	*P* value			
	Interaction	131.7	5	26.33	$F(5,10) = 53.31$	<0.0001			
	Time	244.3	5	48.86	$F(5,10) = 98.91$	<0.0001			
	Column factor	52.63	1	52.63	$F(1,2) = 18.14$	0.0510			
	Subjects (matching)	5.804	2	2.902	$F(2,10) = 5.875$	0.0205			
	Residual	4.94	10	0.494					
	No. of missing values	0							
	Compare each cell mean with the other cell mean in that row.								
	No. of families	1							
	No. of comparisons per family	6							
	Alpha	0.05							
	Sidak's multiple comparisons test	Mean difference	95% CI of difference	Significant?	Summary	Adjusted *P* value			
	SWC – AltSIO								
	Day 0	0.47	−2.502 to 3.442	No	NS	0.9974			
	Day 3	1.12	−1.852 to 4.092	No	NS	0.8351			
	Day 5	1.415	−1.557 to 4.387	No	NS	0.6503			
	Day 31	−3.57	−6.542 to −0.5977	Yes	*	0.0158			
	Day 89	−5.435	−8.407 to −2.463	Yes	***	0.0006			
	Day 378	−11.77	−14.74 to −8.798	Yes	****	<0.0001			
	Test details	Mean 1	Mean 2	Mean difference	SE of difference	N1	N2	*t*	df
	SWC – AltSIO								
	Day 0	73.8	73.33	0.47	0.9462	2	2	0.4967	12
	Day 3	70.13	69.01	1.12	0.9462	2	2	1.184	12
	Day 5	71.06	69.65	1.415	0.9462	2	2	1.495	12
	Day 31	65.9	69.47	−3.57	0.9462	2	2	3.773	12
	Day 89	63.1	68.54	−5.435	0.9462	2	2	5.744	12
	Day 378	57.82	69.59	−11.77	0.9462	2	2	12.44	12

Table S7. Statistical analysis of long-term (>1 y) carbon drawdown experiment (Fig. 3). Continued

B	Table analyzed	STATS_TOC_Jan_2012							
	Two-way RM ANOVA	Matching: stacked							
	Alpha	0.05							
	Source of variation	% of total variation	*P* value	*P* value summary	Significant?				
	Interaction	2.351	0.1087	NS	No				
	Time	78.88	<0.0001	****	Yes				
	Column factor	1.1	0.0414	*	Yes				
	Subjects (matching)	0.004662	0.8638	NS	No				
	ANOVA table	SS	df	MS	*F*(dfn,dfd)	*P* value			
	Interaction	10.93	5	2.186	*F*(5,5) = 3.288	0.1087			
	Time	366.8	5	73.36	*F*(5,5) = 110.3	<0.0001			
	Column factor	5.115	1	5.115	*F*(1,1) = 236.0	0.0414			
	Subjects (matching)	0.02168	1	0.02168	*F*(1,5) = 0.03260	0.8638			
	Residual	3.325	5	0.665					
	No. of missing values	0							
	Compare each cell mean with the other cell mean in that row.								
	No. of families	1							
	No. of comparisons per family	6							
	Alpha	0.05							
	Sidak's multiple comparisons test	Mean difference	95% CI of difference	Significant?	Summary	Adjusted *P* value			
	SWC − SWC + AltSIO								
	Day 0	0.84	−2.677 to 4.357	No	NS	0.9504			
	Day 3	2	−1.517 to 5.517	No	NS	0.3589			
	Day 5	3.69	0.1734 to 7.207	Yes	*	0.0404			
	Day 31	1.445	−2.072 to 4.962	No	NS	0.6616			
	Day 89	0.62	−2.897 to 4.137	No	NS	0.9882			
	Day 378	−1.81	−5.327 to 1.707	No	NS	0.4512			
	Test details	Mean 1	Mean 2	Mean difference	SE of difference	N1	N2	*t*	df
	SWC − SWC + AltSIO								
	Day 0	73.8	72.96	0.84	0.9147	2	1	0.9184	6
	Day 3	70.13	68.13	2	0.9147	2	1	2.187	6
	Day 5	71.06	67.37	3.69	0.9147	2	1	4.034	6
	Day 31	65.9	64.45	1.445	0.9147	2	1	1.58	6
	Day 89	63.1	62.48	0.62	0.9147	2	1	0.6778	6
	Day 378	57.82	59.63	−1.81	0.9147	2	1	1.979	6

Table S7. Statistical analysis of long-term (>1 y) carbon drawdown experiment (Fig. 3). Continued

C	Table analyzed	STATS_TOC_Jan_2012				
	Two-way RM ANOVA	Matching: stacked				
	Alpha	0.05				
	Source of variation	% of total variation	*P* value	*P* value summary	Significant?	
	Interaction	20.75	0.0012	**	Yes	
	Time	57.03	0.0001	***	Yes	
	Column factor	31.31	0.1819	NS	No	
	Subjects (matching)	2.702	0.0082	**	Yes	
	ANOVA table	SS	df	MS	*F*(dfn,dfd)	*P* value
	Interaction	44.41	5	8.881	$F(5,5) = 27.50$	0.0012
	Time	122	5	24.41	$F(5,5) = 75.57$	0.0001
	Column factor	66.99	1	66.99	$F(1,1) = 11.59$	0.1819
	Subjects (matching)	5.782	1	5.782	$F(1,5) = 17.90$	0.0082
	Residual	1.615	5	0.323		
	No. of missing values	0				
	Compare each cell mean with the other cell mean in that row.					
	No. of families	1				
	No. of comparisons per family	6				
	Alpha	0.05				
	Sidak's multiple comparisons test	Mean difference	95% CI of difference	Significant?	Summary	Adjusted *P* value
	AltSIO − SWC + AltSIO					
	Day 0	0.37	−4.858 to 5.598	No	NS	>0.9999
	Day 3	0.88	−4.348 to 6.108	No	NS	0.9907
	Day 5	2.275	−2.953 to 7.503	No	NS	0.6104
	Day 31	5.015	−0.2134 to 10.24	No	NS	0.0599
	Day 89	6.055	0.8266 to 11.28	Yes	*	0.0256
	Day 378	9.96	4.732 to 15.19	Yes	**	0.002

Test details	Mean 1	Mean 2	Mean difference	SE of difference	N1	N2	*t*	df
AltSIO − SWC + AltSIO								
Day 0	73.33	72.96	0.37	1.36	2	1	0.2721	6
Day 3	69.01	68.13	0.88	1.36	2	1	0.6471	6
Day 5	69.65	67.37	2.275	1.36	2	1	1.673	6
Day 31	69.47	64.45	5.015	1.36	2	1	3.688	6
Day 89	68.54	62.48	6.055	1.36	2	1	4.453	6
Day 378	69.59	59.63	9.96	1.36	2	1	7.324	6

Table S8. TOC averaged by density horizon in the California Current, North Pacific

Density (kg m^{-3})	Depth (m)			TOC (μmol L^{-1})	
range	range	mean	s.d.	mean	s.d.
24.5 - 25.0	<50	23.1	19.7	68.6	11.4
25.0 - 25.5	50-70	38.8	22.7	62.9	10.2
25.5 - 26.0	70-100	67.2	37.8	57.2	10.9
26.0 - 26.5	100-320	180.5	71.5	49.2	2.9
26.5 - 26.75	320-400	332.1	24.0	45.9	2.1
26.75 - 27.0	400-500	487.5	59.4	44.7	2.7
27.0 - 28.0	>500	614.5	101.5	43.0	3.1

Samples (n = 1,292) collected from near shore hydrographic stations of the California Cooperative Oceanic Fisheries Investigations (2008–2010; stations <207 km from the coast).

CHAPTER 3

Single strain physiology and community composition of bacteria from coastal and offshore Southern California Bight marine environments

3.1 ABSTRACT

It was recently discovered that an individual bacterial stain, *Alteromonas* sp. AltSIO, has the capacity to consume an equivalent magnitude of ambient dissolved organic carbon (DOC) as diverse free living bacterial communities. In this study we tested the generality of this phenomenon among other bacterial strains. A total of 270 individual bacterial colonies were isolated from freshly collected seawater and a long-term (>1 y) DOC drawdown microcosm community, from which 108 strains were purified and phylogenetically classified. Comparison of growth rates in rich media revealed large differences in growth rate based on original isolation environment, but irrespective of phylogenetic classification. Broad intra-genus differences in growth rate, spanning 12-fold, were observed among isolates collected from the same environment. Apparent dominant bacterial strains isolated from the long-term microcosm were affiliated with genera generally characterized with the capacity for broad carbon utilization and/or with a unique capacity to survive long-term carbon starvation. A subset of phylogenetically diverse strains was screened for positive growth in unamended seawater, then growth and DOC drawdown were assessed among 11 isolates relative to AltSIO and two seawater communities. Results found that no other isolate, besides AltSIO displayed the ability to consume a measurable degree of ambient DOC. Results are discussed in the context of a bacterial community analysis of samples collected from across a dynamic oceanographic front in the California Current Ecosystem (CCE).

3.2 INTRODUCTION

The discovery that a single bacterial strain has the capacity to consume the entire pool of labile dissolved organic matter (DOM) raised fundamental questions about the role that microbial diversity plays in regulating the flux of DOM in the surface ocean. It was hypothesized (Pedler et al. 2014) that physiotypes with broad metabolic capacities and rapid growth rates, such as *Alteromonas* sp. AltSIO, may dominate the recycling of labile DOM in the surface ocean. *Alteromonas* spp. have been observed to account for a major fraction of the active bacterial community during natural phytoplankton blooms (Tada et al. 2011), but their conspicuous rarity in typical non-bloom environmental samples coupled with their near ubiquity in grazer-reduced substrate amended microcosms (Schafer et al. 2000, Beardsley et al. 2003, Nelson and Wear 2014) suggests that these physiotypes are strongly regulated by top-down control. The ecological relevance of such physiotypes and the broader generality of such capacity to consume a significant fraction of the DOM pool remains unknown.

To test the generality of this phenomenon, the system developed in Chapter 2 (Pedler et al. 2014) was employed to test growth and drawdown of individual bacterial strains isolated from the surface ocean relative to diverse native bacterial communities. It was hypothesized that bacteria isolated from the same location by the same technique as that used to isolate AltSIO would select for bacterial strains with similar physiology and capacity to metabolize a significant fraction of the DOM pool. Likewise, it was hypothesized that bacteria isolated from a 1 year old microcosm comprised of marine bacteria that had grown on and consumed nearly all semi-labile

DOM (Pedler et al. 2014) would have a greater capacity to consume semi-labile DOC relative to isolates collected from fresh surface seawater communities.

Within this framework, there were four objectives of this study. First, isolate and purify marine bacteria from surface coastal seawater and from a 1-year-old DOC drawdown microcosm community. Second, classify the phylogenetic distributing of all isolates by sequencing 16S rDNA and classify the general physiology of each by measuring growth rates in rich media (ZoBell 2216). Third, test the capacity of a phylogenetically diverse subset of purified isolates to consume a measurable amount of ambient DOC relative to AltSIO and diverse seawater communities. Fourth, characterize the bacterial community composition along a transect across a dynamic oceanographic front in the California Current Ecosystem (CCE).

3.3 Methods

3.3.1 Isolation of marine bacteria

Seawater was collected from the Scripps Pier on four dates including 24 September 2010, 18 November 2010, 9 December 2010, and 25 Feb 2011 (Table 1). In September and December, whole seawater was spread onto Noble agar (15 g Noble agar L^{-1} 90:10 GF/F seawater:Milli-Q water). To test for the potential to select for and re-isolate AltSIO from the same environment, grazer-free enrichment cultures were set up and sampled November 2010 and February 2011. For enrichment, whole seawater was filtered through a GF/F membrane (0.7 μm nominal) and incubated in the dark at 16^{o}C and sampled by plating 100 μL onto Noble agar on days 0, 5 and 11. Between 24

and 57 individual colonies per sampling date, totaling 155 colonies, were picked and restreaked onto ZoBell agar. Bacteria were purified by successive picking and streaking single colonies between 5 and 6 times each.

3.3.2 Isolation of marine bacteria from 1 year DOC drawdown experiment

After one year of incubation, a seawater community treatment of the Jan 2012 DOC drawdown experiment (Chapter 2) (Pedler et al. 2014) was streaked onto Noble agar and ZoBell agar plates. A total of 115 colonies derived equally from each agar type, were purified as described above (Table 1).

Table 1. Isolation scheme of 270 marine bacteria isolates.

Isolate group	Isolate no.	Agar type	Seawater collection date	Source	Incubation time (days)
NA	1-36	Noble	24 Sept. 2010	Whole SW	0
NA	37-47	Noble	18 Nov. 2010	GF/F SW enrich. 1	0
NA	48-53	Noble	18 Nov. 2010	GF/F SW enrich. 1	5
NA	54-61	Noble	18 Nov. 2010	GF/F SW enrich. 1	11
NA	62-109	Noble	9 Dec. 2010	Whole SW	0
NA	110-120, 154, 155	Noble	25 Feb. 2011	GF/F SW enrich. 2	0
NA	121-135	Noble	25 Feb. 2011	GF/F SW enrich. 2	5
NA	136-153	Noble	25 Feb. 2011	GF/F SW enrich. 2	11
LT	1-56	Noble	7 Jan. 2012	DOC drawdown microcosm	379
LT	57-115	ZoBell	7 Jan. 2012	DOC drawdown microcosm	379

Abbreviations: NA, noble agar; LT, long term; SW, seawater; GF/F, glass fiber filter type F; enrich., enrichment culture; DOC, dissolved organic carbon.

3.3.3 Growth rates and cryopreservation of bacterial isolates

After 5 to 6 successive streakings of single colonies from all isolates, each was inoculated into 7 mL of ZoBell media, and incubated for up to 96 h at 22^{o}C with rotation at 180 revolutions per minute (rpm). Growth was assessed by increases in optical density (O.D.) measured at 600 nm every 12 to 24 h. From each culture two separate 1.5 mL stocks were cryopreserved in glycerol (30% final vol/vol) and DMSO (10% vol/vol) and stored at -80^{o}C.

3.3.4 16S sequencing and phylogenetic identification of pure isolates

Pure isolates were streaked from -80^{o}C glycerol stocks onto ZoBell agar, grown at 22^{o}C, and single colonies were picked using sterile inoculating loops and swirled in 30 µL of TE buffer pre-aliqutoed into 96-well plates. Cells were lysed by 5 successive freeze-thaw cycles (-80 and 96^{o}C), then stored at-20^{o}C. The full length 16S region was amplified by polymerase chain reaction (PCR) using the universal bacterial primers 27F and 1492R (Integrated DNA Technologies, San Diego, CA), 2x PCR master mix (New England Biolabs) and 2 µL of bacterial DNA template in 50 µL (final vol.) reactions. PCR product was cleaned using the Exo-SAP protocol by incubation with exonuclease I (Thermo Scientific, Waltham, MA) and alkaline phosphatase (Affymetrix, Santa Clara, CA) and sequenced (Eton Bioscience, San Diego, CA) using both 27F and 1492R bacterial 16S primers. Forward and reverse sequences for each isolate were aligned, trimmed, edited, and concatenated into a single contiguous consensus sequence (contig) using Sequencher (v. 5.1, Gene Codes

Corp., Ann Arbor, MI). Consensus sequences were exported, compiled into a single FASTA file, then aligned amd queried against the SILVA Incremental Aligner (SINA v1.2.11) (Pruesse et al. 2012). Clustal Omega (McWilliam et al. 2013) and FastTree (Price et al. 2010) were used for multiple sequence alignment and plylogeneitc tree building and Fig Tree (v1.4.0 for Mac OS X; http://tree.bio.ed.ac.uk/) was used for post processing of trees.

3.3.5 DOC drawdown by single bacterial isolates

A total of 28 individual isolates evenly dispersed throughout the phylogenetic tree were plated from -80^{o}C glycerol stocks onto low nutrient 10^{4}x-diluted ZoBell agar plates and grown at 16^{o}C in the dark. Single colonies from each isolate were picked and used to inoculate 50 mL of GF/F-filtered autoclave-sterilized seawater (AFSW). After 48 h of growth, 100 µL of each pure culture was streaked onto ZoBell agar and incubated at 22^{o}C to verify viable cell growth in unamended seawater. Of the isolates that grew in AFSW, 11 were selected and used to inoculate freshly filter-sterilized seawater.

Seawater was collected from the Scripps pier, gravity filtered through a pre-combusted 142 mm GF/F membrane (Millipore, Billerica, MA), and filter sterilized by peristaltic pumping through a pre-flushed 142 mm polyethersulfone membrane (Pall) in a laminar flow hood as previously described for DOC-clean methodology (Chapter 2) (Pedler et al. 2014). Approximately 400 mL of filtered seawater was added to 46 pre-combusted 1L Erlenmeyer glass flasks. AltSIO and 11 pure cultures

preconditioned in AFSW for 3 d were used to inoculate filtered seawater at an initial cell concentration of approximately 10^3 cells/mL (4 mL of pure culture in AFSW was added to 400 mL 0.1 μm FSW). Two different seawater culture treatments were inoculated with either 10% (vol/vol) GF/F filtered seawater or 10% (vol/vol) whole seawater, respectively. Uninoculated filter-sterilized seawater served as a control. All 15 treatments were conducted with 3 biological replicate flasks and incubated at 16^{o}C in the dark. Samples for bacterial abundance were taken daily every 24 h for 5 d and again on d 27. Samples for TOC concentration were taken at day 0, 5, and 27 and measured on a TOC analyzer (Shimadzu 500 V-CSN/TNM-1) by high temperature combustion as described in Chapter 2 (Pedler et al. 2014).

Bacterial carbon biomass in each treatment was calculated by multiplying measured cell abundance by 20 fg C cell^{-1} for all pure isolates and SWC treatments. AltSIO biomass was calculated using measured cell-specific carbon content of 63 fg C cell^{-1} from 5 d old cultures grown in seawater (Chapter 2) (Pedler et al. 2014). Bacterial carbon demand (C incorporated + C respired) was calculated assuming 40% bacterial growth efficiency (BGE) as an approximation of average BGE empirically determined for AltSIO (Pedler et al. 2014).

3.3.6 Bacterial community analysis across an oceanographic front in the California Current Ecosystem

In October 2008, a 9-station, 26-km transect across a deep water oceanographic front (Landry et al. 2012, Ohman et al. 2012, Samo et al. 2012), was

sampled during a cruise (CCE-P0810) as part of the CCE-Long Term Ecological Research Program (LTER) (Fig. 5). Seawater samples were collected from stations 1, 3, 5, 7 and 9, over a 9 h period (21:30 – 05:00, local time) with Niskin bottles on a conductivity/temperature/density (CTD; Sea-Bird Electronics, Inc., Bellevue, WA, USA) rosette. From each station, 4 L of seawater was collected from 6 depths between 0 and 100 m targeting i) surface, ii) mixed layer, iii) upper chlorophyll (chl) max, iv) mid chl max, v) lower chl-max, and vi) below chl-max. Each 4 L sample was divided and filtered onto two duplicate 0.2 μm Sterivex filters (Millipore) and immediately frozen at -80^{o} C. Bacterial cell size was measured from all samples by epifluorescence microscopy as described (Samo et al. 2012, Pedler et al. 2014).

Ribonucleic acid (RNA) and deoxyribonucleic acid (DNA) were extracted from Sterivex filter after housings were opened over dry ice using a -80^{o}C pre-chilled metal pipe cutter. The filter membrane was removed and pulverized in a liquid nitrogen cooled mortar and pestle. Pulverized sample powder was transferred to 4 mL centrifuge tubes set on dry ice and 1.5 to 3 mL TRIzol reagent (Life Technologies) was added. RNA, DNA and protein were extracted from each sample following the manufacturer's protocol. RNA samples were treated with DNase and DNA samples were treated with RNase.

Extracted and purified DNA was used for PCR amplification of an internal region of 16S sequences using primers capped with the pyrosequencing adapter sequences and unique 5bp index barcodes. The 16S primers target the region from basepair positions 341 to 805 in *Escherichia coli* 16S rRNA (Herlemann et al.

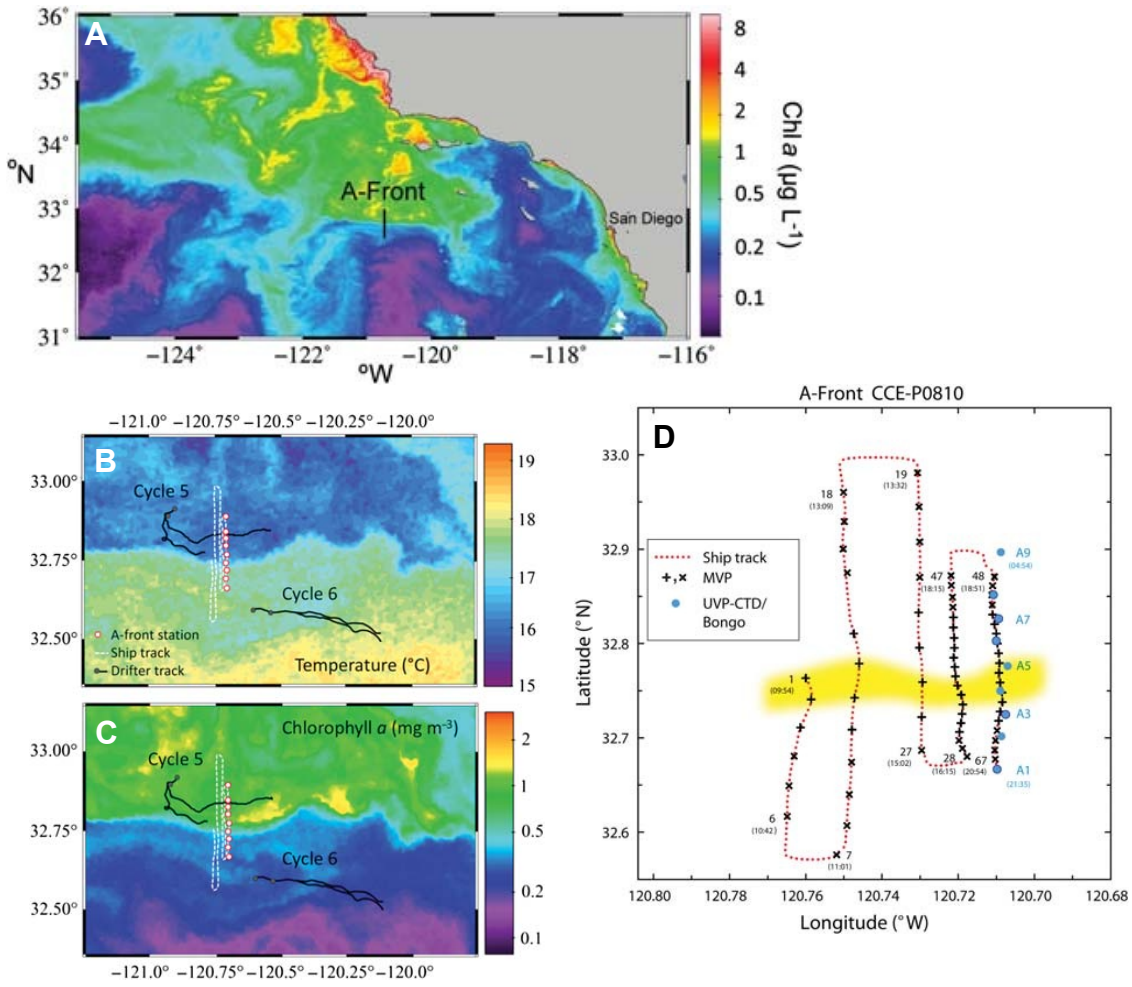

Figure 5. Overview of cruise CCE P0810. A) Satellite image of Chl a in the southern sector of the CCE from (Ohman et al. 2012). Vertical black line indicates the location of the A-Front study. Chl a is merged for 22–25 October 2008 from MERIS, MODIS-Aqua, MODIS-Terra and SeaWiFS data; image courtesy of M. Kahru, SIO. B) and C) Expanded view of the A-Front study region (from A) showing ship tracks during underway crossings of the front (white dashed lines), locations of CTD/net tow sampling stations for the transect study (red circles), and the 2-day drifter paths for experimental process Cycles 5 and 6 (dots show start positions) (Landry et al. 2012). D) Survey and sampling track across A-Front, 24–25 October 2008. Central yellow band indicates the core frontal area. Dotted line is the ship track and (+, x) indicate MVP cast locations and cast numbers (1–67) with local time shown in black, where (x) identifies MVP casts clearly to the south or north of the front and beyond the transitional region. Locations of CTD–UVP5–Rosette, Bongo net, and bacterial community samples shown as blue circles labeled A1–A9, with start times for the first and last stations (Ohman et al. 2012).

2011). Samples were pooled and sequenced on the 454 titanium platform. Roughly 10-15k sequences were attained for each sample. After quality trimming, samples were clustered at the 97% nucleotide identity level using UPARSE (Edgar 2013) to generate operational taxonomic units (OTUs). Sequences were then recruited back to reference OTU sequences to generate counts of OTUs across the sample matrix. Singleton OTUs were disregarded due to the potential of sequencing platform error. To establish taxonomy, reference OTU sequences aligned to the sequences in the SILVA database using SINA (Pruesse et al. 2012, Quast et al. 2013). Sequence reads for each OTU were transformed to relative abundance by normalizing to 1 within each sample. Normalized data were used to calculate relative proportions of major taxa and to calculate relative distances between samples by Bray-Curtis analysis and a dendrogram was constructed by Ward's method in PC-ORD.

3.4 RESULTS

3.4.1 Isolate phylogeny

A total of 270 bacterial colonies were isolated and purified (Table S8). During purification and cryopreservation, 99 isolates became nonviable. Growth rates were measured among the remaining 171 isolates in ZoBell 2216 media. 16S ribosomal DNA was successfully amplified from 137 isolates, of which 111 yielded high quality sequence data, and 108 were classified by >97% sequence similarity (Table S8). Isolate sequences were classified as belonging to 25 different genera from 4 phyla (Fig. 6). The majority of all isolates belonged to either alpha Proteobacteria (n=56) or

Figure 6. Maximum likelihood tree of phylogentitic distribution of Scripps pier bacterial isolate 16S rRNA. A) Top half of tree showing alphaproteobacteria isolates. B) Bottom half of tree showing gammaproteobacteria, Actinobacteria, and Bacteroidetes isolates. Accession numbers of nearest neighbors and environmentally relevant strains are listed in parentheses.

Figure 6. A. Maximum likelihood tree of phylogentitic distribution of Scripps pier bacterial isolate 16S rRNA. Continued

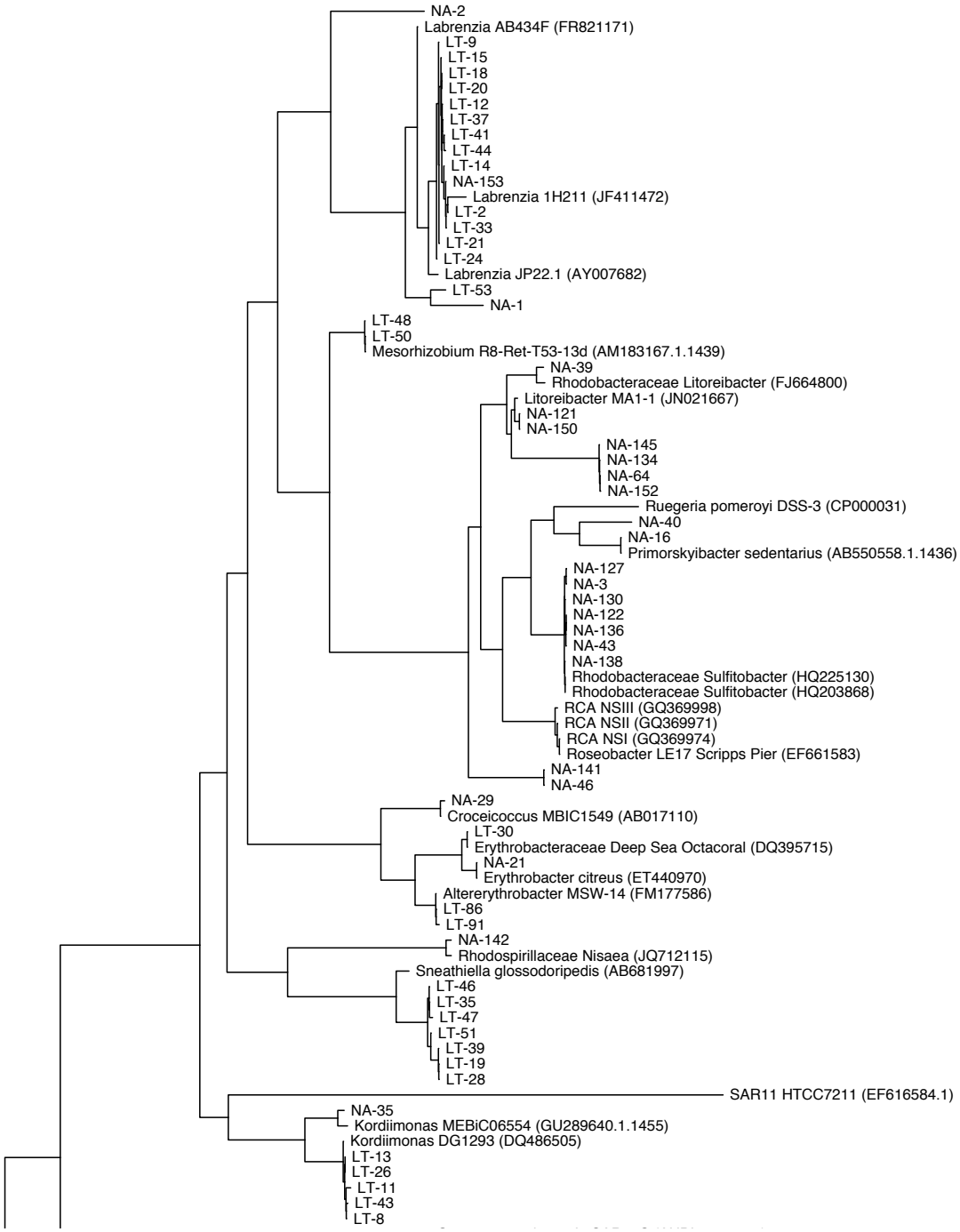

Figure 6. B. Maximum likelihood tree of phylogentitic distribution of Scripps pier bacterial isolate 16S rRNA. Continued.

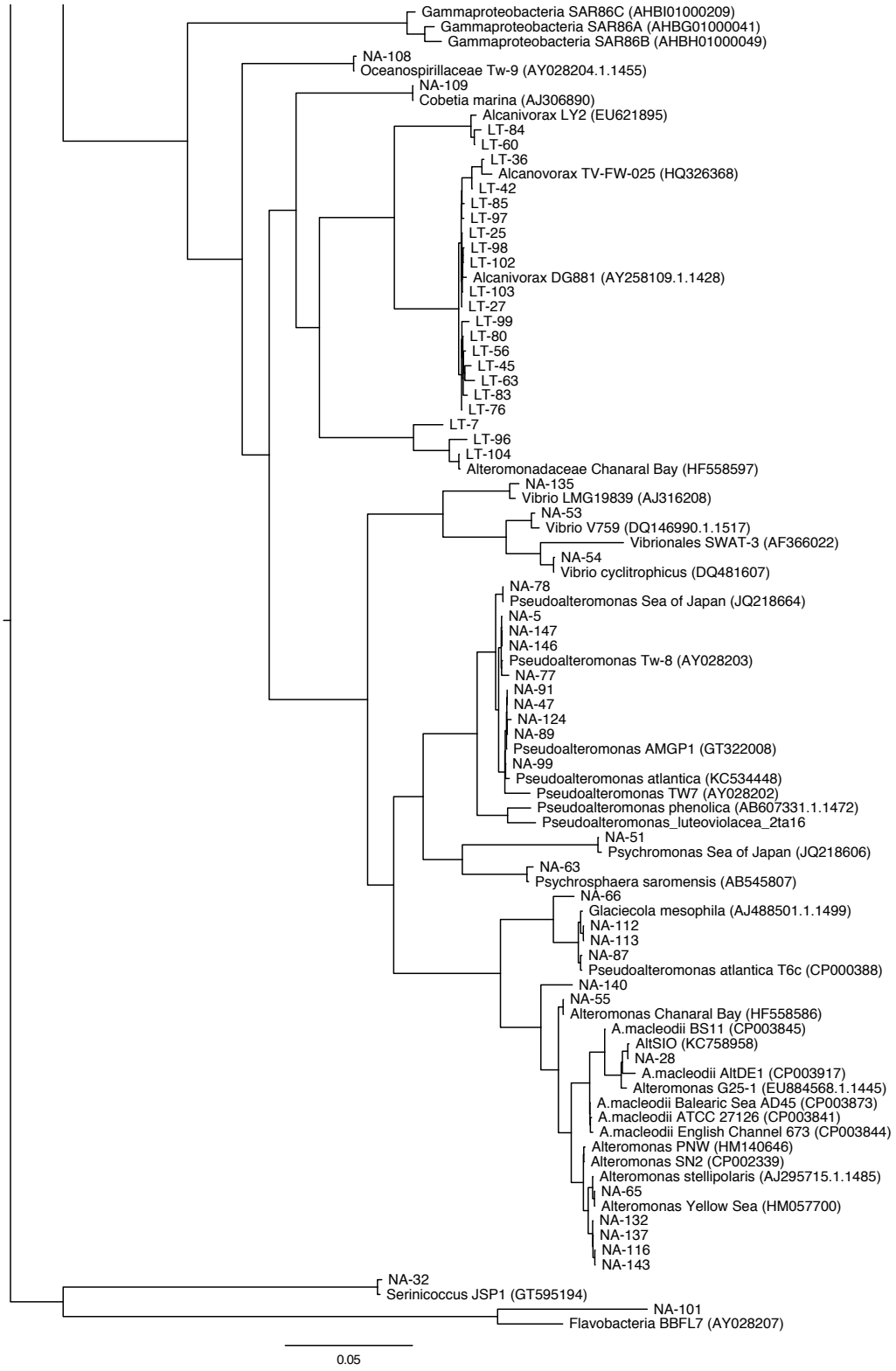

gamma Proteobacteria (n=50), with only one representative each of the Actinobacteria and Bacteroidetes phyla.

Seven genera contained more than five isolate representatives and each was derived exclusively from either NA isolates or LT isolates. *Pseudoalteromonas* (n=10), *Alteromonas* (n=7), and *Sulfitobacteira* (n=7) were comprised entirely of NA isolates. *Labrenzia* (n=14), *Sneathiella* (n=7), *Kordiimonas* (n=6), and *Alcanivorax* (n=18) were made up entirely of LT isolates except for a single NA-derived *Labrenzia*.

Removal of heterotrophic grazers by GF/F filtration did not enrich for gammaproteobacteria. Isolates collected from initial GF/F filtrate were comprised of 12 alpha and 17 gammaproteobacteria, whereas 5 and 11 days of incubations yielded 13 alpha- and 12 gammaproteobacteria. Plating of the 1 year old microcosm seawater community culture on both Noble and ZoBell agar appeared to result in opposite selection, with alphaproteobacteria comprising 80% of the isolates on Noble agar, but only 12% of the isolates on ZoBell agar with the remainder comprised of gammaprotobacteria in each case.

3.4.2 Isolate growth rates in ZoBell 2216 media

Large differences in growth rates were observed between the isolates obtained from Scripps pier seawater (NA isolates) and the isolates from the 1 year DOC drawdown mesocosms (LT isolates) (Table S8). NA isolates had a median and average growth rate of 9.7 and 8.0 generations/day, respectively. Whereas, LT isolates had a

median and average growth rate of 1.1 and 1.3 generations/day, respectively. Phylogenetic classification had no bearing on measured isolate growth rates. For example, among NA isolates, both *Alteromonas* (n=7) and *Pseudoalteromonas* (n=10) genera exhibited growth rates that ranged over 10-fold from 1 to 12 generations/day.

3.4.3 Isolate growth and ambient DOC drawdown in unamended seawater

All bacterial isolates and both seawater communities (SWC) grew in unamended 0.1 μm-filtered seawater. After 5 days of incubation, only two pure cultures, NA-35 and AltSIO, reached an abundance $>10^5$ cells·mL^{-1} (Fig. 7). The SWC inoculated with 10% GF/F filtered seawater reached 6-fold greater cell abundance (1.8×10^6 cells·mL^{-1}) than the SWC inoculated with 10% whole seawater (3.0×10^5 cells·mL^{-1}) (Fig. 7). After 27 days of incubation, no change in TOC concentration was detected in samples from alphaproteobacteria isolates *Sulfitobacter* NA-3, *Kordiimonas* NA-35, *Celeribacter* NA-46, or gammaproteobacteria isolates *Marinobacter* LT-96, *Pseudoalteromonas* NA-47, *Psychromonas* NA-51. Bacterial carbon utilization was calculated for all samples (Table 2). Detectable changes in TOC concentration (> 1 μM C) were apparent in only two samples, AltSIO (4.7 μM C change) and SWC-1 (4.5 μM C change) with corresponding biomass-subtracted changes in DOC concentration of 7.8 and 7.5 μM C, respectively.

3.4.4 Bacterial community analysis across an oceanographic front in the California Current Ecosystem

Table 2. Bacterial isolate abundance and DOC utilization.

	Marinobacter (LT-96)	Sulfitobacter (NA-3)	Kordiimonas (NA-35)	Celeribacter (NA-46)	Pseudoalteromonas (NA-47)	Psychromonas (NA-51)	Vibrio (NA-54)	Glaciecola (NA-66)	Pseudoalteromonas (NA-77)	Cobetia (NA-109)	Alteromonas (NA-116)	Alteromonas (AltSIO)	SWC-1 (10% GF/F)	SWC-2 (10% WSW)
Abundance ($x10^5$ mL^{-1})	0.32	0.76	3.22	0.52	0.44	0.43	0.77	0.63	0.35	0.51	0.97	5.92	18.0 0	2.95
Cell C (uM)	0.05	0.13	0.54	0.09	0.07	0.07	0.13	0.10	0.06	0.09	0.16	3.11	3.00	0.49
delta TOC[a]	0	0	0	0	0	0	nm	nm	nm	nm	nm	nm	nm	nm
delta TOC[b]	0.08	0.19	0.80	0.13	0.11	0.11	0.19	0.16	0.09	0.13	0.24	4.66	4.50	0.74
BCD (uM)	0.13	0.31	1.34	0.22	0.18	0.18	0.32	0.26	0.15	0.21	0.40	7.76	7.49	1.23

Abbreviations are: [a]Measured after 27 d of incubation; [b]Calculated; nm, not measured; BCD, bacterial carbon demand.

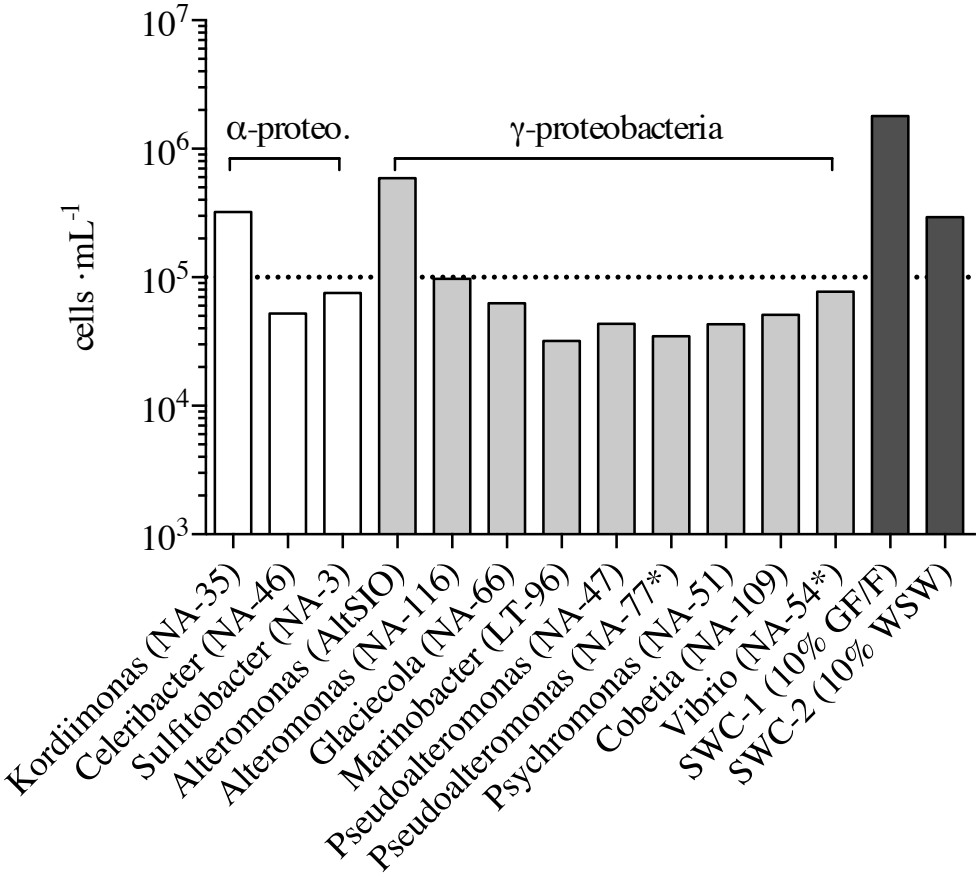

Figure 7. Scripps pier isolate growth in 0.1 μm-filtered seawater. Dotted horizontal line denotes 10^5 cells mL^{-1} for reference. * Denotes isolates from enrichment cultures.

Average cell-specific carbon for all cells (n=17,417) measured across the front measured 21.5 fg C $cell^{-1}$ and ranged from 16.2 to 26 for all samples (Table 3). The highest average C content was measured from all samples collected at 100 m (22.9-25.9 fg C $cell^{-1}$). All depth samples from station A9 showed the highest contribution of large cells (≥ 40 fg C $cell^{-1}$) to total bacterial C biomass (16-24%) relative to other stations. Categorizing by depth, 100 m samples showed the greatest contribution of large bacteria to total bacterial biomass accounting for 15-22% of total bacterial biomass (Table 3).

3.4.5 16S rDNA analysis

The majority (>50%) of all sequences belonged to the Proteobacteria phylum in 30 of 44 total samples (Tables 4 - Table 9). Samples for which Proteobacteria comprised < 50% of total sequence reads were comprised of a higher proportion of Bacteroidetes and/or cyantobacteria (Table 4-9). Bacteroidetes comprised > 30% of all sequence reads in stations A1 surface and mid chl. max, and at the front station A5 in samples from the mixed layer, upper chl max, and mid chl. max (Table 7). Elevated proportions of Bacteroidetes are in general agreement with increased concentration of organic aggregates as measured using an Underwater Vision Profiler (UVP) (Ohman et al. 2012).

Except for cycle 6 surface station 1 (C6-1), alphaproteobacteria comprised 44-88% of all Proteobacteria reads across the front. Within alphaprotobacteira, the SAR11 clade accounted for 28-92% of all reads. Gammaproteobacteria accounted for

Table 3. Bacteria cell biovolume and carbon content across the A-Front study in the CCE (cruise P0810). Samples from the oligotrophic side of the front are marked with blue headers (A1, A3). The front is noted in yellow (A5), and samples from the mesotrophic side of the front are marked with green headers (A7, A9). "Large cells" defined as ≥ 40 fg C cell^{-1}.

		Surface					Mixed layer				
	all samples	A1	A3	Front A5	A7	A9	A1	A3	Front A5	A7	A9
cells counted	*17417*	586	508	463	1095	1137	657	615	465	1039	898
mean biovol. (um^3)	*0.133*	0.162	0.087	0.125	0.097	0.170	0.160	0.087	0.120	0.100	0.184
mean C cell^{-1} (fg)	*21.5*	24.5	17.1	21.3	18.2	24.9	24.6	17.1	20.7	18.0	26.0
% cells > 40 fg C cell^{-1}	*5.7*	8.9	1.2	2.6	2.4	9.3	6.2	1.0	3.2	3.4	12.0
mean C of cells > 40 fg	*50.3*	48.6	49.2	48.6	47.9	53.4	47.9	43.8	46.5	54.4	52.7
% total bac C as "large cells"	*12.5*	17.6	3.4	5.9	6.3	20.0	12.1	2.5	7.2	10.2	24.4

	Upper chl. max.					Mid chl. max.				
	A1	A3	Front A5	A7		A1	A3	Front A5	A7	A9
cells counted	669	589	583	826		512	368	619	859	1142
mean biovol. (um^3)	0.165	0.093	0.105	0.120		0.138	0.082	0.118	0.098	0.156
mean C cell^{-1} (fg)	25.0	17.7	18.9	19.9		22.5	16.2	20.5	18.0	23.9
% cells > 40 fg C cell^{-1}	7.6	2.4	3.1	4.7		5.3	1.4	2.8	2.4	7.6
mean C of cells > 40 fg	49.7	46.7	50.1	58.1		48.5	54.0	45.9	53.6	50.9
% total bac C as "large cells"	15.2	6.3	8.2	13.8		11.4	4.5	6.1	7.3	16.2

	Lower chl. max.					Below chl. max. (100 m)				
	A1	A3	Front A5	A7	A9	A1	A3	Front A5	A7	A9
cells counted	274	311	617	817	791	169	188	210	224	186
mean biovol. (um^3)	0.163	0.173	0.109	0.119	0.179	0.165	0.182	0.164	0.173	0.147
mean C cell^{-1} (fg)	24.4	25.2	19.5	20.3	26.0	24.7	25.9	24.4	25.5	22.9
% cells > 40 fg C cell^{-1}	9.1	9.0	2.6	3.8	10.8	7.1	10.6	9.5	9.8	6.5
mean C of cells > 40 fg	49.2	52.2	48.0	49.1	49.8	52.4	53.9	51.7	48.8	53.0
% total bac C as "large cells"	18.4	18.6	6.4	9.2	20.6	15.1	22.1	20.2	18.8	14.9

13-35% of total Proteobacteria reads across the front, with a general increase in abundance on the mestorophic side of the front (stations A5, A7, A9) and highest proportional abundances, ≥ 30% of total gammaproteobacteria, at 100 m depth at the front and adjacent mestotrophic stations (A5, A7, A9). Except for cycle 6 surface station 1 (C6-1), *Oceanospirralles* accounted for 42-84% of total gammaproteobacteria reads, the majority of which were identified as belonging to the SAR86 cluster. *Oceanospirralles* was generally higher in proportional abundance in surface samples from stations A3-A9. No members of the *Labrenzia* genus were identified within the *Rhodobacterales* order.

Within the gammaproteobacteria, *Alteromonadales* accounted for between 3-38% of total reads across the front, and were highest (29-38%) at station A1 from surface down to the mid chl. max, at the front station A5 within the mid and lower chl. max, and at station A9 within the mid chl. max. In contrast to the generally higher abundance of total gammaproteobacteria reads observed for all samples at 100 m, *Alteromonadales* accounted for only 4-17% of total gammaproteobacteria. Within the *Alteromonadales*, the genus *Alcanivorax* was detected in 15 of 44 samples dispersed across the front and both flanking water mass regions with a proportional abundance of 0.0.1-4.2%. Members of the *Alteromonas* genus were detected in 28 of 44 samples from the front and both flanking water masses and ranged in abundance from 0.1 to 2 % of total gammaproteobacteria reads. On the oligotrophic side of the front, *Alteromonas* genus reads where found in a higher number of samples and with higher proportional abundance than on the mesotrophic side of the front.

Within *Prochlorococcus* and *Synechococcus* sequence reads, *Synechococcus* dominated (≥ 50 %) at all depths from the front and all samples on the mesotrophic side of the front, except the 100 m sample at the front (station A5) where no *Synechococcus* reads were detected. The oligotrophic side of the front was more variable but generally showed a higher proportion of *Prochlorococcus* reads than *Synechococcus* (Tables 4-9). These data are in agreement with microscopy and flow cytometry based estimates of *Prochlorococcus* and *Synechococcus* abundance from the same sample set (Taylor et al. 2012).

Cluster analysis of abundance-normalized OTUs from 44 CCE samples resulted in 3 distinct groups when setting a Bray-Curtis distance measure of 5.6, and accounting for 75% of total information (Fig. 8). Group I was comprised of all samples on the oligotrophic side of the front but also included the mixed layer sample of station A9 from the mesotrophic side of the front; group II contained all samples from the front and the mesotrophic side of the front; and group III contained all samples from 100 m spanning all stations in the transect and Cycle 5 and Cycle 6. Finer scale clustering is observed within each group with lower Bray-Curtis distance cutoffs. Within group II, all samples from the mixed layer through the lower chlorophyll maximum at the front (station A5) clustered together but distinct from all others within the group.

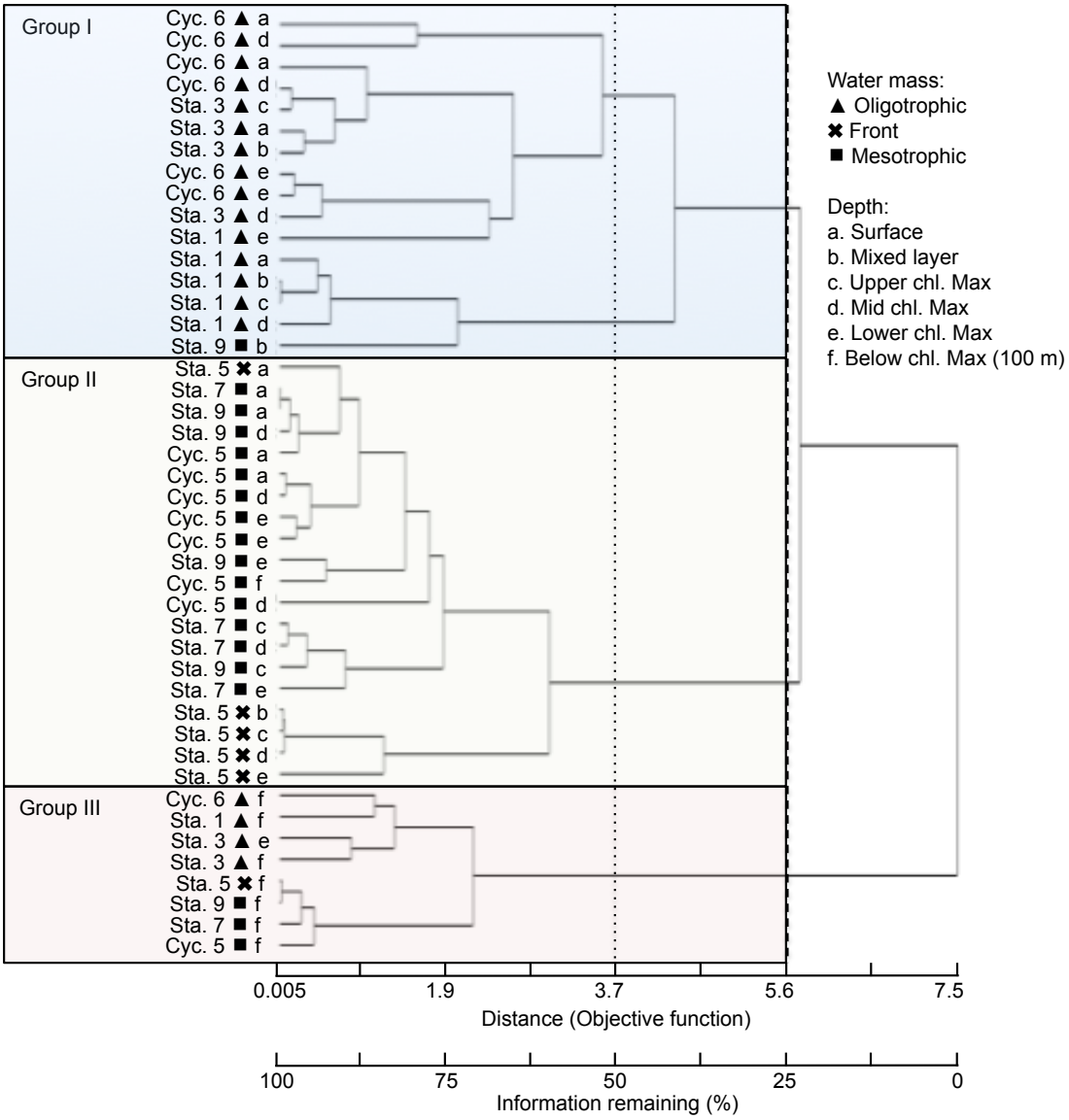

Figure 8. Cluster analysis of 44 samples across CCE A-Front and adjacent flanking water masses from cruise CCE P0810. Abbreviations: Sta., station; Cyc., cycle; chl, chlorophyll.

Table 4. Relative abundance of 16S rDNA sequences for major taxa in the CCE A-Front study. Surface sample.

	C6-1	C6-2	A1	A3	Front A5	A7	A9	C5-1	C5-2
Proteobacteria	0.60	0.45	0.20	0.69	0.60	0.66	0.62	0.63	0.64
Bacteroidetes	0.01	0.04	0.37	0.06	0.22	0.08	0.11	0.14	0.12
Planktomycetes	0.00	0.00	0.00	0.00	0.00	0.00	0.00	0.00	0.00
Cyanobacteria	0.33	0.45	0.36	0.20	0.14	0.22	0.22	0.17	0.20
Proportion of total	0.95	0.94	0.94	0.95	0.96	0.96	0.96	0.95	0.96
Proteobacteria									
Alpha	0.21	0.82	0.69	0.83	0.79	0.81	0.76	0.78	0.77
Beta	0.61	0.02	0.01	0.06	0.01	0.01	0.01	0.01	0.03
Delta	0.06	0.02	0.02	0.01	0.00	0.00	0.01	0.00	0.01
Gamma	0.13	0.14	0.27	0.11	0.19	0.18	0.22	0.20	0.18
Alpha Proteobacteria									
SAR11	0.28	0.62	0.42	0.84	0.66	0.58	0.56	0.52	0.59
Rhodobacterales	0.00	0.11	0.41	0.06	0.20	0.31	0.32	0.33	0.28
Rhodospirillacea	0.00	0.05	0.04	0.01	0.01	0.01	0.01	0.01	0.01
Rickettsiales	0.15	0.19	0.10	0.08	0.09	0.05	0.06	0.09	0.06
Gamma Proteobacteria									
Alteromonadales	0.03	0.20	0.38	0.08	0.18	0.14	0.17	0.11	0.17
Oceanospirillales	0.12	0.67	0.42	0.79	0.79	0.81	0.77	0.84	0.78
SAR86	0.10	0.57	0.34	0.72	0.68	0.58	0.55	0.56	0.50
Cyanobacteria									
Prochlorococcus	0.61	0.90	0.27	0.75	0.43	0.25	0.22	0.21	0.21
Synechococcus	0.39	0.10	0.73	0.25	0.57	0.75	0.78	0.79	0.79

Table 5. Relative abundance of 16S rDNA sequences for major taxa in the CCE A-Front study. Mixed layer.

	A1	A3	Font A5	A9
Proteobacteria	0.38	0.60	0.42	0.26
Bacteroidetes	0.23	0.04	0.36	0.26
Planktomycetes	0.00	0.00	0.00	0.02
Cyanobacteria	0.31	0.29	0.18	0.40
Proportion of total	0.93	0.93	0.96	0.94
Proteobacteria				
Alpha	0.81	0.79	0.87	0.61
Beta	0.00	0.02	0.02	0.04
Delta	0.01	0.02	0.00	0.00
Gamma	0.17	0.16	0.10	0.34
Alpha Proteobacteria				
SAR11	0.60	0.74	0.89	0.48
Rhodobacterales	0.24	0.07	0.05	0.42
Rhodospirillacea	0.03	0.04	0.00	0.02
Rickettsiales	0.12	0.13	0.04	0.02
Gamma Proteobacteria				
Alteromonadales	0.35	0.11	0.20	0.38
Oceanospirillales	0.49	0.78	0.75	0.55
SAR86	0.43	0.68	0.62	0.46
Cyanobacteria				
Prochlorococcus	0.44	0.87	0.26	0.22
Synechococcus	0.56	0.13	0.74	0.78

Table 6. Relative abundance of 16S rDNA sequences for major taxa in the CCE A-Front study. Upper chlorophyll maximum.

			Front		
	A1	A4	A5	A7	A9
Proteobacteria	0.32	0.57	0.42	0.53	0.46
Bacteroidetes	0.29	0.09	0.37	0.07	0.20
Planktomycetes	0.00	0.00	0.00	0.00	0.01
Cyanobacteria	0.32	0.25	0.15	0.35	0.28
Proportion of total	0.93	0.92	0.95	0.95	0.95
Proteobacteria					
Alpha	0.77	0.76	0.88	0.82	0.76
Beta	0.01	0.02	0.01	0.01	0.02
Delta	0.02	0.04	0.00	0.02	0.00
Gamma	0.20	0.18	0.10	0.14	0.22
Alpha Proteobacteria					
SAR11	0.50	0.75	0.92	0.68	0.75
Rhodobacterales	0.29	0.09	0.04	0.21	0.18
Rhodospirillacea	0.04	0.04	0.00	0.01	0.01
Rickettsiales	0.14	0.08	0.02	0.06	0.03
Gamma Proteobacteria					
Alteromonadales	0.33	0.10	0.19	0.19	0.22
Oceanospirillales	0.48	0.79	0.74	0.71	0.71
SAR86	0.41	0.53	0.61	0.45	0.49
Cyanobacteria					
Prochlorococcus	0.41	0.67	0.36	0.27	0.28
Synechococcus	0.59	0.33	0.64	0.73	0.72

Table 7. Relative abundance of 16S rDNA sequences for major taxa in the CCE A-Front study. Mid chlorophyll maximum.

	C6-1	C6-2	A1	A3	Front A5	A7	A9	C5-1	C5-2
Proteobacteria	0.40	0.65	0.31	0.51	0.35	0.61	0.70	0.60	0.58
Bacteriodetes	0.01	0.07	0.36	0.09	0.39	0.09	0.08	0.13	0.12
Planktomycetes	0.02	0.01	0.02	0.01	0.00	0.00	0.00	0.00	0.00
Cyanobacteria	0.49	0.18	0.23	0.28	0.20	0.23	0.17	0.24	0.23
Proportion of total	0.92	0.90	0.91	0.89	0.94	0.93	0.95	0.97	0.93
Proteobacteria									
Alpha	0.49	0.82	0.71	0.69	0.85	0.82	0.76	0.75	0.58
Beta	0.34	0.01	0.01	0.02	0.02	0.01	0.01	0.05	0.20
Delta	0.01	0.03	0.03	0.07	0.00	0.01	0.01	0.01	0.02
Gamma	0.15	0.14	0.25	0.21	0.13	0.16	0.20	0.19	0.19
Alpha Proteobacteria									
SAR11	0.31	0.74	0.46	0.74	0.86	0.75	0.59	0.60	0.38
Rhodobacterales	0.06	0.08	0.33	0.09	0.07	0.15	0.28	0.28	0.37
Rhodospirillacea	0.15	0.05	0.06	0.05	0.01	0.01	0.02	0.01	0.01
Rickettsiales	0.20	0.09	0.12	0.06	0.04	0.04	0.06	0.07	0.16
Gamma Proteobacteria									
Alteromonadales	0.25	0.11	0.38	0.06	0.29	0.14	0.11	0.18	0.18
Oceanospirillales	0.61	0.75	0.45	0.72	0.65	0.77	0.81	0.71	0.76
SAR86	0.06	0.53	0.33	0.28	0.53	0.50	0.49	0.50	0.48
Cyanobacteria									
Prochlorococcus	0.77	0.75	0.27	0.58	0.23	0.27	0.35	0.20	0.25
Synechococcus	0.23	0.25	0.73	0.42	0.77	0.73	0.65	0.80	0.75

Table 8. Relative abundance of 16S rDNA sequences for major taxa in the CCE A-Front study. Lower chlorophyll maximum.

	C6-1	C6-2	A1	A3	Front A5	A7	A 9	C5-1	C5-2
Proteobacteria	0.51	0.44	0.34	0.69	0.44	0.50	0.62	0.64	0.69
Bacteroidetes	0.06	0.08	0.27	0.06	0.19	0.24	0.15	0.11	0.08
Planktomycetes	0.02	0.01	0.02	0.01	0.00	0.02	0.01	0.00	0.01
Cyanobacteria	0.32	0.35	0.14	0.08	0.32	0.15	0.11	0.20	0.20
Proportion of total	0.91	0.89	0.76	0.85	0.96	0.92	0.88	0.94	0.97
Proteobacteria									
Alpha	0.70	0.68	0.72	0.53	0.80	0.71	0.66	0.81	0.75
Beta	0.06	0.04	0.01	0.09	0.02	0.04	0.01	0.02	0.06
Delta	0.08	0.10	0.05	0.17	0.01	0.01	0.05	0.01	0.01
Gamma	0.15	0.17	0.21	0.19	0.17	0.24	0.26	0.16	0.18
Alpha Proteobacteria									
SAR11	0.81	0.72	0.78	0.72	0.74	0.70	0.58	0.65	0.55
Rhodobacterales	0.05	0.08	0.14	0.11	0.14	0.19	0.21	0.20	0.28
Rhodospirillacea	0.07	0.10	0.03	0.07	0.01	0.01	0.04	0.02	0.02
Rickettsiales	0.03	0.05	0.03	0.04	0.07	0.03	0.07	0.06	0.07
Gamma Proteobacteria									
Alteromonadales	0.17	0.14	0.24	0.04	0.31	0.22	0.04	0.14	0.20
Oceanospirillales	0.58	0.59	0.45	0.57	0.65	0.69	0.76	0.75	0.66
SAR86	0.25	0.19	0.21	0.18	0.46	0.46	0.29	0.36	0.39
Cyanobacteria									
Prochlorococcus	0.68	0.71	0.49	0.59	0.20	0.21	0.42	0.17	0.18
Synechococcus	0.32	0.29	0.51	0.41	0.80	0.79	0.58	0.83	0.82

Table 9. Relative abundance of 16S rDNA sequences for major taxa in the CCE A-Front study. Below chlorophyll maximum (100 m).

				Front				
	C6	A1	A3	A5	A7	A9	C5-1	C5-2
Proteobacteria	0.52	0.56	0.66	0.73	0.66	0.73	0.72	0.65
Bacteroidetes	0.10	0.13	0.08	0.08	0.09	0.07	0.09	0.10
Planktomycetes	0.04	0.04	0.00	0.01	0.01	0.01	0.01	0.01
Cyanobacteria	0.14	0.02	0.12	0.02	0.03	0.02	0.10	0.07
Proportion of total	0.80	0.76	0.87	0.84	0.80	0.83	0.92	0.83
Proteobacteria								
Alpha	0.49	0.52	0.60	0.48	0.36	0.45	0.65	0.44
Beta	0.06	0.01	0.05	0.01	0.06	0.01	0.07	0.03
Delta	0.18	0.21	0.17	0.20	0.22	0.23	0.03	0.18
Gamma	0.25	0.24	0.17	0.30	0.35	0.30	0.24	0.35
Alpha Proteobacteria								
SAR11	0.65	0.81	0.82	0.86	0.81	0.87	0.67	0.85
Rhodobacterales	0.11	0.07	0.08	0.03	0.06	0.04	0.19	0.06
Rhodospirillacea	0.16	0.08	0.04	0.06	0.09	0.05	0.02	0.05
Rickettsiales	0.04	0.02	0.05	0.02	0.03	0.02	0.05	0.01
Gamma Proteobacteria								
Alteromonadales	0.17	0.09	0.06	0.05	0.07	0.04	0.09	0.06
Oceanospirillales	0.47	0.53	0.68	0.62	0.62	0.66	0.81	0.65
SAR86	0.06	0.08	0.18	0.07	0.08	0.09	0.41	0.05
Cyanobacteria								
Prochlorococcus	0.66	0.68	0.53	1.00	0.37	0.48	0.32	0.42
Synechococcus	0.34	0.32	0.47	0.00	0.63	0.52	0.68	0.58

3.5 DISCUSSION

3.5.1 Overview of study

The objective of this study was fourfold. First, isolate and purify marine bacteria from surface coastal seawater and from a 1-year-old DOC drawdown microcosm community. Second, classify the phylogenetic distributing of all isolates by sequencing 16S rDNA and classify the general physiology of each by measuring growth rates in rich media (ZoBell 2216). Third, test the capacity of a phylogenetically diverse subset of purified isolates to consume a measurable amount of ambient DOC relative to AltSIO and diverse seawater communities. Fourth, characterize the bacterial community composition along a transect across a dynamic oceanographic front in the California Current Ecosystem (CCE) by 16S rDNA tag pyrosequencing.

3.5.2 Isolate phylogeny

A diverse set of bacterial isolates was successfully purified from whole seawater and a 1-year-old long-term DOC drawdown bacterial microcosm community. Similar to natural seawater communities of the CCE, purified isolates were dominated by alpha and gammaproteobacteria. Surface samples from the mesotrophic region of the CCE were dominated (79-81%) by alphaproteobacteria (Table 4), but purified isolates in this study were comprised of a near equal proportion of alpha and gammaproteobacteria. While purified isolates spanned 25 unique genera, the dominant taxon of each class observed in the CCE, SAR11 clade and SAR86 clade, respectively,

were not among the cultured isolates. This is an expected result given that neither taxa have yet been cultured on agar surfaces.

Among the culturable taxa, there were strains that appeared overrepresented in the long-term DOC drawdown microcosm isolates including *Labrenzia*, *Sneathiella*, *Kordiimonas*, and *Alcanivorax*. The *Labrenzia* genus is generally characterized as motile, bacteriochlorphy a-containing aerobic anoxygenic photoheterotrophs (Biebl et al. 2007). *Sneeathiella* genus type strain MKT133 is characterized as capable of nitrate reduction, has poly-β-hydroxybutyrate inclusions, but does not assimilate glucose, manose or sucrose (Kurahashi et al. 2008). *Kordiimonas* are generally characterized as motile bacteria capable of degrading a wide range of carbon sources (Xu et al. 2011). The *Alcanivorax* genus is most notably characterized as hydrocarbon-degrading marine bacteria that produce triacylglycerol and wax ester storage lipids (Kalscheuer et al. 2007). There are two potential interpretations for the observation that these genera appeared to dominate the culturable bacteria isolates from the 1 year old microcosm community. First, that these bacteria were best equipped for surviving long-term carbon starvation, or second, that these genera became dominant by metabolizing a significant fraction of the semi-labile DOM pool.

The apparent differential selection of gammaproteobacteria on ZoBell agar and alphaproteobacteria on Noble agar from the same 1 year old seawater community supports the general characterization of gamma Proteobacteria as copiotrophic strategists (Lauro et al. 2009). However, this broad categorical distinction may only be appropriate for describing positive selection of different genera, but not necessarily

inferring physiology. It is notable that all isolates from the long-term DOC drawdown microcosm displayed a mean growth rate more than six times slower than isolates from freshly collected seawater, regardless of phylogenetic affiliation (Table S8). Likewise, isolates collected from the same environment within the same genus, *Alteromonas* for example, displayed growth rates that ranged 12-fold under the same conditions. Together, these data suggest that phylogenetic classification may be valuable for predicting general metabolic capacities shared within or among genera, but physiological rates of individual strains may be more strongly influenced by adaptation to local resource supply and environmental conditions.

3.5.3 Isolate growth and ambient DOC drawdown in unamended seawater

The primary objective of isolating a wide diversity of marine bacteria was to test the capacity of individual bacterial strains to consume a measurable degree of ambient DOC. A total of 270 isolates were originally isolated, and approximately half of those were successfully purified, phylogenetically classified by >1000 bp length 16S sequences, with measured growth rates, and cryogenically preserved for future studies. A total of 28 phylogenetically diverse isolates were selected and screened for positive growth in unamended seawater. Those which showed rapid growth in seawater were then selected for the full experiment testing growth in and consumption of ambient DOM.

While it was hypothesized that bacterial strains isolated from the same environment by the same technique would display a similar capacity to consume

ambient DOC as *Alteromonas* sp. AltSIO, results of these experiments found that no other bacterial strain tested exhibited the capacity to significantly effect measurable changes in DOC concentration when grown in isolation (Fig. 7; Table 2). Besides AltSIO, only one isolate, alphaproteobacterium *Kordiimonas* NA-35, produced a cell yield $>10^5$ mL^{-1}, yet no change in TOC concentration was detected in this treatment. These data suggest that the broad physiological capacity of AltSIO to consume an ecologically relevant fraction of ambient DOC, on par with mixed seawater communities, is not common among readily culturable marine bacteria. While this is an unexpected result, it provides additional impetus to use AltSIO a model to study the apparent unique metabolic requirements that enable efficient consumption of ambient surface ocean DOM.

3.5.4 Bacterial community analysis across an oceanographic front in the California Current Ecosystem (CCE)

A transect was sampled across a highly dynamic front delineating characteristically mesotrophic and oligotrophic oceanographic regimes in the CCE. 16S rDNA tag pyrosequencing identified 1053 OTUs within the sample set. Cluster analysis of 44 samples showed three distinct groups comprised mainly of oligotrophic samples in one group, mesotrophic and front samples in a second group, while all samples from 100 m depth formed a separate third group. These deep samples were characterized as having a relatively high proportion of gammaproteobacteria (Table 9) relative to other depths sampled and were also characterized with large bacteria (≥ 40

fg C $cell^{-1}$) accounting for a significant fraction of total bacterial biomass (Table 3). Finer scale differences showed that within the second group, comprised of mesotrophic samples, the mixed layer through the lower chlorophyll maximum of the front clustered together as unique from all others within that group. These samples within the front were characterized by a relatively high abundance of Bacteroidetes, primarily Flavobacteria, concomitant with a high concentration of diatoms (Taylor et al. 2012), and organic aggregates (Ohman et al. 2012). Members of the Bacteroidetes phyla are commonly observed attached to particulate organic matter (Delong et al. 1993), with preferential uptake of polymers over monomers, and are abundant during and following algal blooms (Pinhassi et al. 2004, Teeling et al. 2012).

While SAR11 and SAR86 both dominated the alpha and gammaproteobacteria, respectively, they each showed a general increase in relative abundance immediately at the front (station A5) from the surface to the lower chlorophyll maximum. This observation is in contrast to what would have been predicted because neither SAR11 nor SAR86 show the genetic requirements for attachment to surfaces or hydrolysis of aggregates, and both have relatively streamlined genomes that may preclude taking full advantage of molecularly complex, recently produced diatom-derived DOM (Giovannoni et al. 2005, Dupont et al. 2012).

The most prominent difference of all 100 m samples, and the most likely contributor driving their divergence from all other samples, is the emergence of deltaproteobacteria. This class was nearly absent from all other depths sampled, but comprised up to 23% of all Proteobacteria in 100 m samples and was comprised

primarily of *Desulfobacterales* and the SAR324 clade (Marine group B). The SAR324 clade is commonly found to peak in abundance in the upper mesopelagic aphotic zone below the deep chlorphyll maximum in the Atlantic and Pacific Oceans (Giovannoni et al. 1996, Fuhrman and Davis 1997, Treusch et al. 2009). Desulfobacterales are characterized as sulfate reducers (Muyzer and Stams 2008) and commonly found in oxygen minimum zones (Canfield et al. 2010) and suboxic marine environments (Rodriguez-Mora et al. 2013). The presence of these two taxa serve as a rational explanation to the observed clustering differences of 100 m bacterial communities from all other samples and provides insight into the transition from the upper auxic photic zone to a substantially different biogeochemical environment.

3.6 ACKNOWLEDGMENTS

We are grateful for the assistance of two volunteers, Benjamin Negrete Jr., high school Biology teacher a Excelsior Academy San Diego, and Emily Shaffer, undergraduate student at UC San Diego who were both instrumental in isolate purification,16S rRNA gene sequencing, and isolate-specific DOC drawdown experiments. Chief scientist Michael Landry, Co-PI Mark Ohman, and all participants of the CCE A-Front study including the captain and crew of the R/V Melville are greatly acknowledged for facilitating sample collection at sea. M. Landry and M. Ohman are also thanked for granting copyright permission to use images that appear in Fig. 5 of this dissertation and originally published in Landry et al. (2012) and Ohman et al. (2012). Scientists at the J. Craig Venter Institute including Chris Dupont, Andy Allen, Hong Zheng, Jing Bai, Ariel Rabines, and Alex Richter are greatly acknowledged for their help processing and analyzing DNA and RNA samples from the CCE. Characterization of bacterial activity across the CCE A-Front was conducted as a collaborative study with Ty Samo. Thank you to Magali Porrachia for assistance with running and troubleshooting the TOC analyzer.

Chapter 3, in part, is being prepared for submission for publication of the material. Pedler, B. E., Samo, T. J., Dupont, C. L., Allen, A. E., Landry, M. R., Azam, F. The dissertation author was the primary investigator and author of this material.

Chapter 3, in part, is also being prepared for submission for publication of the material. Pedler, B. E., Shaffer, E., Aluwihare, L. I., Azam, F. The dissertation author was the primary investigator and author of this material.

3.7 REFERENCES

Beardsley, C., J. Pernthaler, W. Wosniok, and R. Amann. 2003. Are readily culturable bacteria in coastal North Sea waters suppressed by selective grazing mortality? Applied and Environmental Microbiology **69**:2624-2630.

Biebl, H., R. Pukall, H. Luensdorf, S. Schulz, M. Allgaier, B. J. Tindall, and I. Wagner-Doebler. 2007. Description of Labrenzia alexandrii gen. nov., sp nov., a novel alphaproteobacterium containing bacterlochlorophyll a, and a proposal for reclassification of Stappia aggregata as Labrenzia aggregata comb. nov., of Stappia marina as Labrenzia marina comb. nov and of Stappia alba as Labrenzia alba comb. nov., and emended descriptions of the genera Pannonibacter, Stappia and Roseibium, and of the species Roseibium denhamense and Roseibium hamelinense. International Journal of Systematic and Evolutionary Microbiology **57**:1095-1107.

Canfield, D. E., F. J. Stewart, B. Thamdrup, L. De Brabandere, T. Dalsgaard, E. F. Delong, N. P. Revsbech, and O. Ulloa. 2010. A cryptic sulfur cycle in oxygen-minimum-zone waters off the chilean coast. Science **330**:1375-1378.

Delong, E. F., D. G. Franks, and A. L. Alldredge. 1993. Phylogenetic diversity of aggregate-attached vs free-living marine bacterial assemblages. Limnology and Oceanography **38**:924-934.

Dupont, C. L., D. B. Rusch, S. Yooseph, M.-J. Lombardo, R. A. Richter, R. Valas, M. Novotny, J. Yee-Greenbaum, J. D. Selengut, D. H. Haft, A. L. Halpern, R. S. Lasken, K. Nealson, R. Friedman, and J. C. Venter. 2012. Genomic insights to SAR86, an abundant and uncultivated marine bacterial lineage. Isme Journal **6**:1186-1199.

Edgar, R. C. 2013. UPARSE: highly accurate OTU sequences from microbial amplicon reads. Nature Methods **10**:996-998.

Fuhrman, J. A., and A. A. Davis. 1997. Widespread archaea and novel bacteria from the deep sea as shown by 16S rRNA gene sequences. Marine Ecology Progress Series **150**:275-285.

Giovannoni, S. J., M. S. Rappe, K. L. Vergin, and N. L. Adair. 1996. 16S rRNA genes reveal stratified open ocean bacterioplankton populations related to the Green

Non-Sulfur bacteria. Proceedings of the National Academy of Sciences of the United States of America **93**:7979-7984.

Giovannoni, S. J., H. J. Tripp, S. Givan, M. Podar, K. L. Vergin, D. Baptista, L. Bibbs, J. Eads, T. H. Richardson, M. Noordewier, M. S. Rappe, J. M. Short, J. C. Carrington, and E. J. Mathur. 2005. Genome streamlining in a cosmopolitan oceanic bacterium. Science **309**:1242-1245.

Herlemann, D., M. Labrenz, K. Jurgens, S. Bertilsson, J. Waniek, and A. Andersson. 2011. Transitions in bacterial communities along the 2000 km salinity gradient of the Baltic Sea. Isme Journal **5**:1571-1579.

Kalscheuer, R., T. Stoeveken, U. Malkus, R. Reichelt, P. N. Golyshin, J. S. Sabirova, M. Ferrer, K. N. Timmis, and A. Steinbuechel. 2007. Analysis of storage livid accumulation in Alcanivorax borkumensis: Evidence for alternative triacylglycerol biosynthesis routes in bacteria. Journal of Bacteriology **189**:918-928.

Kurahashi, M., Y. Fukunaga, S. Harayarna, and A. Yokota. 2008. Sneathiella glossodoripedis sp nov., a marine alphaproteobacterium isolated from the nudibranch Glossodoris cincta, and proposal of Sneathiellales ord. nov and Sneathiellaceae fam. nov. International Journal of Systematic and Evolutionary Microbiology **58**:548-552.

Landry, M. R., M. D. Ohman, R. Goericke, M. R. Stukel, K. A. Barbeau, R. Bundy, and M. Kahru. 2012. Pelagic community responses to a deep-water front in the California Current Ecosystem: overview of the A-Front Study. Journal of Plankton Research **34**:739-748.

Lauro, F., D. McDougald, T. Thomas, T. Williams, S. Egan, S. Rice, M. DeMaere, L. Ting, H. Ertan, J. Johnson, S. Ferriera, A. Lapidus, I. Anderson, N. Kyrpides, A. Munk, C. Detter, C. Han, M. Brown, F. Robb, S. Kjelleberg, and R. Cavicchioli. 2009. The genomic basis of trophic strategy in marine bacteria. Proceedings of the National Academy of Sciences of the United States of America **106**:15527-15533.

McWilliam, H., W. Li, M. Uludag, S. Squizzato, Y. M. Park, N. Buso, A. P. Cowley, and R. Lopez. 2013. Analysis Tool Web Services from the EMBL-EBI. Nucleic Acids Research **41**:W597-W600.

Muyzer, G., and A. J. M. Stams. 2008. The ecology and biotechnology of sulphate-reducing bacteria. Nature Reviews Microbiology **6**:441-454.

Nelson, C. E., and E. K. Wear. 2014. Microbial diversity and the lability of dissolved organic carbon. Proceedings of the National Academy of Sciences **111**:7166-7167.

Ohman, M. D., J. R. Powell, M. Picheral, and D. W. Jensen. 2012. Mesozooplankton and particulate matter responses to a deep-water frontal system in the southern California Current System. Journal of Plankton Research **34**:815-827.

Pedler, B. E., L. I. Aluwihare, and F. Azam. 2014. Single bacterial strain capable of significant contribution to carbon cycling in the surface ocean. Proceedings of the National Academy of Sciences **111**:7202-7207.

Pinhassi, J., M. M. Sala, H. Havskum, F. Peters, O. Guadayol, A. Malits, and C. Marrase. 2004. Changes in bacterioplankton composition under different phytoplankton regimens. Applied and Environmental Microbiology **70**:6753-6766.

Price, M. N., P. S. Dehal, and A. P. Arkin. 2010. FastTree 2-Approximately Maximum-Likelihood Trees for Large Alignments. Plos One **5**:e9490.

Pruesse, E., J. Peplies, and F. O. Gloeckner. 2012. SINA: Accurate high-throughput multiple sequence alignment of ribosomal RNA genes. Bioinformatics **28**:1823-1829.

Quast, C., E. Pruesse, P. Yilmaz, J. Gerken, T. Schweer, P. Yarza, J. Peplies, and F. O. Gloeckner. 2013. The SILVA ribosomal RNA gene database project: improved data processing and web-based tools. Nucleic Acids Research **41**:D590-D596.

Rodriguez-Mora, M. J., M. I. Scranton, G. T. Taylor, and A. Y. Chistoserdov. 2013. Bacterial community composition in a large marine anoxic basin: a Cariaco Basin time-series survey. Fems Microbiology Ecology **84**:625-639.

Samo, T., B. Pedler, G. Ball, A. Pasulka, A. Taylor, L. Aluwihare, F. Azam, R. Goericke, and M. Landry. 2012. Microbial distribution and activity across a

water mass frontal zone in the California Current Ecosystem. Journal of Plankton Research **34**:802-814.

Schafer, H., P. Servais, and G. Muyzer. 2000. Successional changes in the genetic diversity of a marine bacterial assemblage during confinement. Archives of Microbiology **173**:138-145.

Tada, Y., A. Taniguchi, I. Nagao, T. Miki, M. Uematsu, A. Tsuda, and K. Hamasaki. 2011. Differing Growth Responses of Major Phylogenetic Groups of Marine Bacteria to Natural Phytoplankton Blooms in the Western North Pacific Ocean. Applied and Environmental Microbiology **77**:4055-4065.

Taylor, A. G., R. Goericke, M. R. Landry, K. E. Selph, D. A. Wick, and M. J. Roadman. 2012. Sharp gradients in phytoplankton community structure across a frontal zone in the California Current Ecosystem. Journal of Plankton Research **34**:778-789.

Teeling, H., B. Fuchs, D. Becher, C. Klockow, A. Gardebrecht, C. Bennke, M. Kassabgy, S. Huang, A. Mann, J. Waldmann, M. Weber, A. Klindworth, A. Otto, J. Lange, J. Bernhardt, C. Reinsch, M. Hecker, J. Peplies, F. Bockelmann, U. Callies, G. Gerdts, A. Wichels, K. Wiltshire, F. Glockner, T. Schweder, and R. Amann. 2012. Substrate-controlled succession of marine bacterioplankton populations induced by a phytoplankton bloom. Science **336**:608-611.

Treusch, A. H., K. L. Vergin, L. A. Finlay, M. G. Donatz, R. M. Burton, C. A. Carlson, and S. J. Giovannoni. 2009. Seasonality and vertical structure of microbial communities in an ocean gyre. Isme Journal **3**:1148-1163.

Xu, X. W., Y. Y. Huo, X. D. Bai, C. S. Wang, A. Oren, S. Y. Li, and M. Wu. 2011. Kordiimonas lacus sp. nov., isolated from a ballast water tank, and emended description of the genus Kordiimonas. International Journal of Systematic and Evolutionary Microbiology **61**:422-426.

CHAPTER 4

Physiological and genomic insights into the role of bacterial metabolism on the alteration and efficient removal of marine dissolved organic matter

4.1 ABSTRACT

The marine bacteria *Alteromonas* sp. strain AltSIO was previously found to degrade a significant fraction of marine dissolved organic matter (DOM). In this study, the broad potential of AltSIO to significantly alter and consume ambient marine DOM, with particular attention to carbohydrates, was investigated by multiple approaches including direct physiological measurements, genome analysis, and DOM composition characterization from incubation experiments. Results show that AltSIO has a particularly broad capacity to degrade carbohydrates. Growth in seawater incubations with individual neutral sugars and radiolabeled sugar uptake experiments showed that AltSIO preferentially utilizes disaccharides and galactose, but does not incorporate or respire glucose. Genome analysis confirms that this strain lacks a glucose-specific permease required for the exogenous uptake of glucose, but is endowed with a number of carbohydrate-specific transporters not found in genomes of closely related bacterial strains. Genomic insights also show the potential to reduce nitrate, a high capacity to scavenge iron, and a complete chemotaxis apparatus potentially used for disaccharide acquisition. DOM characterization by ultrahigh resolution mass spectrometry shows that AltSIO and diverse seawater communities significantly alter the composition of ambient DOM.

4.2 INTRODUCTION

Bacteria are the primary biotic force responsible for remineralizing DOM, and myriad metabolic strategies for survival on this resource have emerged. Some have

evolved into metabolically streamlined specialists, *a la* Pelagibacter ubique SAR11 (Giovannoni et al. 2005), with small genomes, small cell size, and relatively narrow metabolic capacity. Others have evolved to employ a strategy characterized by rapid growth rates, large cell and genome size, and relatively broad metabolic potential (Lauro et al. 2009). *Alteromonas* sp. strain AltSIO has been shown to grow rapidly in unamended seawater with only ambient DOC and thus falls within the category of a generalist.

Approximately 40% of total marine DOC in the surface ocean is comprised of carbohydrates (Pakulski and Benner 1994) and the majority therein is characterized as hydrolysable neutral sugars (McCarthy et al. 1996, Aluwihare et al. 1997, Skoog and Benner 1997). These sugars include fucose, rhamnose, arabinose, galactose, glucose, mannose, and xylose, and together have a wide range of reported bioavailabity for bacterial degradation (Cowie and Hedges 1994, Kirchman et al. 2001). It is important to note that concentrations of these sugars are measured in seawater after acid hydrolysis, and are thus not necessarily found as free monosaccharides in seawater. In fact, the majority of neutral sugars in the surface ocean exist as oligosaccharides and polysaccharides (Benner 2002).

In this study, the broad potential of AltSIO to significantly alter and consume ambient marine DOM, with particular attention on carbohydrates, was investigated by multiple approaches including direct physiological measurements, genome analysis, and DOM composition characterization. Physiology experiments included characterization of enzyme activity, testing oxidation of 95 individual substrates,

growth response in neutral sugar-amended seawater incubations, and radiolabeled sugar incorporation measurements. Additional insight into potential physiological capacity of AltSIO was provided by genomic analysis. The ability of AltSIO to significantly alter ambient DOM composition was investigated in a time course experiment characterizing DOM composition by Fourier transform ion cyclotron resonance mass spectrometry (FT-ICR-MS) (Kujawinski et al. 2009, Bhatia et al. 2010).

4.3 Methods

4.3.1 Alteromonas AltSIO hydrolytic enzyme activity

Ectoenzyme activity of AltSIO was assayed using fluorogenic substrates (Hoppe 1983, Hoppe et al. 1988) derived from 7-amino-4-methylcoumarin (AMC) and 4-methyl-umbelliferone (MUF) as described (Martinez et al. 1996). Protease activity was measured as the hydrolysis rate of leucine-AMC. α-D-glucosidase was assayed as the hydrolysis rates of MUF α-D-glucoside. β-D-galactosidase was measured as the hydrolysis rate of MUF-β-D-galactoside. MUF-oleate was used to assay lipase activity. AltSIO was grown in overnight culture in ZoBell media, pelleted by centrifugation at 6000xg for 5 min, and washed 2x with AFSW, and resuspended in AFSW for enzyme assay incubations at 22^{o}C.

AltSIO was streaked onto a low nutrient ZoBell/1000 agar plate from a -80^{o}C cryogenically preserved glycerol stock, grown for 2 d at 22^{o}C, then a single colony was used to inoculate a liquid culture for growth in AFSW. After 3 d of growth in and

while still in exponential growth phase, 3 mL aliquots were added to 7 mL autoclave-sterilized borosilicate glass tubes and incubated in the dark in triplicate with 20 μM of each fluorogenic substrate. Blanks consisted of AFSW incubated in triplicate with each substrate. Solutions of MUF and AMC were used to generate standard curves.

4.3.2 Bacterial isolate-specific single substrate metabolism

The ability to metabolize a suite of 95 individual substrates was tested using BioLog GN2 microplates (Biolog, Inc., Hayward, CA) containing broad chemical classes including polysaccharides, carbohydrates, carboxylic acids, organic acids, amino acids, and peptides.

Single substrate metabolism of five bacterial isolates was tested including *Alteromonas* sp. strain AltSIO, *Pseudoalteromonas* TW7, *Vibrionacea* SWAT-3, Flavobacerium BBFL7, and Roseobacter *Rugeria pomeroyii* DSS-3. Bacteria were grown in ZoBell medium (5 g peptone, 1 g yeast extract, L^{-1} seawater) in over night culture, shaken at 170 rpm at 22^{o}C. Cultures were pelleted by centrifugation at 6,000xg, and washed 2x with autoclave-sterilized, GF/F-filtered Scripps pier seawater (AFSW). Cells were resuspended in AFSW to a final cell density of 50% transmittance (~0.30 optical density at 600nm), equivalent to approximately 10^8 cells mL^{-1} per manufacturer's recommendation. Cell suspensions (150 μL) of each isolate were added to three separate 96-well plates and incubated in the dark. In addition to single substrates, each well contained the redox indicator tetrazolium violet, which served as an indicator of cellular respiration. Inoculated wells without substrate served

as the control. Development of insoluble purple tetrazolium salt was measured by the absorbance at 590 nm using a microplate reader (Molecular Devises). Measurements were made after 2 h of inoculation, then every 24 h for 5 d. Each individual well was scored as "positive" if the absorbance measured ≥ 2x the absorbance of the blank well within 48h. Each isolate was scored as "positive" for the ability to metabolize a particular substrate if at least 2 of 3 replicate plates indicated a positive result.

4.3.3 AltSIO growth response to single sugars in seawater

AltSIO was grown from a -80^{o}C glycerol stock as described above, and inoculated into AFSW, grown for 4 d in the dark at 16^{o}C, transferred to a fresh batch of AFSW, grown for 2 d, then used to inoculate 3.5 L of freshly collected 0.1 µm filtered seawater. Seawater was collected from the Scripps pier on 18 March 2014 during an incoming tide as described in Chapter 1. Briefly, whole seawater was gravity filtered through pre-combusted GF/F filters, then filtered through a pre-flushed 0.1 µm PES filter membrane using a peristaltic pump. AltSIO was grown in 0.1 µm FSW for 5.5 d to allow for the consumption of labile DOM, then 200 mL of the culture was aliquoted into 15 1-L precombusted glass Erlenmeyer flasks. To each treatment flask, 1 µM NH_4NO_3 and 2 µM of each sugar was added. Additional treatments included 2 x 10^4 x diluted ZoBell media, a DOC re-feed where AltSIO was diluted ~90% and replenished with the original 0.1 µm FSW. Two controls included the addition of i) 1 µM NH_4NO_3 only, and ii) no addition. Samples for bacterial counts were collected in duplicate for a total of 5d. Initially, samples were collected every 2 h

for 12 h, then every 6h for 12 h, then every 24 h for the remainder of the experiment. On day 5, samples were diluted 10^3x and 10^4x and plated onto ZoBell agar to assay total viable cells by enumeration of colony forming units (CFU). Samples for TOC analysis were collected at d 0 before and after sugar addition, and at d 5.

4.3.4 AltSIO incorporation of individual sugars

The incorporation by *Alteromonas* AltSIO of ^{14}C-glucose (Moravek Biochemicals, Inc., Brea, CA), ^{14}C-fructose (Moravek Biochemicals, Inc., Brea, CA), and ^{14}C-galactose (MP Biomedicals) was tested. AltSIO was grown in AFSW for 2 to 4 d at 16^{o}C as described above, then incubated with 50 nM radiolabeled glucose (255 mCi/mmol), fructose (240 mCi/mmol), and galactose (108 mCi/mmol) for 16 h. Formaldehyde (2% final conc. vol/vol) was added to formaldehyde-killed controls prior to substrate addition. After incubation, treatment and control samples were divided into 2 mL aliquots in triplicate, cells were pelleted by centrifugation at 16,000xg at 4^{o}C for 10 m, and supernatant was transferred to new 2 mL tubes by pipet and saved. Cells were washed with 1 mL ice cold AFSW, centrifuged a second time as above, supernatant was poured off, and 1 mL of EcoLite liquid scintillation cocktail (MP Biomedicals, Solon, OH) was added to each tube. All samples were placed on ice while individual tubes were being processed. From each sample, 100 µL of supernatant was removed and added to a scintillation vial with 5 mL scintillation cocktail to quantify total radioactivity in solution. Remaining supernatant was immediately frozen at -20^{o}C. Each sample was counted for ^{14}C

disintegrations per minute (DPM) by liquid scintillation counter (PerkinElmer) for 10 minutes.

4.3.5 AltSIO uptake and incorporation of L-leucine

The uptake and incorporation by *Alteromonas* AltSIO of ^{3}H-L-leucine was tested. AltSIO was grown in AFSW as described for single sugar uptake assays. AltSIO was incubated with a calculated concentration of 1, 3 and 10 nM ^{3}H-L-leucine (144 Ci/mmol) for 1.5 h at 16^{o}C. Control samples were placed on ice 15 m prior to substrate addition and remained on ice for the duration of the experiment. All samples were processed in an identical manner to ^{14}C-sugar uptake experimental procedures.

4.3.6 Alteromonas AltSIO cell-specific C, N, P ratios

AltSIO was inoculated into 0.1 μm filtered, 8-month aged, seawater collected from Bergen Norway, and grown in the dark at 22^{o}C for 10 d. Samples were collected on d 0, 1, 2, 3, and 10. Measurements were made for bacterial abundance, TOC concentration, and transmission electron microscopy (TEM) and TEM X-ray microanalysis (XRMA) to calculate individual cell C, N, and P ratios as described (Norland et al. 1995).

4.3.7 Alteromonas AltSIO genome sequence

A single colony of AltSIO was picked from a freshly streaked agar plate and used to inoculate 50 mL of ZoBell media. The culture was grown overnight at 22^{o}C

and shaken at 170 rpm. Cells were pelleted (24 x 1 mL) by centrifugation at 8000 xg for 5 min. Supernatant was discarded and DNA extraction and cleanup was performed using the Nucleospin Tissue DNA extraction kit (Machery Nagel). Initial DNA concentration and purity was assayed using a NanoDrop spectrophotometer (Thermo Fisher Scientific), followed by the Quanti-it PicoGreen dsDNA quantification kit (Invitrogen). Purified DNA was sent to the U.S. Dept. of Energy Joint Genome Institute (JGI) for sequencing as part of the Community Science Program (CSP). DNA was sequenced through JGI's Microbial Standard Draft Genome and Microbial Paired Ends pipelines using Illumina HiSeq 2000, and Improved Draft Finishing using PacBio sequencing. The permanent draft genome was analyzed using JGI's Integrated Microbial Genomes Expert Review (IMG-ER) online portal (Markowitz et al. 2009).

4.3.8 Impact of AltSIO on dissolved organic matter composition measured by FT-ICR-MS

Prior to seawater filtration, 3 separate 0.1 μm Supor membrane cartridge filters (Pall, AcroPak 1000) were flushed with Milli-Q water, filled and soaked with 0.01 M trace metal grade HCL for 24 h, then flushed again with Milli-Q water for 1 h prior to seawater filtration. Seawater was collected from the Scripps pier in 40 L batches using two 20 L acid-washed polycarbonate carboys and used to fill two 200 L drums lined with Teflon bags. Whole seawater was filtered through a 0.1 μm cartridge filters (~150L/cartridge) using a peristaltic pump fitted with PharMed BPT Masterfled tubing (Cole-Parmer, Vernon Hills, IL) connected to Teflon tubing (Nalgene, Rochester,

NY). Filtrate was dispensed into 15 20L fluorinated high density polyethylene (F-HDPE) carboys. Each carboy was filled with ~1 L of filtrate at a time and sequentially rotated through in an effort to maintain sample homogeneity between carboys. Filtered seawater was then stored at 16°C for 12 h before a second filtration through a new pre-cleaned 0.1 µm cartridge filter performed in a ultraviolet (UV) light-sterilized laminar flow hood. Filtrate was dispensed into acid washed, milli-q rinsed, UV-sterilized, 20 L polycarbonate carboys that had been previously rinsed 2x with ~500 mL 0.1 µm FSW.

4.3.8.1 Experimental setup

Experimental treatments included i) AltSIO in pure culture (6 carboy replicates); ii) free-living seawater community (SWC) comprised of 10% GF/F FSW (3 carboy replicates); iii) SWC inoculated with AltSIO (3 carboy replicates); and iv) bacteria free, filter-sterilized seawater control (1 carboy). Carboys were sampled for bacterial abundance and TOC daily for 10 d, and on d 40. On d 2, 3, 5, and 10, ~2L from duplicate carboys of each treatment was filtered onto 0.2 µm Sterivex (Millipore, Billerica, MA) cartridge filters using a peristaltic pump and immediately frozen at -80°C for later nucleic acid analysis. On d 0, 3, 5, 10, and 41 1L was samples were collected for DOC analysis by ultra high resolution mass spectrometry.

4.3.8.2 FT-ICR-MS DOM sample collection

Using a peristaltic pump, one liter of sample was filtered through 0.2 µm Omnipore PTFE hydrophilic Teflon membranes (Millipore) placed inside 47 mm

PTFE filter holders (Cole-Parmer) attached to Teflon tubing (Nalgene) and connected to PharMed BPT tubing (Masterflex) with Teflon connector fittings (Cole-Parmer). The complete filtration setup including all tubing, filter holder, and filter was flushed with 1L of Milli-Q, then ~400 mL seawater sample prior to DOM sample collection. Filtered seawater was collected in 1L polycarbonate containers after rinsing with 10% trace metal grade HCl, and followed by Milli-Q water, then rinsed 2x with ~200 mL filtered sample. DOM samples were then acidified to pH 2.5 by addition of 16 drops of 12M trace metal grade HCl dispensed from a Teflon dropper, and stored at 4^{o}C in the dark until DOM extraction.

4.3.8.3 FT-ICR-MS DOM Extraction

DOM was extracted from 0.2 μm-filtered seawater using 6 mL Bond Elut PPL solid phase extraction cartridges (Agilent) as described by Dittmar et al. (2008). Briefly, cartridges were rinsed with 8 x 1 mL of 100% methanol (Optima grade), then 1L seawater samples were loaded onto and passed through a cartridge using an extraction manifold, vacuum pump, and Teflon tubing. The cartridge was then rinsed with 8 x 1 mL of 0.01 M HCL and dried for 5 m with the vacuum on. DOM was eluted from the column with 2 x 4 mL 100% methanol by gravity, transferred to combusted amber glass vials with Teflon lined caps (National Scientific), and stored at -20^{o}C.

4.3.8.4 Analysis of DOM by FT-ICR-MS

Ultrahigh resolution mass spectrometry was performed using a Thermo Scientific 7 Tesla electrospray ionization Fourier transform ion, cyclotron resonance, mass spectrometer (ESI FT-ICR-MS) located at the Woods Hole Oceanographic Institution as described (Bhatia et al. 2010, Soule et al. 2010). Immediately preceding MS analysis, samples were dried under a steady stream of N_2 gas, dissolved in ultrapure water to a concentration of 1 mg/ml and a 1:4 dilution of each sample was prepared in 50:50 MeOH:water for analysis in negative ion mode. Dilutions were prepared immediately before analysis to limit ester formation (McIntyre and McRae 2005).

4.3.8.5 FT-ICR-MS Data processing and statistical analysis

Spectra were aligned as described (Soule et al. 2010) to generate a list of m/z values from all spectra and compiled into a single matrix of 24 samples by 15, 298 peaks with unique atomic masses. The relative peak heights were then transformed to presence (peak height = 1) or absence (peak height = 0) and normalized to the total number of m/z values within each spectrum. This transformation does not account for differences in relative peak height between m/z values within and among spectra. A distance matrix cluster analysis (e.g. (Koch et al. 2005) was calculated between all samples using Bray–Curtis distance measure and Ward's linkage method and using PC-ORD. One sample was removed from all analysis because it failed to ionize and produce a comparable number of detectable peaks relative to all other samples. Two

additional samples were removed from the analysis because they did not ionize efficiently on the instrument, and thus were not comparable to other samples.

Data processing and statistical analyses were preformed using GraphPad Prism® for Mac OS X version 6.0C (GraphPad Software, Inc., La Jolla, CA), PC-ORD 6 (MjM Software Design, Gleneden Beach, Oregon), and Matlab R2013a for Mac OS X version 8.1.0.604 (Mathworks, Inc., Natick, MA).

4.4 RESULTS

4.4.1 Single compound metabolism

A comparative analysis of the AltSIO metabolic profile with four other phyogenetically diverse bacterial strains was conducted by testing the capacity to metabolize 95 individual substrates of broad chemical classes (Fig. 9 and Table S13). Results show that AltSIO has the capacity to metabolize the broadest range of substrates in all chemical categories relative to other isolates tested (Fig 9). AltSIO showed a positive metabolic response for 62 compounds compared with 29, 36, 40, and 18 for TW7, SWAT3, DSS-3, and BBFL-7, respectively. AltSIO showed particular affinity for carbohydrate processing, showing a positive metabolic capacity for nearly twice as many carbohydrates as the two other gammaproteobacteria, Pseudoalteromonas sp. TW7 and Vibrio sp. SWAT3. AltSIO metabolized all L-amino acids tested, but no D-amino acids (Table S13).

4.4.2 Ateromonas AltSIO hydrolytic enzyme activity

AltSIO displayed measureable enzyme activity for all enzymes tested except for lipase (Table 10). Cell-specific enzyme activities were comparable to the range of those measured among 44 marine bacterial strains isolated from the Scripps pier (Martinez et al. 1996) and demonstrates that AltSIO has the capacity to hydrolyze leucine from aminopeptides, and galactose, glucose, and phosphate moieties from organic polymers. While measurements of protease and alkaline phosphatase were relatively low compared with the maximum range observed for other isolates (4.2–3810, and 0.7– 410 x 10^{-18} mole $cell^{-1}$ hr^{-1}, respectively), AltSIO cell-specific α-D-glucosidase activity was 50% greater than the highest measured rate among 44 marine isolates from the Scripps pier (Martinez et al. 1996).

Table 10. AltSIO cell-specific hydrolytic enzyme activity

Enzyme	Hydrolysis rate (10^{-18} mole $cell^{-1}$ hr^{-1})	
	mean	s.d.
Leucine aminopeptidase	46.3	1.9
Alkaline phosphatase	35.8	0.8
β-D-galactosidase	18.8	3.8
α-D-glucosidase	12.5	4.3
lipase	n.d.	

4.4.3 Alteromonas AltSIO cell-specific C, N, P ratios

Experimental results of cellular C:N:P measurements during DOC drawdown are summarized in Table 11. Between d 0 and d 10, cell abundance increased from

~10^5 to 3.7 x 10^6 cells mL^{-1}, and TOC concentration decreased from 127 to 70 μM C. Cellular ratios of C:N:P were high relative to average marine bacteria that typically have a C:P ratio of 50 (Fagerbakke et al. 1996). TEM analysis showed the presence of electron-light cellular inclusions in AltSIO cells (Fig. 10). Similar inclusions were observed among FISH-identified *Vibrio splendidus* cells in a seawater mesocosms experiment amended with excess glucose (Ovreas et al. 2003). The *V. spendidus* cells had a measured C:N:P ratio of 260:37:1 (Ovreas et al. 2003) using the same method and same instrument as was used in this study.

4.4.4 AltSIO growth response to single sugars in 0.1 μm filtered seawater

The metabolic capacity of AltSIO to utilize specific sugars including disaccharides, monosaccharaides, hexose sugars and pentose sugars was tested. The potential for the addition of specific sugars to stimulate co-metabolism of operationally defined semi-labile DOM was also tested by first incubating AltSIO for 5 d in ambient DOM (0.1 μm filtered seawater) to exhaust the labile DOM fraction. AltSIO was supplemented with 1 μM ammonium nitrate and 2 μM of each sugar. A control treatment amended with only NH_4NO_3 was included to test for the potential for nitrogen limitation on otherwise labile DOC.

The growth response was quantified as total cell abundance and total viable cells in 11 sugar treatments, one treatment of complex substrate addition comprised of dilute ZoBell media, ambient DOM replenishment, a NH_4NO_3-only control, and a negative control with no substrate or NH_4NO_3 addition. After 5 d of incubation, large

Table 11. C:N:P elemental ratios of AltSIO grown in marine DOM. Elemental ratios are the average of measurements made on 37-45 cells per time point. The mean C:N:P of 124 cells collected from d 1-3 measured 212:54:1. n.m., not measured.

Time (d)	TOC, µmol C L^{-1} (± s.d.)	Cells mL^{-1} (± s.d.)	C:N:P (atom · $atom^{-1}$)
0	126.5 (1.7)	1.02×10^5 (9.03×10^4)	n.m.
1	129.5 (2.2)	3.32×10^5 (8.21×10^4)	279:49:1
2	118.6 (0.6)	5.61×10^5 (1.99×10^5)	217:61:1
3	73.7 (1.0)	3.43×10^6 (1.30×10^5)	179:49:1
10	70.2 (0.6)	3.69×10^6 (1.84×10^5)	n.m.

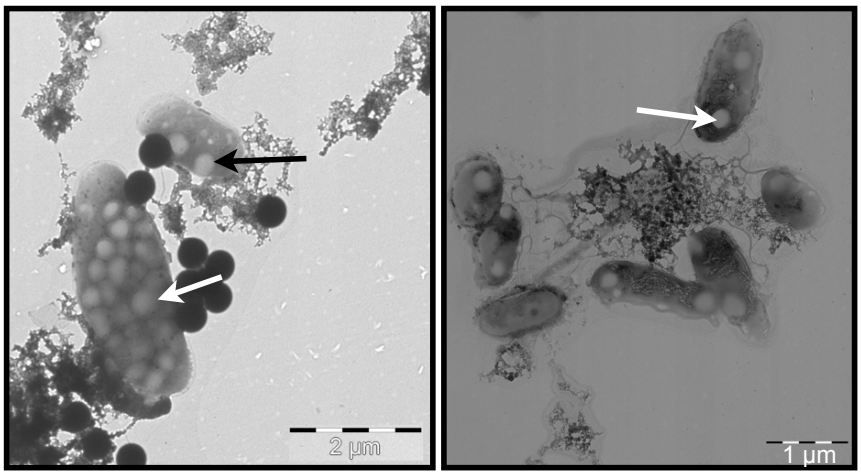

Figure 10. Transmission electron microscopy (TEM) images of non-fixed, non-stained, air-dried Alteromonas sp. AltSIO cells grown in 0.1 µm filtered aged seawater. Scale bars are 2 µm (left panel) and 1 µm (right panel). Electron-light cellular inclusions are noted with red arrows. Electron dense spheres in left panel are latex reference beads.

differences in total cell abundance and viable cell counts were observed between treatments (Fig 11A). Cell abundance above that measure in the NH_4NO_3-only control was only observed in 4 treatments including sucrose, mannose, galactose, and dilute ZoBell media amendments (Fig. 11A).

TOC measurements were made to determine the initial ambient TOC concentration of the filtered source water, the total concentration of carbon added in each substrate treatment, and the decrease in TOC concentration after 5 d. Because TOC measurements were analyzed from unfiltered samples, decreases in TOC concentration are directly attributed to bacterial carbon respiration. Measurable decreases in TOC after 5 d of incubation were detected in 10 of the 15 treatments. No measurable changes in TOC concentration were detected in the fucose, rhamnose, sorbose, and fructose or DOC re-feed treatments. The greatest absolute changes in TOC concentration were observed in sucrose, maltose, galactose and dilute ZoBell substrate additions. DOC drawdown of each treatment was calculated by subtracting bacterial biomass carbon from measured TOC concentrations. Biomass C was calculated by multiplying total cell concentration by empirically derived AltSIO-specific carbon content of 63 fg C $cell^{-1}$ (Chapter 2) (Pedler et al. 2014). Three sugar amendments including maltose, galactose, and sucrose resulted in enhanced DOC drawdown below initial pre-amendment TOC concentration by 8.2, 6.2, and 4.7 µM C, respectively.

4.4.5 AltSIO incorporation of ^{14}C-labeled sugars and ^{3}H-labeled L-leucine

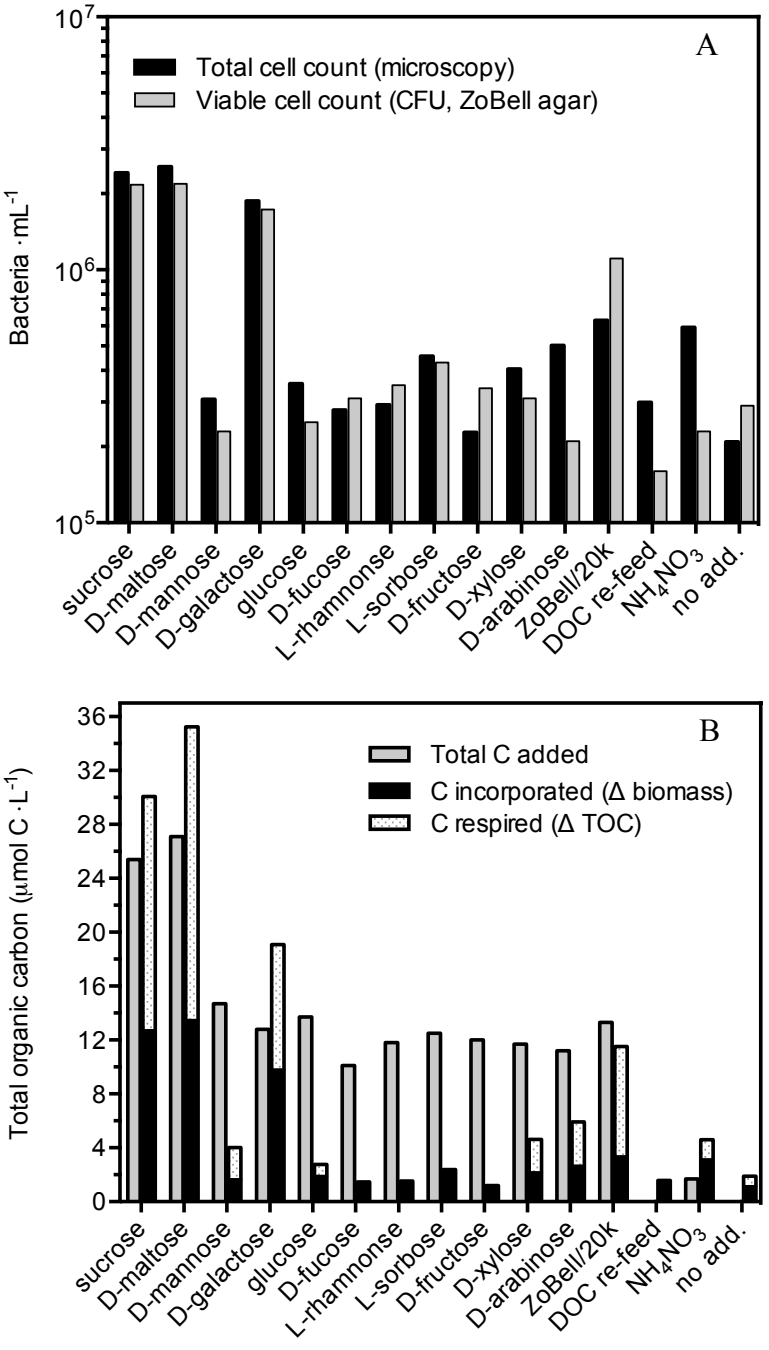

Figure 11. AltSIO growth and metabolic response to neutral sugar-amended 0.1 µm-filtered seawater. A) Bacterial abundance measured by direct cell counts via microscopy, and viable cell counts measured by colony forming units (CFU) on ZoBell agar plates. B) Sugar treatment-specific metabolic carbon partitioning measured by changes in bacterial biomass and TOC concentration as determined by high temperature combustion.

In two separate experiments, the incorporation of ^{14}C-labeled glucose was not detectable when incubated with 100 nM substrate for 1 h (Table 12). Incubation of the same batch culture on the same day under identical conditions showed that AltSIO actively incorporated ^{3}H-L-leucine at a rate of 0.4, 0.7, and 3.0 amol cell^{-1} h^{-1} when incubated with 0.7, 2.1, and 6.9 nM leucine, respectively (Table 12). Longer incubations (15.8 h) with ^{14}C -labeled glucose, fructose, and galactose (individually) showed negligible incorporation of glucose and fructose (0.063 and 0.009 x 10^{-18} mol cell^{-1}), but a total incorporation of 13.01 x 10^{-18} mol cell^{-1} of galactose at a rate of 0.82 ± 0.26 x 10^{-18} mol cell^{-1} h^{-1}. With an average cell size of 0.72 μm^3 (Pedler et al. 2014, Chapter 2), equivalent to an internal cell volume 0.72 x 10^{-15} L, AltSIO incorporated galactose to an internal concentration of 18 mM.

4.4.6 Alteromonas AltSIO 16S phylogeny and genome sequence

The genome sequence of AltSIO consisted of 4.6 Mbp assembled into a single DNA scaffold/chromosome with 4040 total genes, and 3941 protein coding genes with associated function predictions for 80% (Table S9). AltSIO shares ~99% 16S sequence homology with *Alteromonas macleodii* strains i) Balearic Sea AD45, ii) Aegean Sea MED64, and iii) AltDE1 isolated from 1000 m depth of the Eastern Mediterranean Sea (Fig. 12). However, average nucleotide identity (ANI; http://enve-omics.ce.gatech.edu/) scores comparing AltSIO with AD45, AltDE1, and MED64, measured 86.06, 85.55, and 85.41 % respectively. Thus, using ANI as a classifying metric AltSIO is a separate bacterial species. Despite their nucleotide differences,

Table 12. Radiolabeled glucose, fructose, galactose, and leucine uptake measured in AltSIO grown in GF/F-filtered, autoclave sterilized aged seawater.

Exp. Date	Culture batch ID, age (d)	Cell abundance (mL^{-1})	Substrate & spec. act. ($Ci \cdot mmol^{-1}$)	Substrate addition (10^{-9} mol • L^{-1})	Incubation time (h)	Incorporated (10^{-18} mol • $cell^{-1}$)	Incorporation rate (10^{-18} mol • $cell^{-1}$ • h^{-1})	Incorporated substrate conc. $cell^{-1}$ (10^{-3} mol • L^{-1})
7 Apr. 2014	A, 2	n.m.	^{14}C-glucose (0.255)	100	1.1	n.d.		
10 Apr. 2014	B, 3	5.84 x 10^4	^{14}C-glucose (0.255)	100	1.0	n.d.		
11 Apr. 2014	B, 4	2.59 x 10^5	^{14}C-glucose (0.255)	52	15.8	0.063 ± 0.020	0.004 ± 0.001	0.088 ± 0.000
11 Apr. 2014	B, 4	2.59 x 10^5	^{14}C-fructose (0.240)	43	15.8	0.009 ± 0.020	0.001 ± 0.001	0.013 ±0.027
11 Apr. 2014	B, 4	2.59 x 10^5	^{14}C-galactose (0.108)	23	15.8	13.01 ± 4.14	0.82 ± 0.26	18.07 ± 5.74
10 Apr. 2014	B, 3.5	1.82 x 105	^{3}H-Leucine (144)	0.7	1.4	0.57 ± 0.09	0.40 ± 0.06	0.79 ± 0.12
10 Apr. 2014	B, 3.5	1.82 x 105	^{3}H-Leucine (144)	2.1	1.4	1.05 ± 0.88	0.73 ± 0.62	1.46 ± 1.22
10 Apr. 2014	B, 3.5	1.82 x 105	^{3}H-Leucine (144)	6.9	1.4	4.35 ± 1.34	3.04 ± 0.93	6.04 ± 1.86

Values with associated error are mean ± standard deviation of 3 to 4 methodological vial replicates. Abbreviations: n.m., not measured; Exp., experiment; n.d., not detected; spec. act., radioisotope specific activity.

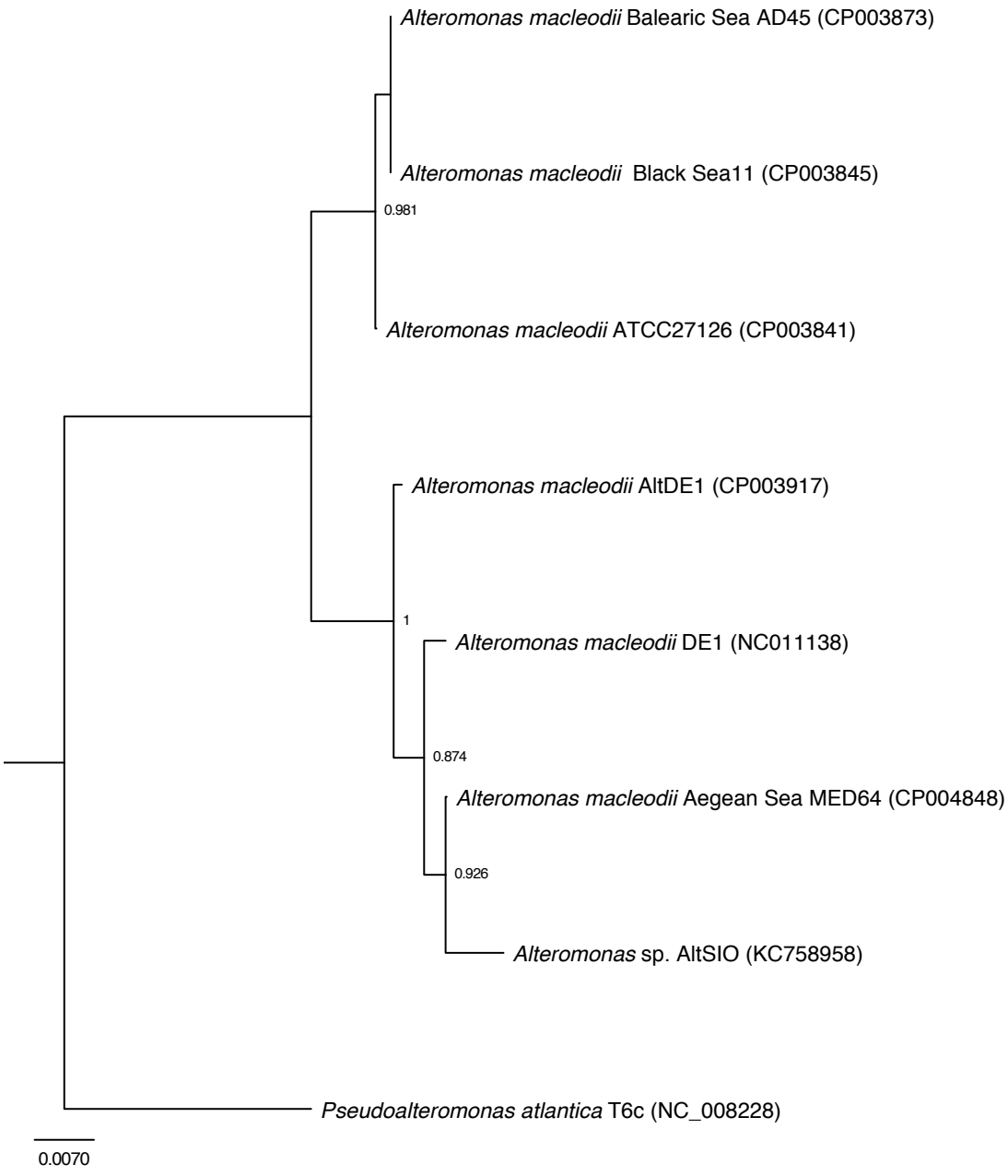

Figure 12. Maximum likelihood phylogenetic tree of the 16S rRNA gene of AltSIO relative to closely related *Alteromonas macleodii* strains with publicly available genomes (JGI IMG). Confidence values are indicated at each node (n=1000 permutations). Scale bar represents phylogenetic distance of 0.007.

general genome characteristic and predicted clusters of orthologous groups (COGs) of proteins show that the AltSIO genome is highly similar to the *A. macleodii* strains with a nearly identical number of genes in each COG category (Table S10).

A total of 87 COGs were identified with predicted functions related to carbohydrate metabolism (Table S11). Six carbohydrate-processing COGs were identified as unique to AltSIO and absent from all 3 other *Alteromonas macleodii* genomes, and an additional 8 COGs absent from at least one other genome. Except for the predicted exopolysaccharide biosynthesis protein, all other unique COGs were characterized as having a role in carbohydrate metabolism. No carbohydrate-related COGs identified in any of the *A. macleodii* strains were absent from the AltSIO genome. A total of 38 COGs were identified as unique to AltSIO (Table S12), and while spanning all predicted functions, they were dominated by sugar transport and sugar metabolism functions.

Three of the unique COGs had predicted functions specific to outer membrane modifications and/or stabilization, including i) celD, a protein involved in bacterial cellulose biosynthesis, ii) sortase, a surface protein transpeptidase involved in attaching proteins to the cell wall, and iii) a COG identified as bacterial surface proteins containing Ig-like domains. Additionally, AltSIO has 31 genes related to maintaining membrane potential, 21 specific to H+/Na+ translocation for energizing its flagellar motor, and 10 specific to the F-type ATPase superfamily.

Additional genes unique to AltSIO include cytochrome c551/c552 and a nitrate/nitrite transporter. Cytochrome c551/c552 plays a role in electron transport

during respiration, and in *Pseudomonas aeruginosa*, functions as an electron donor for the nitrate reductase enzyme (Bertini et al. 2006). Based on KEGG orthology, AltSIO has all required components to execute nitrate and nitrite reduction including nitrate/nitrite periplasmic binding proteins, permeases, transporters and nitrate and nitrite reductases.

AltSIO possesses two ferridoxins not present in *A. macloedii*, NAD+ reductase (hcaD), an iron-containing odixoreductase, and 2Fe-2S (fdx) involved in iron-sulfur cluster biogenesis (Schroder et al. 2003). AltSIO also has 57 separate protein coding genes annotated as belonging to the outer membrane receptor (OMR) superfamily of membrane transporters. All OMRs were annotated as transporters for iron, iron-siderophores, or vitamin B12 (cobolamin), including a divalent cation Fe2/Zn2 permease. The three *A. macleodii* strains had a comparable number (42 to 59) of Fe-related OMRs. In contrast, Pelagibacter ubique, SAR11 (HTCC 1062) has just a single protein annotated as belonging to the TonB/OMR superfamily of transporters.

Additional genes of notable predicted functions, but not unique to AltSIO include 3 genes related to 3-hydroxybutyrate dehydrogenase and/or depolymerase involved in the synthesis and breakdown of β-hydroxybutyrate storage bodies (ketone bodies) to citric acid, and a carbon-starvation response gene (cstA) involved in nutrient scavenging in *Escherichia coli* (Schultz and Matin 1991). Lastly, AltSIO and the four *A. macleodii* genomes all contain complete annotated bacterial chemotaxis systems coupled with the chemotaxis pathway-associated dipeptide binding and

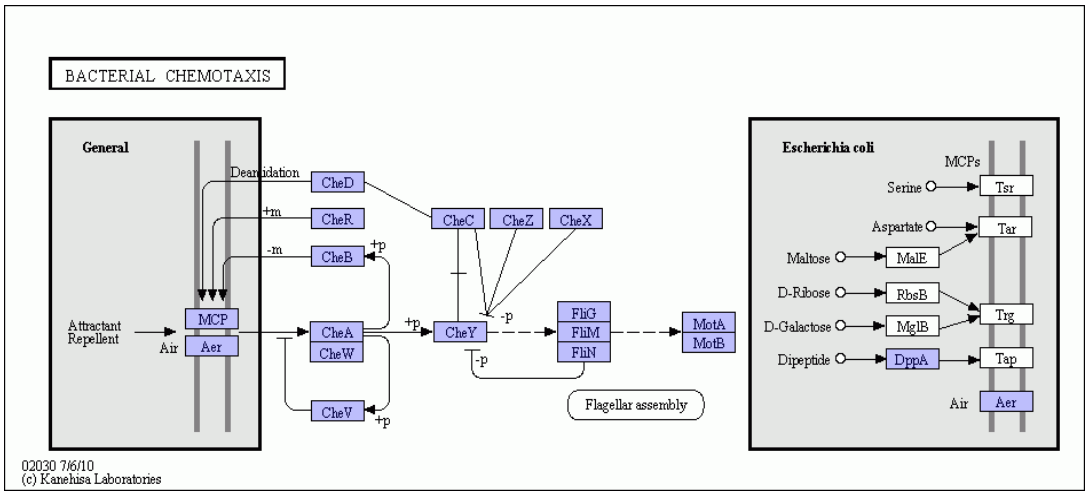

Figure 13. KEGG pathway of bacterial (*E. coli*) chemotaxis in with enzymes present in AltSIO genome highlighted with filled purple boxes.

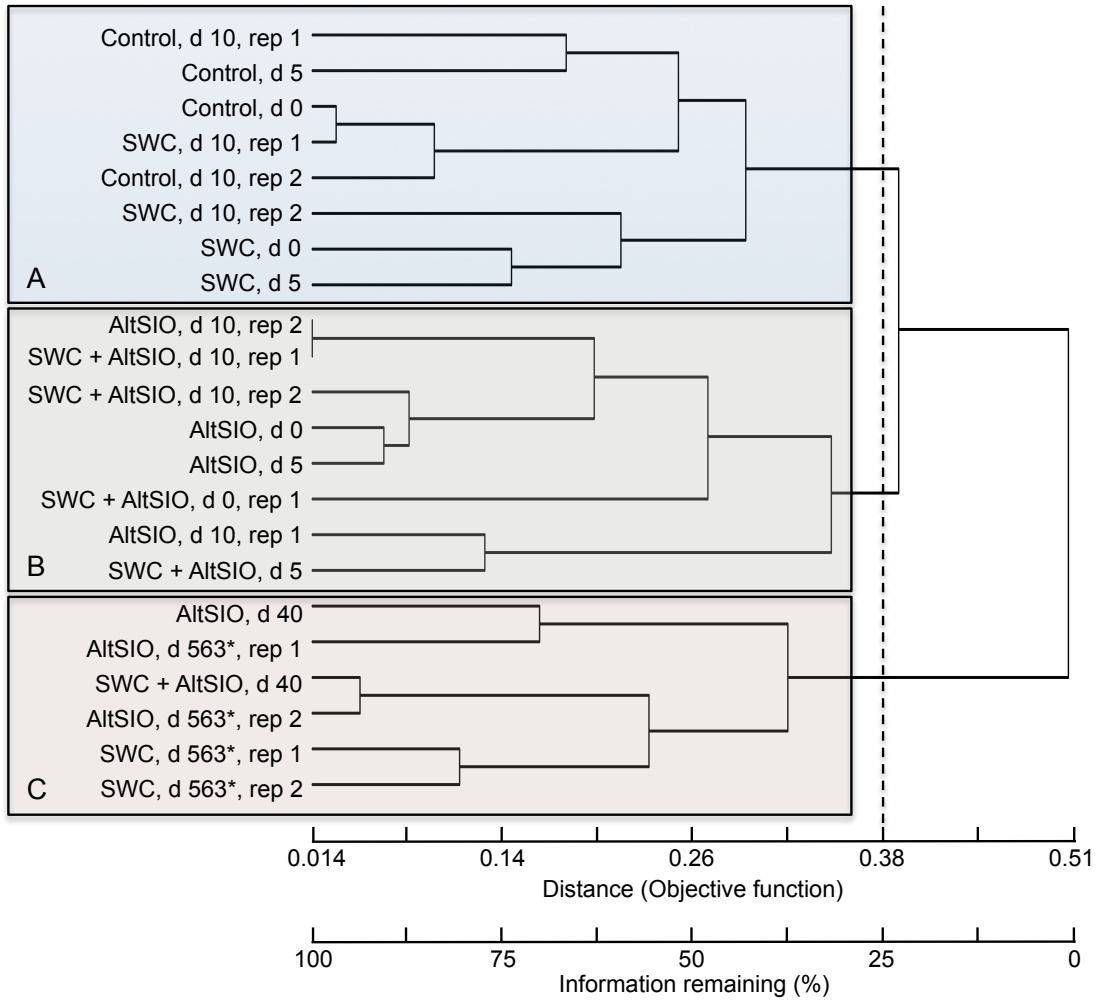

Figure 14. Linkage dendrogram of presence/absence FT-ICR-MS peak data of 22 samples calculated from Bray-Curtis distance and Ward's method. All samples are from the June 2013 DOC drawdown experiment, except those labeled d 563*, which are derived from the January 2012 DOC drawdown experiment (Pedler et al. 2014) (Chapter 2).

transport system, DppA (Fig 13). In *Escherichia coli,* this periplasmic binding protein is also required for the uptake of exogenous heme iron (Letoffe et al. 2006).

4.4.7 Impact of AltSIO on dissolved organic matter composition relative to a diverse bacterial community—FT-ICR-MS sample analysis

Cluster analysis of presence/absence data from 15298 mass peaks was used to classify similarity between 22 samples. Delineating samples based on a Bray-Curtis distance of 0.38 (objective function) with ~25 percent of information remaining, resulted in three distinct groups (groups A, B, and C) (Fig 14). Group A consisted of all SWC and bacteria-free control samples from experimental sampling time points ≤ d 10. Group B consisted of all AltSIO and SWC+AltSIO treatments from sampling time points ≤ d 10. Group C was comprised of AltSIO, SWC, and SWC+AltSIO from time points ≥ d 40 including d 563 samples collected from the January 2012 DOC drawdown mesocosms (Chapter 2) (Pedler et al. 2014).

4.5 DISCUSSION

4.5.1 AltSIO sugar metabolism and potential impact on marine dissolved organic matter composition

4.5.1.1 Metabolism of 95 individual substrates

To better understand how AltSIO may alter the composition of ambient DOM, we tested the substrate-specific physiology of AltSIO via a series of experiments. Substrate metabolism assays tested the ability of AltSIO to utilize 95 different

substrates relative to four other, phygenetically diverse, marine bacteria. These results support the conclusion that AltSIO has broad metabolic potential to utilize a wide spectrum of substrates. Even compared to vibrio and pseudoalteromonas strains that are often characterized as 'generalist', 'opportunist', or 'copiotrophic' genera (Schafer et al. 2000, Beardsley et al. 2003, Lauro et al. 2009, Nelson and Carlson 2012), AltSIO stands out in its ability to utilize >50% more compounds than *Rugeria pomeroii* DSS-3, which showed the next highest metabolic response (Table S13).

4.5.1.2 Utilization of neutral sugars in seawater

We then sought to investigate the ability of AltSIO to metablolize a suite of individual, neutral sugars that together make up a significant fraction of marine DOM. Incubation with individual sugars in seawater suggests that AltSIO preferentially metabolizes sucrose, maltose, and galactose. Given that cell abundance and TOC concentrations in the glucose-amended treatments were not significantly different from controls, this suggests that AltSIO does not utilize glucose for anabolism or catabolism. This is an unexpected result since sucrose and maltose are both disaccharides of glucose. Furthermore, glucose provides the most efficient form of cellular energy production, yielding 38 ATPs when directed through glycolysis and the citric acid cycle (Madigan and Brock 2009).

4.5.1.3 ^{14}C-sugar incorporation and enzyme activity

To further investigate the apparent selective discrimination of sugar utilization, the ability of AltSIO to incorporate specific sugars was tested by incubating pure cultures with ^{14}C-labeled glucose, fructose, and galactose. Results from three separate experiments confirmed that AltSIO showed little to no measureable incorporation of glucose when incubated with 50-100 nM substrate. Incorporation of fructose was also negligible (Table 12). Galactose was the only substrate tested that showed significant incorporation which measured 13.0 amol·cell^{-1} at a rate of 0.83 amol·cell^{-1}·h^{-1} (Table 12). These data support the observations of AltSIO biomass growth and DOC utilization response when amended with individual sugars in labile-DOM-exhausted seawater (Fig. 11 A, B).

Genomic analysis showed that AltSIO lacks the glucose permease (KEGG EC 2.7.1.69) required for the extracellular transport of glucose across the outer membrane. In *E. coli*, uptake of exogenous glucose is dependent upon this phosphotransferase enzyme, but galactose can be transported even in the absence of phosphotransferase activity (Kornberg and Riordan 1976). Conversely, AltSIO is equipped with galactokinase (galK) involved in active transport and phosphorylation of galactose. AltSIO displayed a relatively high, cell-specific, α-glucosidase hydrolysis rate (Table 10) relative to 44 bacterial strains collected from the Scripps pier (Martinez et al. 1996), and has genes for both α- and β-glucosidase encoded in its genome. These enzymes are both involved in the metabolism of galactose, sucrose, starch and other olig- and polysaccharides by exohydrolysis of 1-4-α-glucosidic linkages and β-D-glucosyl residues to release α-D-glucose and β-D-glucose, respectively.

4.5.2. Interplay between DOM composition and broad bacteria group-specific physiology

In a cross-ocean basin analysis of dissolved combined neutral sugars (DCNS) Goldberg et al (2011) found that, as DCNS concentrations decreased with increasing water mass age, the mole % of glucose became enriched relative to galactose. This finding was robust across the North Atlantic, South Pacific and the Bermuda Atlantic Time Series site (BATS) (Goldberg et al. 2009, Goldberg et al. 2011). It is important to note that these measurements are performed on acid-hydrolyzed DOM and thus decreases in total 'glucose equivalents' include oligo- and polysaccharides. These data nevertheless provide strong evidence that galactose moieties, in some form, are selectively and preferentially degraded by heterotrophic microbial communities.

Direct measurement of neutral monosaccharide concentrations in the open ocean region of the equatorial Pacific by high-pressure anion exchange (as apposed to hydrolysis of HMW DOM) showed that glucose accounted for 47 -79% of total neutral sugars, whereas galactose accounted for 0-2% of total measurable monomers (Rich et al. 1996). In the same study, it was found that ^{3}H-labled glucose accounted for 15-47% of total bacterial production, and 30-60% of glucose uptake was respired (uptake of galactose was not measured) (Rich et al. 1996). From the observation that measurable glucose concentrations were highest and galactose were lowest in this environment, it was concluded that glucose supported the majority of bacterial carbon production and respiration, whereas utilization of galactose was presumed to be

relatively insignificant (Rich et al. 1996). However, this interpretation of stock concentration ignores the potential differences in turnover rate between these substrates. As an example, concentrations of inorganic phosphate (P) often fall below the limit of detection (~2 nM) in the P-limited eastern Mediterranean, whereas measured bacterial-mediated turnover rates have been found to be as rapid as 40 minutes (Thingstad et al. 1998). Without comparative data on uptake and turnover rates of other monosaccharides, or even oligosaccharides from the same sample set or environment, the relative importance of each remains unknown.

In estuarine environments, 15-30% of the total bacterial population was found to incorporate ^{3}H-glucose, with *Alphaproteobacteria* accounting for 60% of uptake (Elifantz et al. 2005). In a study testing bacterial-group-specific uptake of low molecular weight compounds in the coastal northwestern Mediterranean Sea, 10-30% of total bacteria were found to incorporate glucose during a seasonal cycle, with uptake again dominated by *Alphaproteobacteria* (Alonso-Saez and Gasol 2007). Less than 10% of Bacteroidetes and gammaproteaobacteria cells incorporated glucose, but a higher proportion (10-60%) of cells in these groups from the same sample set incorporated amino acids and ATP (Alonso-Saez and Gasol 2007).

The ability of AltSIO to remove the entire labile pool of DOM in coastal surface seawater (Pedler et al. 2014) (Chapter 2), yet not utilize free glucose, suggests that glucose monomers may not comprise a significant fraction of labile DOM in coastal the environment from which it was isolated (Southern California Bight). Additionally, if the observed physiology of AltSIO is representative of other

physiotypes that rapidly consume labile DOM, the preferential utilization of sucrose, a disaccharide of glucose + fructose, and maltose, a disaccharide of two glucose monomers, suggests that disaccharides may serve as more relevant proxies for measuring labile DOM dynamics in the surface ocean. This interpretation relies on the hypothesis that the metabolic capacity of bacterial communities are shaped by the local resource composition. This hypothesis is supported by the observed shift in the utilization of enantiomeric amino acids by bacterioplankton from the surface ocean to the oceans interior; surface-dwelling bacterial communities almost exclusively utilize L-amino acids where they are most abundant, whereas mesopelagic communities primarily consume D-amino acids where the DOM pool is largely devoid of L-enantiomeric forms (Perez et al. 2003).

With regard to substrate source, Pakulski and Benner (1994) found that monosaccharide concentrations varied little with depth throughout the entire water column (0-4000 m) in the Atlantic and Pacific Oceans, whereas polysaccharides displayed a 5-fold decrease from the surface down to the oxygen minima and accounted for ~78% of total hydrolysable carbohydrates (Pakulski and Benner 1994). These data suggest that polysaccharides are more dynamically responsive than monosaccharides to bacterial decomposition within the total carbohydrate pool.

4.5.3 Ecological survival strategy of AltSIO inferred from measured physiology and genomic insights

Single substrate assays with 95 single substrates (Fig 9, Table S13) and comparative genomic analysis has shown that even among closely related bacterial strains, AltSIO has an increased propensity for broad carbohydrate metabolism and sugar transport. The presence of cytochorome c551/c552, nitrate reductase, and 57 outer membrane transporters related to TonB, Fe and siderophore transport suggest that nitrate and iron acquisition may play an important role in its ability to utilize the majority of the labile DOM pool. A complete suite of genes for chemotaxis coupled to dipeptide transporters suggests that AltSIO may use this strategy to increase its overall acquisition of nitrogen and/or heme iron. There are a number of genes that may contribute to the observed ability of AltSIO to remain viable and respond rapidly after prolonged periods of carbon starvation (Chapter 2) (Pedler et al. 2014). These include the carbon-starvation response gene (cstA), poly-β-hydroxybuterate synthesis and polymerization genes used for energy storage, and a large number of genes involved in H+ transport for maintaining membrane potential. Cellular inclusions similar to those observed in *V. splendidus* were also observed in AltSIO cells and both strains displayed C:P ratios more than five times larger than that found in the average marine bacterium (Fagerbakke et al. 1996, Ovreas et al. 2003, Thingstad et al. 2005). This observation has been described as the 'whinnie the pooh' strategy (Thingstad et al. 2005), whereby cells indulge on a non-limiting resource (C) to form cellular inclusions, increasing the effective surface area to volume ratio, and thus increasing diffusion-limited nutrient uptake. The C:P ratio of AltSIO cells showed a decrease with increasing incubation time (Table 11), which suggest that either i) the presence of

inclusions resulted in a higher proportion of P incorporation, or that ii) it began to metabolize the inclusions as a source of energy as substrate concentrations decreased.

4.5.4 Alteration of dissolved organic matter composition by AltSIO relative to a diverse bacterial community

It has been established that AltSIO has the capacity to consume the same magnitude of DOC as diverse bacterial communities (Pedler et al. 2014) (Chapter 2), but its effect on DOM composition was unknown. To test how AltSIO metabolism may alter DOM composition relative to a diverse bacterial community, a time course of solid-phase-extracted marine DOM (Dittmar et al. 2008) was analyzed by ultra high resolution mass spectrometry (Bhatia et al. 2010, Soule et al. 2010). Cluster analysis by Bray-Curtis distance measure of >15,000 molecular formulae from 22 samples showed three distinct groups (Fig 13). All samples incubated for 10 or fewer days split into two groups, with all samples containing AltSIO clustering separately from those where AltSIO was not added. Samples collected immediately after treatment inoculation (d 0 samples) clustered separately according to the presence or absence of AltSIO, presumably without sufficient time to significantly alter DOM composition, and this suggests that there was likely a distinguishing AltSIO-specific biosignature (Kujawinski et al. 2009) carried over from the initial AltSIO seed culture. No significant changes in DOM composition were detected between samples spanning 10 d of incubation for either of the respective groups. While differences between groups A and B (≤10 d) were large, approximately 20% data similarity was found between

these groups by Bray-Curtis distance matrix. Conversely all samples incubated for ≥ 40 d show no degree of overlap with samples from earlier time points, regardless of treatment. Given that samples incubated for 40 d were most similar to samples incubated for 1.5 y from separate sources of water, this suggests that incubation time was the prime detriment of changes in DOM composition. In other words, by the time significant differences in DOM composition became detectable, differences of each treatment appeared equally dissimilar from the initial conditions. These data suggest that AltSIO significantly alters the composition of marine DOM and it does so at a level similar to that produced by a diverse microbial assemblage.

4.6 ACKNOWLEDGEMENTS

We thank Elizabeth Kujawinski, Melissa Soule, Crystal Breier, and Krista Longnecker for assistance running and analyzing FT-ICR-MS samples. Single substrate sugar metabolism experiments were conducted with the help of Emily Shaffer. Isolate-specific enzyme activity and BioLog substrate metabolism assays were conducted with Kalani Reyes as part of the UCSD Summer Training Academy for Research in the Sciences (STARS) and the Scripps Undergraduate Research Fellowship (SURF) programs.

Chapter 4, in part, is being prepared for submission for publication of the material. Pedler, B. E., Leon Zyas, R. I., Aluwihare, L. I., Azam, F. The dissertation author was the primary investigator and author of this material.

4.7 REFERENCES

Alonso-Saez, L., and J. M. Gasol. 2007. Seasonal variations in the contributions of different bacterial groups to the uptake of low-molecular-weight compounds in northwestern Mediterranean coastal waters. Applied and Environmental Microbiology **73**:3528-3535.

Aluwihare, L. I., D. J. Repeta, and R. F. Chen. 1997. A major biopolymeric component to dissolved organic carbon in surface sea water. Nature **387**:166-169.

Beardsley, C., J. Pernthaler, W. Wosniok, and R. Amann. 2003. Are readily culturable bacteria in coastal North Sea waters suppressed by selective grazing mortality? Applied and Environmental Microbiology **69**:2624-2630.

Benner, R. 2002. Chemical composition and reactivity. Pages 59-90 *in* D. A. Hansell and C. A. Carlson, editors. Biogeochemistry of Marine Dissolved Organic Matter. Elsevier Science, USA.

Bertini, I., G. Cavallaro, and A. Rosato. 2006. Cytochrome c: Occurrence and functions. Chemical Reviews **106**:90-115.

Bhatia, M. P., S. B. Das, K. Longnecker, M. A. Charette, and E. B. Kujawinski. 2010. Molecular characterization of dissolved organic matter associated with the Greenland ice sheet. Geochimica Et Cosmochimica Acta **74**:3768-3784.

Cowie, G. L., and J. I. Hedges. 1994. Biochemical indicators of diagenetic alteration in natural organic matter mixtures. Nature **369**:304-307.

Dittmar, T., B. Koch, N. Hertkorn, and G. Kattner. 2008. A simple and efficient method for the solid-phase extraction of dissolved organic matter (SPE-DOM) from seawater. Limnology and Oceanography-Methods **6**:230-235.

Elifantz, H., R. R. Malmstrom, M. T. Cottrell, and D. L. Kirchman. 2005. Assimilation of polysaccharides and glucose by major bacterial groups in the Delaware Estuary. Applied and Environmental Microbiology **71**:7799-7805.

Fagerbakke, K. M., M. Heldal, and S. Norland. 1996. Content of carbon, nitrogen, oxygen, sulfur and phosphorus in native aquatic and cultured bacteria. Aquatic Microbial Ecology **10**:15-27.

Giovannoni, S. J., H. J. Tripp, S. Givan, M. Podar, K. L. Vergin, D. Baptista, L. Bibbs, J. Eads, T. H. Richardson, M. Noordewier, M. S. Rappe, J. M. Short, J. C. Carrington, and E. J. Mathur. 2005. Genome streamlining in a cosmopolitan oceanic bacterium. Science **309**:1242-1245.

Goldberg, S. J., C. A. Carlson, M. Brzezinski, N. B. Nelson, and D. A. Siegel. 2011. Systematic removal of neutral sugars within dissolved organic matter across ocean basins. Geophysical Research Letters **38**.

Goldberg, S. J., C. A. Carlson, D. A. Hansell, N. B. Nelson, and D. A. Siegel. 2009. Temporal dynamics of dissolved combined neutral sugars and the quality of dissolved organic matter in the Northwestern Sargasso Sea. Deep-Sea Research Part I-Oceanographic Research Papers **56**:672-685.

Hoppe, H. G. 1983. Significance of exoenzymatic activities in the ecology of brackish water - measurements by means of methylumbelliferyl substrates. Marine Ecology Progress Series **11**:299-308.

Hoppe, H. G., S. J. Kim, and K. Gocke. 1988. Microbial decomposition in aquatic environments combined process of extracellular enzyme activity and substrate uptake. Applied and Environmental Microbiology **54**:784-790.

Kirchman, D. L., B. Meon, H. W. Ducklow, C. A. Carlson, D. A. Hansell, and G. F. Steward. 2001. Glucose fluxes and concentrations of dissolved combined neutral sugars (polysaccharides) in the Ross Sea and Polar Front Zone, Antarctica. Deep-Sea Research Part Ii-Topical Studies in Oceanography **48**:4179-4197.

Koch, B. P., M. R. Witt, R. Engbrodt, T. Dittmar, and G. Kattner. 2005. Molecular formulae of marine and terrigenous dissolved organic matter detected by electrospray ionization Fourier transform ion cyclotron resonance mass spectrometry. Geochimica Et Cosmochimica Acta **69**:3299-3308.

Kornberg, H. L., and C. Riordan. 1976. Uptake of galactose into *Escherichia coli* by facilitated diffusion. Journal of General Microbiology **94**:75-89.

Kujawinski, E. B., K. Longnecker, N. V. Blough, R. Del Vecchio, L. Finlay, J. B. Kitner, and S. J. Giovannoni. 2009. Identification of possible source markers in marine dissolved organic matter using ultrahigh resolution mass spectrometry. Geochimica Et Cosmochimica Acta **73**:4384-4399.

Lauro, F., D. McDougald, T. Thomas, T. Williams, S. Egan, S. Rice, M. DeMaere, L. Ting, H. Ertan, J. Johnson, S. Ferriera, A. Lapidus, I. Anderson, N. Kyrpides, A. Munk, C. Detter, C. Han, M. Brown, F. Robb, S. Kjelleberg, and R. Cavicchioli. 2009. The genomic basis of trophic strategy in marine bacteria. Proceedings of the National Academy of Sciences of the United States of America **106**:15527-15533.

Letoffe, S., P. Delepelaire, and C. Wandersman. 2006. The housekeeping dipeptide permease is the *Escherichia coli* heme transporter and functions with two optional peptide binding proteins. Proceedings of the National Academy of Sciences of the United States of America **103**:12891-12896.

Madigan, M. T., and T. D. Brock. 2009. Brock biology of microorganisms. Pearson/Benjamin Cummings.

Markowitz, V. M., K. Mavromatis, N. N. Ivanova, I. M. A. Chen, K. Chu, and N. C. Kyrpides. 2009. IMG ER: a system for microbial genome annotation expert review and curation. Bioinformatics **25**:2271-2278.

Martinez, J., D. C. Smith, G. F. Steward, and F. Azam. 1996. Variability in ectohydrolytic enzyme activities of pelagic marine bacteria and its significance for substrate processing in the sea. Aquatic Microbial Ecology **10**:223-230.

McCarthy, M., J. Hedges, and R. Benner. 1996. Major biochemical composition of dissolved high molecular weight organic matter in seawater. Marine Chemistry **55**:281-297.

McIntyre, C., and C. McRae. 2005. Proposed guidelines for sample preparation and ESI-MS analysis of humic substances to avoid self-esterification. Organic Geochemistry **36**:543-553.

Nelson, C., and C. Carlson. 2012. Tracking differential incorporation of dissolved organic carbon types among diverse lineages of Sargasso Sea bacterioplankton. Environmental Microbiology **14**:1500-1516.

Norland, S., K. M. Fagerbakke, and M. Heldal. 1995. Light-element analysis of individual bacteria by X-ray microanalysis. Applied and Environmental Microbiology **61**:1357-1362.

Ovreas, L., D. Bourne, R. A. Sandaa, E. O. Casamayor, S. Benlloch, V. Goddard, G. Smerdon, M. Heldal, and T. F. Thingstad. 2003. Response of bacterial and viral communities to nutrient manipulations in seawater mesocosms. Aquatic Microbial Ecology **31**:109-121.

Pakulski, J. D., and R. Benner. 1994. Abundance and distribution of carbohydrates in the ocean. Limnology and Oceanography **39**:930-940.

Pedler, B. E., L. I. Aluwihare, and F. Azam. 2014. Single bacterial strain capable of significant contribution to carbon cycling in the surface ocean. Proceedings of the National Academy of Sciences **111**:7202-7207.

Perez, M., C. Pausz, and G. Herndl. 2003. Major shift in bacterioplankton utilization of enantiomeric amino acids between surface waters and the ocean's interior. Limnology and Oceanography **48**:755-763.

Rich, J. H., H. W. Ducklow, and D. L. Kirchman. 1996. Concentrations and uptake of neutral monosaccharides along 140 degrees W in the equatorial Pacific: Contribution of glucose to heterotrophic bacterial activity and the DOM flux. Limnology and Oceanography **41**:595-604.

Schafer, H., P. Servais, and G. Muyzer. 2000. Successional changes in the genetic diversity of a marine bacterial assemblage during confinement. Archives of Microbiology **173**:138-145.

Schroder, I., E. Johnson, and S. de Vries. 2003. Microbial ferric iron reductases. Fems Microbiology Reviews **27**:427-447.

Schultz, J. E., and A. Matin. 1991. Molecular and functional-characterization of a carbon starvation gene of Escherichia coli. Journal of Molecular Biology **218**:129-140.

Skoog, A., and R. Benner. 1997. Aldoses in various size fractions of marine organic matter: Implications for carbon cycling. Limnology and Oceanography **42**:1803-1813.

Soule, M. C. K., K. Longnecker, S. J. Giovannoni, and E. B. Kujawinski. 2010. Impact of instrument and experiment parameters on reproducibility of ultrahigh resolution ESI FT-ICR mass spectra of natural organic matter. Organic Geochemistry **41**:725-733.

Thingstad, T. F., L. Ovreas, J. K. Egge, T. Lovdal, and M. Heldal. 2005. Use of non-limiting substrates to increase size; a generic strategy to simultaneously optimize uptake and minimize predation in pelagic osmotrophs? Ecology Letters **8**:675-682.

Thingstad, T. F., U. L. Zweifel, and F. Rassoulzadegan. 1998. P limitation of heterotrophic bacteria and phytoplankton in the northwest Mediterranean. Limnology and Oceanography **43**:88-94.

Figure S2. KEGG pathway of glycolysis in AltSIO**.** Purple filled boxes denote genes present in the AltSIO genome with annotated KEGG orthology to enzymes involved each respective reaction. Note the absence of enzyme EC 2.7.1.69, glucose phosphotransferase, required for the import of extracellular glucose.

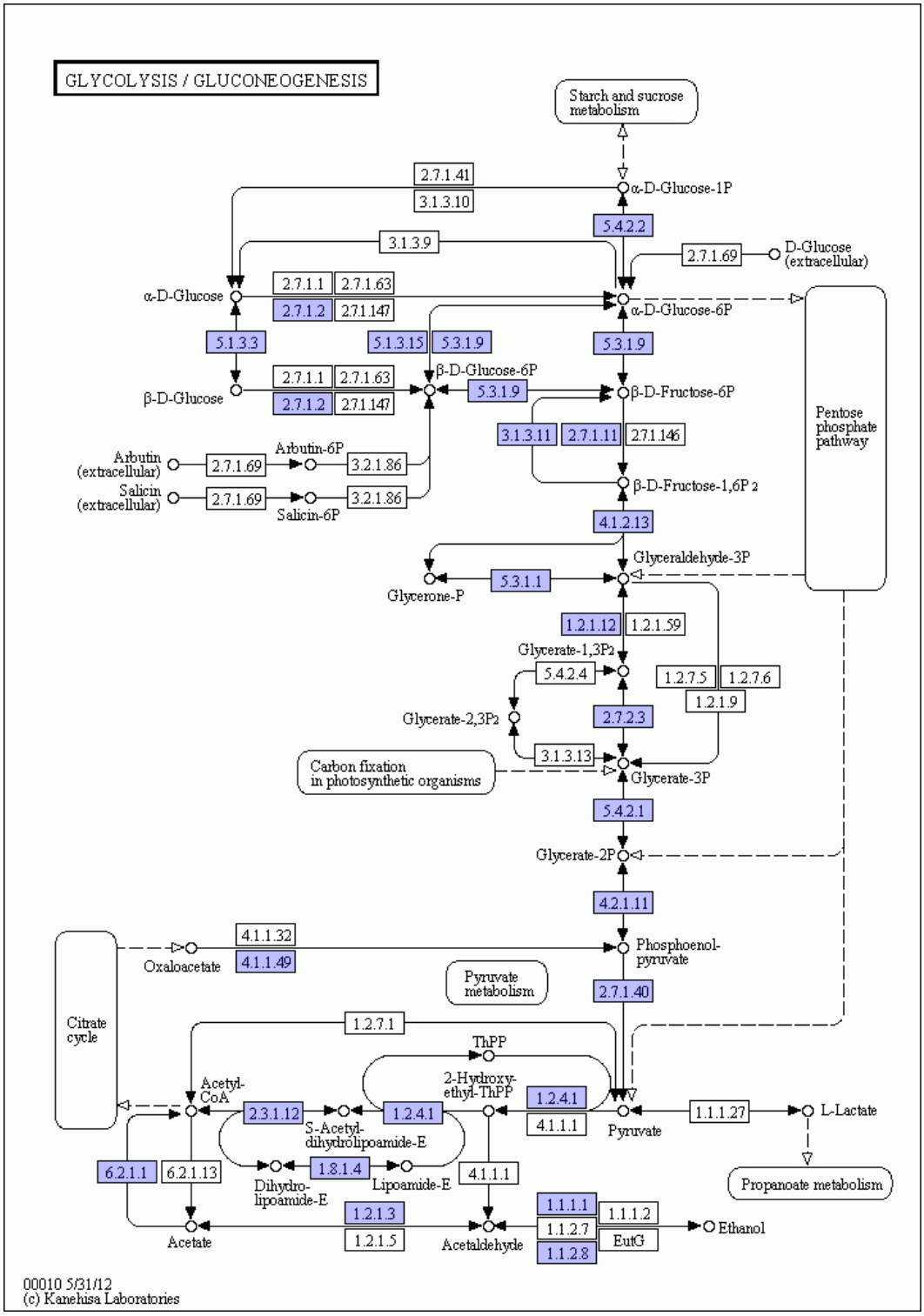
GLYCOLYSIS / GLUCONEOGENESIS
Starch and sucrose metabolism
2.7.1.41
3.1.3.10
α-D-Glucose-1P
5.4.2.2
3.1.3.9
2.7.1.69
D-Glucose (extracellular)
α-D-Glucose
2.7.1.1
2.7.1.63
2.7.1.2
2.7.1.147
α-D-Glucose-6P
5.1.3.3
5.1.3.15
5.3.1.9
5.3.1.9
β-D-Glucose-6P
β-D-Glucose
β-D-Fructose-6P
Pentose phosphate pathway
Arbutin (extracellular)
Arbutin-6P
3.2.1.86
Salicin (extracellular)
Salicin-6P
3.1.3.11
2.7.1.11
2.7.1.146
β-D-Fructose-1,6P2
4.1.2.13
Glyceraldehyde-3P
Glycerone-P
5.3.1.1
1.2.1.12
1.2.1.59
Glycerate-1,3P2
5.4.2.4
1.2.7.5
1.2.7.6
1.2.1.9
Glycerate-2,3P2
2.7.2.3
3.1.3.13
Carbon fixation in photosynthetic organisms
Glycerate-3P
5.4.2.1
Glycerate-2P
4.2.1.11
4.1.1.32
4.1.1.49
Oxaloacetate
Phosphoenol-pyruvate
Pyruvate metabolism
2.7.1.40
Citrate cycle
1.2.7.1
ThPP
Acetyl-CoA
2-Hydroxy-ethyl-ThPP
1.2.4.1
2.3.1.12
1.2.4.1
4.1.1.1
Pyruvate
1.1.1.27
L-Lactate
S-Acetyl-dihydrolipoamide-E
6.2.1.1
6.2.1.13
1.8.1.4
Dihydro-lipoamide-E
Lipoamide-E
4.1.1.1
Propanoate metabolism
1.2.1.3
1.2.1.5
1.1.1.1
1.1.2.7
1.1.2.8
1.1.1.2
EutG
Ethanol
Acetate
Acetaldehyde
00010 5/31/12
(c) Kanehisa Laboratories

Figure S3. Diagram of KEGG pathways of metabolism. Enzymes annotated in the AltSIO genome as catalyzing specific reactions within each pathway are noted by minuscule blue shaded boxes overlain upon pinprick-sized nodes.

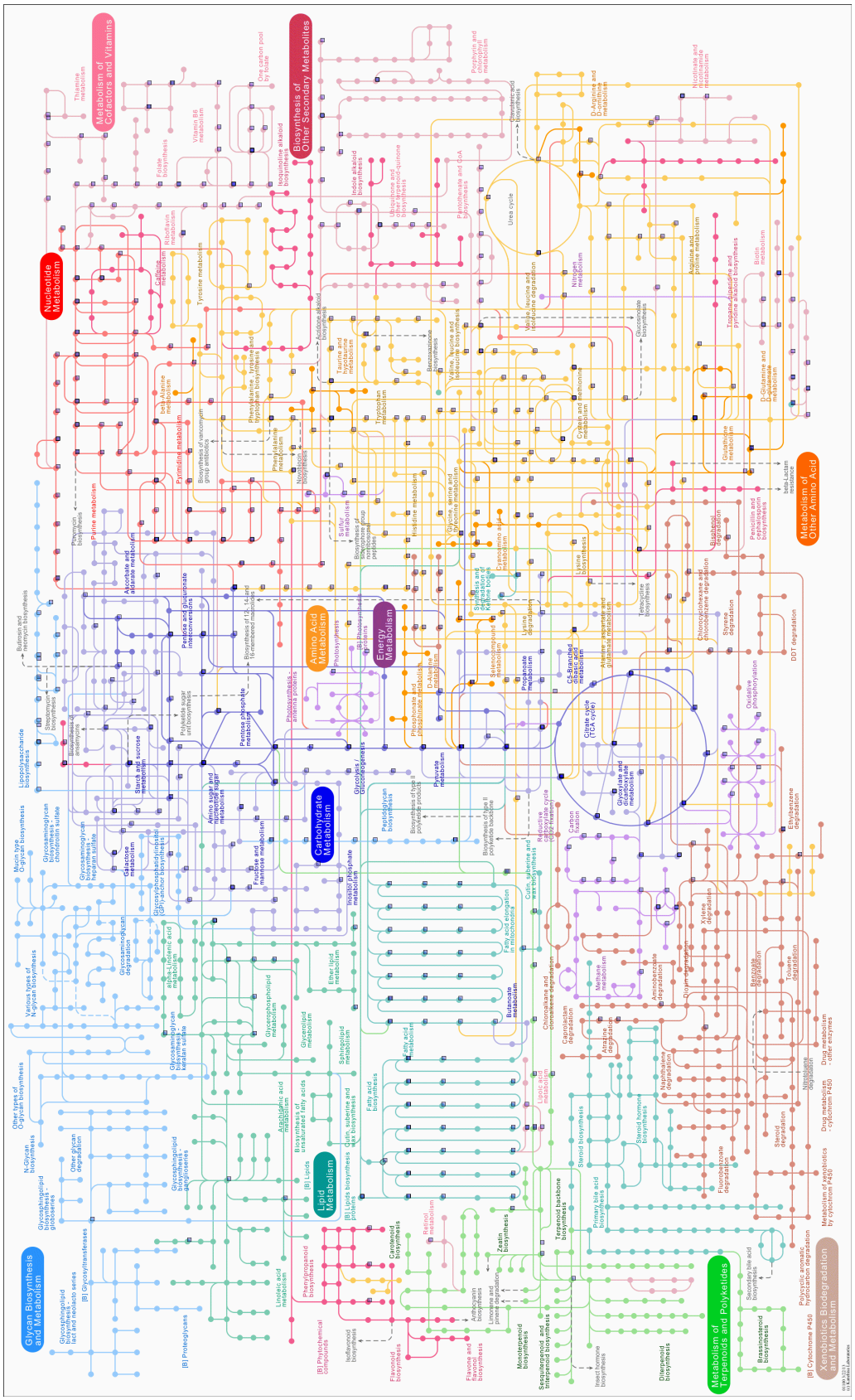
Metabolism of Cofactors and Vitamins
Biosynthesis of Other Secondary Metabolites
Nucleotide Metabolism
Amino Acid Metabolism
Energy Metabolism
Carbohydrate Metabolism
Lipid Metabolism
Metabolism of Other Amino Acid
Glycan Biosynthesis and Metabolism
Metabolism of Terpenoids and Polyketides
Xenobiotics Biodegradation and Metabolism

Table S9. General characteristics of AltSIO (ALT99) genome

	Number	% of Total
DNA, total number of bases	4635666	100.00%
DNA coding number of bases	4092372	88.28%
DNA G+C number of bases	2024478	43.67%
DNA scaffolds	1	100.00%
Genes total number	4040	100.00%
Protein coding genes	3941	97.55%
Pseudo Genes	42	1.04%
RNA genes	99	2.45%
rRNA genes	16	0.40%
5S rRNA	6	0.15%
16S rRNA	5	0.12%
23S rRNA	5	0.12%
tRNA genes	72	1.78%
Other RNA genes	11	0.27%
Protein coding genes with function prediction	3245	80.32%
without function prediction	696	17.23%
Protein coding genes with enzymes	987	24.43%
w/o enzymes but with candidate KO based enzymes	14	0.35%
Protein coding genes connected to Transporter Classification	475	11.76%
Protein coding genes connected to KEGG pathways	1042	25.79%
not connected to KEGG pathways	2899	71.76%
Protein coding genes connected to KEGG Orthology (KO)	1996	49.41%
not connected to KEGG Orthology (KO)	1945	48.14%
Protein coding genes connected to MetaCyc pathways	969	23.99%
not connected to MetaCyc pathways	2972	73.56%
Protein coding genes with COGs	2689	66.56%
with KOGs	1366	33.81%
with Pfam	3355	83.04%
with TIGRfam	1332	32.97%
with IMG Terms	328	8.12%
with IMG Pathways	160	3.96%
with IMG Parts List	138	3.42%
in paralog clusters	2956	73.17%
in Chromosomal Cassette	4040	100.00%
Chromosomal Cassettes	434	-
Biosynthetic Clusters	24	-
Genes in Biosynthetic Clusters	195	4.83%
Fused Protein coding genes	30	0.74%
Protein coding genes coding signal peptides	508	12.57%
Protein coding genes coding transmembrane proteins	1006	24.90%
COG clusters	1734	64.48%
KOG clusters	779	28.97%
Pfam clusters	2265	67.51%
TIGRfam clusters	1136	85.29%

Table S10. Clusters of orthologous groups (COG) of proteins categorized by function for AltSIO genome relative to closely related *Alteromonas macleodii* strains. Abbreviations: (), total number of genes in COGs; n, number of genes; %, percent of total genes.

			Alteromonas macleodii					
	AltSIO (3031)		AD45 (3011)		MED64 (2906)		DE1 (3017)	
COG Categories	n	%	n	%	n	%	n	%
[E] Amino acid transport and metabolism	231	7.6	240	8.0	222	7.6	219	7.3
[G] Carbohydrate transport and metabolism	142	4.7	147	4.9	134	4.6	143	4.7
[D] Cell cycle control, cell division, chromosome partitioning	30	1.0	32	1.1	34	1.2	38	1.3
[N] Cell motility	99	3.3	101	3.4	89	3.1	87	2.9
[M] Cell wall/membrane/envelope biogenesis	175	5.8	172	5.7	174	6.0	169	5.6
[B] Chromatin structure and dynamics	2	0.1	2	0.1	2	0.1	2	0.1
[H] Coenzyme transport and metabolism	123	4.1	121	4.0	126	4.3	126	4.2
[V] Defense mechanisms	43	1.4	39	1.3	49	1.7	50	1.7
[C] Energy production and conversion	189	6.2	174	5.8	191	6.6	206	6.8
[S] Function unknown	258	8.5	258	8.6	244	8.4	249	8.3
[R] General function prediction only	370	12.2	361	12.0	355	12.2	356	11.8
[P] Inorganic ion transport and metabolism	165	5.4	172	5.7	154	5.3	159	5.3
[U] Intracellular trafficking, secretion, and vesicular transport	91	3.0	90	3.0	90	3.1	92	3.1
[I] Lipid transport and metabolism	128	4.2	119	4.0	111	3.8	116	3.8
[F] Nucleotide transport and metabolism	70	2.3	67	2.2	65	2.2	64	2.1
[O] Posttranslational modification, protein turnover, chaperones	126	4.2	124	4.1	132	4.5	131	4.3
[L] Replication, recombination and repair	125	4.1	136	4.5	138	4.8	175	5.8
[A] RNA processing and modification	1	0.0	1	0.0	1	0.0	1	0.0
[Q] Secondary metabolites biosynthesis, transport and catabolism	60	2.0	50	1.7	44	1.5	60	2.0
[T] Signal transduction mechanisms	210	6.9	220	7.3	180	6.2	189	6.3
[K] Transcription	220	7.3	216	7.2	194	6.7	209	6.9
[J] Translation, ribosomal structure and biogenesis	173	5.7	169	5.6	177	6.1	176	5.8
Not in COGs	1351	33.4	1371	33.8	1303	33.4	1702	38.6

Table S11. Enumeration of COGs with predicted carbohydrate processing function within genomes of AltSIO and *Alteromonas macleodii* strains AD45, MED64, and DE1.

			Alteromonas macleodii strain		
ID	Name & predicted function	Alt SIO	AD 45	MED 64	DE 1
COG3734	2-keto-3-deoxy-galactonokinase	1	0	0	0
COG0395	ABC-type sugar transport system, permease component	1	0	0	0
COG1175	ABC-type sugar transport systems, permease components	1	0	0	0
COG1621	Beta-fructosidases (levanase/invertase)	1	0	0	0
COG5039	Exopolysaccharide biosynthesis protein	1	0	0	0
COG0662	Mannose-6-phosphate isomerase	1	0	0	0
COG0296	1,4-alpha-glucan branching enzyme	2	1	1	1
COG0800	2-keto-3-deoxy-6-phosphogluconate aldolase	3	3	2	3
COG3836	2,4-dihydroxyhept-2-ene-1,7-dioic acid aldolase	1	1	0	0
COG0126	3-phosphoglycerate kinase	1	1	1	1
COG1640	4-alpha-glucanotransferase	1	1	1	1
COG0205	6-phosphofructokinase	1	1	1	1
COG0362	6-phosphogluconate dehydrogenase	1	1	1	1
COG0363	6-phosphogluconolactonase/Glucosamine-6-phosphate isomerase/deaminase	1	1	3	3
COG1682	ABC-type polysaccharide/polyol phosphate export systems, permease component	2	2	2	2
COG1134	ABC-type polysaccharide/polyol phosphate transport system, ATPase component	1	1	1	1
COG1653	ABC-type sugar transport system, periplasmic component	3	0	1	1
COG3839	ABC-type sugar transport systems, ATPase components	1	0	1	0
COG0448	ADP-glucose pyrophosphorylase	1	1	1	1
COG3345	Alpha-galactosidase	1	1	0	0
COG1501	Alpha-glucosidases, family 31 of glycosyl hydrolases	2	2	1	1
COG2814	Arabinose efflux permease	12	6	8	9
COG0483	Archaeal fructose-1,6-bisphosphatase and related enzymes of inositol monophosphatase family	1	1	1	1
COG3250	Beta-galactosidase/beta-glucuronidase	1	2	1	2
COG1472	Beta-glucosidase-related glycosidases	4	3	3	3
COG2723	Beta-glucosidase/6-phospho-beta-glucosidase/beta-galactosidase	2	1	1	1
COG4464	Capsular polysaccharide biosynthesis protein	1	1	1	1
COG0537	Diadenosine tetraphosphate (Ap4A) hydrolase and other HIT family hydrolases	2	2	2	2
COG0129	Dihydroxyacid dehydratase/phosphogluconate dehydratase	2	2	4	4
COG0148	Enolase	1	1	1	1
COG3001	Fructosamine-3-kinase	1	1	1	1
COG0158	Fructose-1,6-bisphosphatase	1	1	3	1
COG3588	Fructose-1,6-bisphosphate aldolase	1	1	1	1
COG0406	Fructose-2,6-bisphosphatase	2	2	1	1

Table S11. Enumeration of COGs with predicted carbohydrate processing function within genomes of AltSIO and *Alteromonas macleodii* strains AD45, MED64, and DE1. Continued.

			Alteromonas macleodii strain		
ID	Name & predicted function	Alt SIO	AD 45	MED 64	DE 1
COG0738	Fucose permease	5	9	5	5
COG0153	Galactokinase	1	1	1	1
COG2017	Galactose mutarotase and related enzymes	1	1	1	2
COG0058	Glucan phosphorylase	1	1	1	1
COG0837	Glucokinase	1	1	3	3
COG3265	Gluconate kinase	1	1	1	0
COG4993	Glucose dehydrogenase	2	2	1	1
COG0364	Glucose-6-phosphate 1-dehydrogenase	1	1	3	3
COG0166	Glucose-6-phosphate isomerase	1	1	1	1
COG2133	Glucose/sorbosone dehydrogenases	3	3	2	4
COG0057	Glyceraldehyde-3-phosphate dehydrogenase/erythrose-4-phosphate dehydrogenase	3	3	3	3
COG0580	Glycerol uptake facilitator and related permeases (Major Intrinsic Protein Family)	1	1	1	1
COG0297	Glycogen synthase	1	1	1	1
COG0366	Glycosidases	6	6	6	6
COG2610	H+/gluconate symporter and related permeases	1	2	2	1
COG3622	Hydroxypyruvate isomerase	1	1	1	1
COG0246	Mannitol-1-phosphate/altronate dehydrogenases	1	2	1	1
COG1803	Methylglyoxal synthase	1	1	1	1
COG1820	N-acetylglucosamine-6-phosphate deacetylase	1	2	1	1
COG2942	N-acyl-D-glucosamine 2-epimerase	1	1	0	1
COG2211	Na+/melibiose symporter and related transporters	2	1	1	2
COG0451	Nucleoside-diphosphate-sugar epimerases	4	3	5	3
COG0036	Pentose-5-phosphate-3-epimerase	1	1	1	1
COG2513	PEP phosphonomutase and related enzymes	1	1	1	1
COG0697	Permeases of the drug/metabolite transporter (DMT) superfamily	2	3	3	3
COG0574	Phosphoenolpyruvate synthase/pyruvate phosphate dikinase	1	1	1	1
COG0033	Phosphoglucomutase	1	1	1	1
COG0588	Phosphoglycerate mutase 1	1	1	1	1
COG0279	Phosphoheptose isomerase	1	1	2	1
COG1109	Phosphomannomutase	3	3	3	2
COG2190	Phosphotransferase system IIA components	1	1	1	1
COG1762	Phosphotransferase system mannitol/fructose-specific IIA domain (Ntr-type)	1	1	1	1
COG1925	Phosphotransferase system, HPr-related proteins	1	1	1	1
COG2971	Predicted N-acetylglucosamine kinase	1	3	1	1
COG2956	Predicted N-acetylglucosaminyl transferase	1	1	1	2
COG0702	Predicted nucleoside-diphosphate-sugar epimerases	1	1	1	1

Table S11. Enumeration of COGs with predicted carbohydrate processing function within genomes of AltSIO and *Alteromonas macleodii* strains AD45, MED64, and DE1. Continued.

			Alteromonas macleodii strain		
ID	Name & predicted function	Alt SIO	AD 45	MED 64	DE 1
COG0061	Predicted sugar kinase	1	1	1	1
COG0063	Predicted sugar kinase	1	1	1	1
COG0726	Predicted xylanase/chitin deacetylase	2	1	1	1
COG2379	Putative glycerate kinase	1	0	0	1
COG0469	Pyruvate kinase	1	1	3	3
COG0120	Ribose 5-phosphate isomerase	1	1	1	1
COG0235	Ribulose-5-phosphate 4-epimerase and related epimerases and aldolases	2	2	2	2
COG0524	Sugar kinases, ribokinase family	4	4	3	2
COG1082	Sugar phosphate isomerases/epimerases	2	2	2	2
COG2271	Sugar phosphate permease	1	2	0	0
COG0176	Transaldolase	1	1	1	2
COG1940	Transcriptional regulator/sugar kinase	2	1	1	2
COG1349	Transcriptional regulators of sugar metabolism	2	2	2	2
COG0021	Transketolase	1	1	1	2
COG0149	Triosephosphate isomerase	1	1	2	1
COG1523	Type II secretory pathway, pullulanase PulA and related glycosidases	2	2	2	2
COG0676	Uncharacterized enzymes related to aldose 1-epimerase	1	1	1	1

Table S12. COGs of predicted transporters present in AltSIO genome but absent from *Alteromonas macleodii* strains AD45, MED64, and DE1.

COG ID	AltSIO-specific COGs
COG4654	Cytochrome c551/c552
COG2223	Nitrate/nitrite transporter
COG5653	Protein involved in cellulose biosynthesis (CelD)
COG3764	Sortase (surface protein transpeptidase)
COG5492	Bacterial surface proteins containing Ig-like domains
COG3917	2-hydroxychromene-2-carboxylate isomerase
COG3734	2-keto-3-deoxy-galactonokinase
COG3971	2-keto-4-pentenoate hydratase
COG0395	ABC-type sugar transport system, permease component
COG1175	ABC-type sugar transport systems, permease components
COG1621	Beta-fructosidases (levanase/invertase)
COG5039	Exopolysaccharide biosynthesis protein
COG0790	FOG: TPR repeat, SEL1 subfamily
COG5212	Low-affinity cAMP phosphodiesterase
COG0662	Mannose-6-phosphate isomerase
COG0760	Parvulin-like peptidyl-prolyl isomerase
COG0810	Periplasmic protein TonB, links inner and outer membranes
COG5302	Post-segregation antitoxin (ccd killing mechanism protein) encoded by the F plasmid
COG4671	Predicted glycosyl transferase
COG3607	Predicted lactoylglutathione lyase
COG1985	Pyrimidine reductase, riboflavin biosynthesis
COG1305	Transglutaminase-like enzymes, putative cysteine proteases
COG0446	Uncharacterized NAD(FAD)-dependent dehydrogenases
COG5429	Uncharacterized secreted protein
COG2246	Predicted membrane protein
COG3326	Predicted membrane protein
COG3371	Predicted membrane protein
COG3619	Predicted membrane protein
COG3768	Predicted membrane protein
COG1714	Predicted membrane protein/domain
COG3535	Uncharacterized conserved protein
COG5470	Uncharacterized conserved protein
COG2841	Uncharacterized protein conserved in bacteria
COG3222	Uncharacterized protein conserved in bacteria
COG3533	Uncharacterized protein conserved in bacteria
COG3828	Uncharacterized protein conserved in bacteria
COG4683	Uncharacterized protein conserved in bacteria

Table S12. COGs of predicted transporters present in AltSIO genome but absent from Alteromonas macleodii strains AD45, MED64, and DE1. Continued.

Gene ID	AltSIO-specific Transporters
2526020432	sorbitol ABC transporter membrane protein/mannitol ABC transporter membrane protein
2526020431	sorbitol-binding protein/mannitol-binding protein
2526020433	sorbitol ABC transporter membrane protein/mannitol ABC transporter membrane protein
2526020434	sorbitol ABC transporter ATP-binding protein/mannitol ABC transporter ATP-binding protein

Table S13. Biolog GN2 microplate data showing isolate-specific oxidation of 95 screened substrates.

Chem. class	Type	Compound	Alteromonas AltSIO	Pseudoalteromonas TW7	Vibrio SWAT -3	R. Pomeroyi DSS-3	Flavabacteria BBFL7
		Total utilized	**62**	**29**	**36**	**40**	**18**
polymer	cyclic glucose oligosaccharide	α-Cyclodextrin	+	+			+
polymer	saccharide	Dextrin	+	+	+	+	+
polymer	polysaccharide	Glycogen	+	+	+		+
polymer	polysorbate	Tween 40	+	+	+	+	+
polymer	polysorbate	Tween 80	+	+	+	+	
carbohydrate	monosaccharide hexose sugar	α-D-Glucose	+	+	+		
carbohydrate	monosaccharide, C-2 epimer of glucose	D-Mannose	+		+		
carbohydrate	monosaccharide, C-4 epimer of glucose	D-Galactose	+	+			
carbohydrate	monosaccharide	D-Fructose	+	+	+		
carbohydrate	disaccaride of glucose	Sucrose	+	+	+		+
carbohydrate	disaccaride of glucose	Maltose	+	+	+		+
carbohydrate	sugar	α-D-Lactose	+	+			
carbohydrate	hexosoe deoxy sugar	L-Fucose					
carbohydrate	monosaccharide, aldopentose	L-Arabinose					
carbohydrate	methyl pentose	L-Rhamnose					
carbohydrate	monosaccharide	D-Psicose	+		+		
carbohydrate	disaccharide	D-Melibiose	+	+			
carbohydrate	disaccharide	D-Cellobiose	+	+	+		
carbohydrate	disaccharide	Gentiobiose	+			+	
carbohydrate	disaccharide	Lactulose	+				
carbohydrate	disaccharide	D-Trehalose	+		+		
carbohydrate	disaccharide	Turanose	+				
carbohydrate	trischaccharide	D-Raffinose	+				
carbohydrate	monosaccharide	β-Methyl-D-Glucoside	+				
carbohydrate	pentose sugar alcohol	Adonitol					
carbohydrate	sugar alcohol	D-Arabitol					
carbohydrate	sugar alcohol	D-Mannitol	+	+	+		
carbohydrate	sugar alcohol	D-Sorbitol	+		+		
carbohydrate	sugar alcohol	i-Erythritol					

Table S13.Biolog GN2 microplate data showing isolate-specific oxidation of 95 screened substrates. Continued.

Chem. class	Type	Compound	Alteromonas AltSIO	Pseudoalteromonas TW7	Vibrio SWAT -3	R. Pomeroyi DSS-3	Flavabacteria BBFL7
carbohydrate	sugar alcohol	m-inositol					
carbohydrate	sugar alcohol	Xylitol					
carbohydrate	amino sugar	N-Acetyl-D-Galactosamine					
carbohydrate	amino sugar	N-Acetyle-D-Glucosamine		+	+	+	
amino acid	nonpolar	L-Alanine	+	+	+	+	+
amino acid	Nonionizable polar	L-Asparagine	+	+	+	+	
amino acid	Ionizable: acidic	L-Aspartic Acid	+		+	+	
amino acid	Ionizable: acidic	L-Glutamic Acid	+	+	+	+	+
amino acid	ionizable basic	L-Histidine	+				
amino acid	nonpolar	L-Leucine	+	+		+	
amino acid	non-DNA encoded	L-Ornithine	+			+	
amino acid	nonpolar	L-Phenylalanine	+			+	
amino acid	nonpolar	L-Proline	+	+	+	+	
amino acid	Nonionizable polar	L-Serine	+	+	+	+	+
amino acid	Nonionizable polar	L-Threonine	+	+	+	+	+
amino acid derivitive	peptide	L-Alanyl-Glycine	+	+	+	+	+
amino acid derivitive	Ionizable: acidic	Glycyl-L-Aspartic Acid			+	+	+
amino acid derivitive	Ionizable: acidic	Glycyl-L-Glutamic Acid	+	+	+	+	+
amino acid derivitive	peptide	L-Pyroglutamic Acid				+	
amino acid derivitive	peptide	Hydroxy-L-Proline	+			+	
amino acid	nonpolar	D-Alanine				+	
amino acid	Nonionizable polar	D-Serine					
amino acid peptide	Lys-Met peptide	D,L-Catnitine					
	glutamate, succinic acid precursor	γ-Aminobutyric Acid				+	
	catabolic intermediate of L-hisitidine	Urocanic Acid					
	tRNA nucleoside	Inosine	+	+	+		
purine	RNA nucleoside	Uridine	+	+	+		
pyrimidine	DNA nucleoside	Thymidine			+		
amine		Phenyl ethylamine					
amine		Putrescine					

Table S13. Biolog GN2 microplate data showing isolate-specific oxidation of 95 screened substrates. Continued.

Chem. class	Type	Compound	Alteromonas AltSIO	Pseudoalteromonas TW7	Vibrio SWAT -3	R. Pomeroyi DSS-3	Flavabacteria BBFL7
amine		2-Aminoethanol					
		2,3-Butanediol					
	triglyceride backbone	Glycerol	+			+	
sugar phosphate		D,L, α-Glycerol Phosphate	+		+		
sugar phosphate		α-D-Glucose-1-Phosphate	+				
sugar phosphate		D-Glucose-6-Phosphate	+				
carboxylic acid		Pyruvic Acid Methyl Ester	+	+		+	
carboxylic acid		Succinic Acid Mono-Methyl Ester				+	+
organic acid		Acetic Acid	+	+	+	+	+
organic acid		Cis-Aconitic Acid	+		+	+	
organic acid		Citric Acid	+		+	+	
carboxylic acid		Formic Acid					
carbohydrate		D-Galactonic Acid Lactone					
carboxylic acid		D-Galacturonic Acid	+				
organic acid		D-Gluconic Acid	+				
carboxylic acid		D-Glucosaminic Acid	+				
carboxylic acid		D-Glucuronic Acid	+				
carboxylic acid		α-Hydroxybutyric Acid				+	
carboxylic acid		β-Hydroxybutyric Acid	+			+	
carboxylic acid		γ-Hydroxybutyric Acid				+	
carboxylic acid		p-Hydroxyphenylacetic Acid					
carboxylic acid		Itaconic Acid					
carboxylic acid		α-Ketobutyric Acid	+		+	+	+
organic acid		α-Ketoglutaric Acid	+		+	+	
organic acid		α-Ketovaleric Acid				+	
carboxylic acid		D,L-Lactic Acid	+			+	
dicarboxylic acid		Malonic Acid	+				
carboxylic acid		Propionic Acid	+			+	+
cyclitol	cyclic polyol	Quinic Acid	+				
		D-Saccharic Acid	+				
carboxylic acid		Sebacic Acid					
dicarboxylic acid		Succinic Acid	+		+	+	
		Bromosuccinic Acid			+	+	

Table S13. Biolog GN2 microplate data showing isolate-specific oxidation of 95 screened substrates. Continued.

Chem. class	Type	Compound	Alteromonas AltSIO	Pseudoalteromonas TW7	Vibrio SWAT -3	R. Pomeroyi DSS-3	Flavabacteria BBFL7
carboxylic acid		Succinamic Acid	+			+	
		Glucoronamide					
oligopeptide	cyclic	L-Alaninamide	+	+		+	+